N° d'ordre: 2010telb0155

Sous le sceau de l'Université européenne de Bretagne

Télécom Bretagne

en habilitation conjointe avec l'Université de Bretagne-Sud

Ecole Doctorale-sicma

Advanced Hybrid-ARQ Receivers for Broadband MIMO Communications

---

Thèse de Doctorat

Mention: *Sciences pour l'ingénieur*

Présenté par **Houda CHAFNAJI**

Département: Signal & Communications

Soutenue le 09 Novembre 2010

Jury:

M. Emmanuel Boutillon, Professeur, UBS, (Président de jury)
M. Jean-Pierre Cances, Professeur, Xlim, Université de Limoges (Rapporteur)
M. Stéphane Azou, Maître de Conf. (HDR), UBO, (Rapporteur)
M. Ramesh Pyndiah, Professeur, Telecom Bretagne, (Examinateur)
M. Halim Yanikomeroglu, Professeur, l'université de Carleton, Canada (Examinateur)
M. Samir Saoudi, Professeur, Telecom Bretagne, (Directeur de thèse)
M. Tarik Ait-idir, Professeur Assistant, INPT, Maroc, (Invité)

(13) **O mankind, indeed We have created you from male and female and made you peoples and tribes that you may know one another.**

The noble Qur'an, Chapter 49

To my parents

Acknowledgments

All praise is due to God Almighty, the Beneficent, the Merciful. Without His blessings and guidance, my accomplishments would never have been possible.

First of all, I would like to thanks my thesis supervisor, Prof. Samir Saoudi, for giving me the opportunity to conduct this research work under his supervision, for his invaluable advice, guidance and support. My deepest gratitude goes to my colleague, co-supervisor and friend, Prof. Tarik Ait-Idir from INPT Rabat. He has always been accessible and very helpful. I am also grateful to Prof. Halim Yanikomeroglu from Carleton University Ottawa for accepting to co-supervise the last part of my work on cooperative communications. Samir, Tarik and Halim tireless efforts, advice and guidance let me learn valuable lessons which would definitely help me in my career.

Many thanks are due to the members of my doctoral committee, Prof. Emmanuel Boutillon, Prof. Jean Pierre Cances, Prof. Stéphane Azou, and Prof. Ramesh Pyndiah for their valuable time and efforts. I am truly honored to have such a great examining committee.

Last, but not least, I am deeply grateful to my parents for their neverending care, constant love, endless support, and encouragement.

Abstract

Multiple input multiple output (MIMO) and hybrid–automatic repeat request (ARQ) are two major techniques that allow to improve the transmission rate and quality over the wireless link. In MIMO techniques, the spatial dimension of the MIMO channel is exploited through the use of multiple antennas at both the transmitter and receiver sides. This translates into an improvement in the spectrum efficiency and/or the link quality. Hybrid–ARQ protocols provide an important source of time diversity through the combination of channel coding and ARQ. This is performed with the aid of packet combining techniques where erroneous data packets are kept in the receiver to help detect/decode retransmitted frames. In broadband MIMO communications, the MIMO wireless link suffers from intersymbol interference (ISI) caused by multipath propagation. This effect can be mitigated using channel equalization and/or hybrid–ARQ. This thesis focuses on the joint design of the packet combiner and the channel equalizer for MIMO ARQ transmissions over the broadband wireless channel. We propose a low-complexity turbo combining approach for MIMO ARQ transmissions where packet combining is performed at each ARQ round by exchanging soft information in an iterative fashion between the soft packet combiner and the soft–input–soft–output (SISO) decoder. The proposed combining approach is extended to a general case of unknown co-channel interference (CCI)-limited MIMO channels. We also propose two packet combining algorithms for code division multiple access (CDMA) MIMO-based wireless packet access where multi-code transmission suffers from severe performance degradation due to the loss of code orthogonality caused by both interchip interference (ICI) and co-antenna interference (CAI). In the first algorithm, equalization and packet combining are jointly performed at the chip-level. In the second algorithm, chip-level equalization and despreading are separately carried out for each transmission, then packet combining is performed at the level of the soft demapper. In the last part of this thesis, we focus on packet combining for multi–relay systems and derive a communication model in such a way that the destination can see the received signals during the relaying slots as direct retransmissions from the source. The derived communication model is of a great importance as it allows packet combining and channel equalization to be jointly performed using the concept of virtual receive antennas.

Keywords: Broadband MIMO, ARQ, multi-code CDMA, cooperative relaying, turbo packet combining, frequency domain equalization.

Résumé

MIMO et hybrid-ARQ font partie des principales techniques qui permettent d'améliorer le taux de transmission ainsi que la qualité du lien sans fil. Dans les techniques MIMO, la dimension spatiale du canal MIMO est exploitée par l'utilisation de plusieurs antennes au niveau de l'émetteur et du récepteur. Cela se traduit par une amélioration de l'efficacité spectrale et/ou la qualité du lien. Les protocoles hybrid-ARQ constituent une importante source de diversité temporelle grâce à la combinaison du codage de canal avec l'ARQ. Ceci est réalisé à l'aide des techniques de combinaison où les paquets de données erronés sont conservés dans le récepteur pour aider à détecter/décoder les trames retransmises. Dans les communications MIMO large bande, la liaison sans fil MIMO souffre des interférences entre symboles causées par la propagation à trajets multiples. Cet effet peut être atténué en utilisant l'égalisation du canal et/ou l'hybrid-ARQ. Cette thèse porte sur la conception conjointe de la combinaison des paquets et de l'égalisation du canal pour les transmissions MIMO ARQ sur le canal large bande sans fil. Nous proposons une approche de combinaison itérative à faible complexité pour les transmissions MIMO ARQ où la combinaison de paquets est effectuée en échangeant l'information soft de façon itérative entre le combinateur à entrée soft et le décodeur SISO. L'approche de combinaision proposée est généralisée au cas des transmissions MIMO limitées par l'effet des interférences co-canal non connues. Nous proposons également deux algorithmes de combinaison pour les systems CDMA-MIMO où les transmissions multi-code souffrent de grave dégradation des performances due à la perte d'orthogonalité entre les codes. Dans le premier algorithme, l'égalisation et la combinaison des paquets sont accomplies conjointement au niveau chip. Dans le deuxième algorithme, l'égalisation au niveau chip et le désétalement sont effectués séparément pour chaque transmission, puis la combinaison des paquets est effectuée au niveau du démodulateur soft. Dans la dernière partie de cette thèse, nous nous concentrons sur la combinaison des paquets pour les systèmes à relais multiples et nous dérivons un modèle de communication de telle sorte que la destination peut voir les signaux reçus pendant les intervalles temporels du relayage comme des retransmissions directes à partir de la source. Le modèle de communication dérivé est d'une grande importance car il permet d'effectuer la combinaison des paquets conjointement avec l'égalisation en utilisant la notion des antennes virtuelles au niveau de la réception.

Mots-clefs: MIMO large bande, ARQ, multi-code CDMA, relais coopératifs, combinaison des paquets itérative, égalisation dans le domaine fréquentiel.

List of Notations and Acronyms

*, $^\top$, and $^{\mathrm{H}}$	conjugate, transpose, and Hermitian transpose, respectively
$\lvert . \rvert$	absolute value
$\lceil x \rceil$	ceiling of x, i.e., the smallest integer greater than or equal to x
$\otimes$	Kronecker product
$\mathbf{0}_{N \times Q}$	all zero $N \times Q$ matrix
$\mathbb{E}[.]$	mathematical expectation of the argument $(.)$
$\mathbb{C}$	set of complex number
$\mathbf{A}_{l'}^{\mathrm{CCI}^{(k)}}$	matrix characterizing the scattering environment between the CCI transmitter and receiver
$\boldsymbol{b}$	coded and interleaved frame
$\mathbf{b}_t$	coded and interleaved sub-stream transmitted over antennas t
$b_{t,j,m}$	coded and interleaved mth bit corresponding to symbol transmitted over antenna t at channel use j
C	number of assigned orthogonal codes per user
$\mathbf{E}_{i,N}$	$N \times NT$ zero matrix where the ith $N \times N$ block is equal to $\mathbf{I}_N$ with $i = 0, \cdots, T-1$
E_{AB}	average energy of A $\rightarrow$ B link
E_k	average energy at slot k
$\mathbf{e}_{t,i}$	$(N_T i + t)$th vector of the canonical basis
$\delta_{m,n}$	Kronecker symbol, i.e., $\delta_{m,n} = 1$ for $m = n$ and $\delta_{m,n} = 0$ for $m \neq n$
D	destination terminal
$\underline{\mathbf{D}}_i^{(k)}$	recursive variable to store channel frequency responses corresponding to round $1, \cdots, k$
$\mathrm{diag}\{\mathbf{X}\}$	row vector corresponding to the diagonal of $\mathbf{X}$
$\mathrm{diag}\{\mathbf{X}_1, \cdots, \mathbf{X}_M\}$	$MN \times MQ$ matrix whose diagonal blocks are $\mathbf{X}_1, \cdots, \mathbf{X}_M \in \mathbb{C}^{N \times Q}$
$\mathrm{diag}\{\mathbf{x}\}$	$N \times N$ diagonal matrix whose diagonal entries are the elements of the complex vector $\mathbf{x} \in \mathbb{C}^N$
$\mathbf{F}_{t,i}^{(k)}$	unconditional MMSE filter corresponding to antenna t and channel use i at ARQ round k

$\mathbf{g}_{t,j}^{(k)}$	equivalent channel gain vector at the equalizer output corresponding to transmissions $1, \cdots, k$, channel use i, and transmit antenna t
$g_{t,i}$	equivalent channel gain at the equalizer output corresponding to channel use i, and transmit antenna t
$\boldsymbol{\mathcal{H}}^{(k)}$	block circulant matrix at the kth ARQ round
$\mathbf{H}_l^{(k)}$	channel matrix of path l at the kth ARQ round
$\mathbf{H}_{l'}^{\mathrm{CCI}^{(k)}}$	channel matrix of path l at the kth ARQ round corresponding to the link between the co-channel interferer transmitter and the receiver
$\mathbf{H}_l^{(\mathrm{AB})}$	channel matrix of path l corresponding to the A $\rightarrow$ B link
$h_{r,t,l}^{(k)}$	fading channel connecting the tth transmit and the rth receive antennas of path l at the kth ARQ round
$\underline{\boldsymbol{\mathcal{H}}}^{(k)}$	block circulant matrix of the virtual MIMO channel after k ARQ round
$\underline{\mathbf{H}}_l^{(k)}$	channel matrix of lth tap of the virtual MIMO channel after k ARQ round
$\mathbf{I}_N$	the $N \times N$ identity matrix
i	channel use index
j	index of transmitted symbol in CDMA systems
L	number of taps
L_{AB}	number of taps corresponding to the A $\rightarrow$ B link
L'	number of taps in the MIMO link between the interferer transmitter and the receiver
l	MIMO tap index
l'	tap index of the MIMO link between the interferer transmitter and the receiver
l_{AB}	normalized distance between terminal A and terminal B
$\mathrm{lcm}(M_1, \cdots, M_k)$	least common multiple of $M_1, \cdots, M_k$
K	ARQ delay
k	ARQ round index
$\mathcal{M}$	number of bits per symbol
M	number of transmit antennas in the point to point virtual MIMO system
M_{D}	number of the destination receive antennas
M_k	number of transmit antennas at slot k
M_{R_k}	number of the kth relay transmit and receive antennas
M_{S}	number of the source transmit antennas
N	length of Walsh code
N_{iter}	number of turbo iterations
N_k	number of virtual receive antennas in the equivalent fixed rate MIMO system
$\underline{N}_k$	number of virtual receive antennas in the point to point virtual MIMO system after k slots

N_R	number of receive antennas
N_T	number of transmit antennas
$N_T^{'}$	number of transmit antennas of the co–channel interferer
$\mathbf{n}^{(k)}$	thermal noise block vector at ARQ round k
$\mathbf{n}_i^{(k)}$	thermal noise vector at channel use i and ARQ round k
$\underline{\mathbf{n}}^{(k)}$	thermal noise present in the virtual MIMO system
n	number of turbo iteration index
R_k	kth relay terminal
$\mathbf{R}_{N_R}$	correlation matrix controlling the receive antenna arrays
$\mathbf{R}_{N_T^{'}}$	correlation matrix controlling the transmit antenna arrays
$\mathcal{R}$	transmission rate
$\mathcal{R}_k$	transmission rate at slot k
$\mathrm{rank}\,\{\mathbf{X}\}$	rank of matrix $\mathbf{X}$
r	receive antenna index
$\mathbf{r}_{t,j}^{(k)}$	tth antenna despreading module output vector at discrete time j corresponding to transmissions $1, \cdots, k$
$r_{t,j}^{(k)}$	tth antenna despreading module output at discrete time j corresponding to transmission k
$\mathcal{S}$	symbol constellation set
$\mathcal{S}_\beta^m$	set of symbols having the mth bit set to β
$\mathcal{S}_\beta^{m,t,i}$	set of symbol vectors having the mth bit in symbol $s_{t,i}$ set to $\beta \in \{0,1\}$
S	source terminal
$\mathbf{s}$	transmitted symbol vector
$\mathbf{s}_i$	transmitted symbol vector at channel use i
$\mathbf{s}_i^{(k)}$	transmitted symbol vector at channel use i and slot k
$s_{t,i}$	symbol transmitted over antenna t at channel use i
$s_{t,i}^{(k)}$	symbol transmitted over antenna t at channel use i and slot k
$s_{t,n,i}$	symbol transmitted by antenna t at channel use i and using Walsh code $\mathbf{w}_n$
$s_{t',i}^{\mathrm{CCI}^{(k)}}$	co-channel interferer transmitted symbol over antenna t at channel use i
$\mathbf{s}^{(\mathrm{CP})}$	transmitted symbol vector including cyclic-prefix word
$\tilde{\mathbf{s}}$	conditional mean of $\mathbf{s}$
$\tilde{\mathbf{s}}_{f_i}$	discrete Fourier transform $\tilde{\mathbf{s}}$ at frequency bin i
$\tilde{\mathbf{s}}_{\|t,i}$	conditional mean of $\mathbf{s}$ with zero at the $(N_T i + t)$th position
T	number of channel use
T_c	length of the chip block transmitted over each antenna in CDMA systems
T_{CP}	length of CP symbol word
$T_{CP}^{(k)}$	length of CP symbol word inserted at slot k

T_k	number of channel use at slot k
T_s	length of the symbol block transmitted over each antenna in CDMA systems
t	transmit antenna index
t'	transmit antenna index of the co–channel interferer
$\mathrm{tr}\{\mathbf{X}\}$	trace of $\mathbf{X}$
$\mathbf{U}_T$	$T \times T$ unitary matrix whose (m,n)th element is $(\mathbf{U}_T)_{m,n} = \frac{1}{\sqrt{T}} \exp\left\{-j\frac{2\pi mn}{T}\right\}$ for m, $n = 0, \cdots, T-1$, where $j = \sqrt{-1}$
$\mathbf{U}_{T,N}$	$TN \times TN$ matrix defined as $\mathbf{U}_{T,N} \triangleq \mathbf{U}_T \otimes \mathbf{I}_N$
$\mathbf{X}$	transmitted chip matrix
$\mathbf{x}_i$	transmitted chip vector at channel use i
$x_{t,i}$	transmitted chip over antenna t at channel use i
$(\mathbf{X})_{m,m}$	mth diagonal entry of matrix $\mathbf{X}$
$\mathbf{x}_f$	DFT of $\mathbf{x} \in \mathbb{C}^Q$, i.e., $\mathbf{x}_f = \mathbf{U}_Q\,\mathbf{x}$
$\mathbf{W}$	multi-code CDMA spreading matrix
$\mathbf{w}_n$	nth Walsh code
$\mathbf{w}^{(k)}$	co-channel interference plus noise single-round block vector
$\mathbf{w}_i^{(k)}$	co-channel interference plus noise single-round vector at channel use i
$\underline{\mathbf{w}}^{(k)}$	co-channel interference plus noise multi-round block vector
$\underline{\mathbf{w}}_i^{(k)}$	co-channel interference plus noise multi-round vector at channel use i
$\mathbf{y}^{(k)}$	received block vector, after the cyclic-prefix removal, at ARQ round k
$\mathbf{y}_i^{(k)}$	received signal, after the cyclic-prefix removal, at channel use i and ARQ round k
$\mathbf{y}_{f_i}^{(k)}$	discrete Fourier transformof $\mathbf{y}^{(k)}$ at frequency bin i
$\overline{\mathbf{y}}^{(k)}$	soft ISI-free received vector
$\underline{\mathbf{y}}^{(k)}$	virtual received signal block vector after k round
$\underline{\mathbf{y}}_i^{(k)}$	virtual received signal at channel use i after k round
$\underline{\tilde{\mathbf{y}}}_f^{(k)}$	recursive variable to store received signals corresponding to round $1, \cdots, k$
$\mathbf{z}_f^{(k)}$	MMSE estimate on $\mathbf{s}_f$ at ARQ round k
$z_{t,i}^{(k)}$	MMSE estimate corresponding to antenna t and channel use i at ARQ round k
$\mathbf{\Gamma}^{(k)}$	new multi-round frequency domain forward filter used in the recursive implementation algorithm
$\mathbf{\Theta}_k$	covariance of CCI plus noise $\mathbf{w}_i^{(k)}$
$\underline{\mathbf{\Theta}}_k$	covariance of CCI plus noise block vector $\mathbf{w}^{(k)}$

$\mathbf{\Theta}_k^{\mathrm{CCI}}$	CCI covariance at ARQ round $k = 1, \cdots, K$
$\boldsymbol{\theta}_{t,i}^{(k)}$	residual interference covariance matrix at the input of the demapper corresponding to transmissions $1, \cdots, k$, channel use i, and transmit antenna t
$\theta_{t,i}$	residual interference variance at the input of the demapper corresponding to channel use i, and transmit antenna t
κ	path loss exponent
$\mathbf{\Lambda}^{(k)}$	channel frequency response corresponding to round k
$\mathbf{\Lambda}_i^{(k)}$	channel frequency response corresponding to round k and channel use i
$\underline{\mathbf{\Lambda}}^{(k)}$	block diagonal matrix gathering the channel frequency responses corresponding to rounds $1, \cdots, k$
$\underline{\mathbf{\Lambda}}_i^{(k)}$	channel frequency response at channel use i corresponding to virtual MIMO channel after k ARQ round
$\lambda_m\{s\}$	operator extracting the mth bit labeling the symbol s
$\tilde{\mathbf{\Xi}}$	unconditional covariance matrix of transmitted symbols or chips
$\mathbf{\Xi}_i$	conditional covariance matrix of transmitted symbols or chips at channel use i
ρ	encoder rate
ρ_k	rank of CCI covariance at ARQ round k
$\underline{\mathbf{\Sigma}}_k$	covariance of CCI plus noise block vector $\underline{\mathbf{w}}^{(k)}$
$\mathbf{\Sigma}_k$	block diagonal matrix gathering covariance matrices corresponding to rounds $1, \cdots, k$
σ^2	thermal noise variance at the receiver side
σ_l^2	energy of tap l
$\sigma_{t,i}^2$	conditional variance of symbol $s_{t,i}$ or chip $x_{t,i}$
$\boldsymbol{\phi}_{t,i}$	vector of *a priori* LLRs of bits corresponding to symbol $s_{t,i}$
$\phi_{t,i,m,n}^{(a)}(k)$	*a-priori* LLR value corresponding to coded and interleaved bits $b_{t,i,m}$ available at iteration n of slot k
$\phi_{t,i,m,n}^{(e)}(k)$	extrinsic LLRs values corresponding to coded and interleaved bits $b_{t,i,m}$ at iteration n of slot k
$\mathbf{\Phi}^{(k)}$	frequency domain MMSE forward filter
$\underline{\mathbf{\Phi}}^{(k)}$	multi-round frequency domain MMSE forward filter
$\mathbf{\Psi}^{(k)}$	frequency domain MMSE backward filter
$\underline{\mathbf{\Psi}}^{(k)}$	multi-round frequency domain MMSE backward filter
$\mathbf{\Omega}^{(k)}$	new multi-round frequency domain backward filter used in the recursive implementation algorithm

ACK	positive acknowledgment
AF	amplify-and-forward
ARQ	automatic repeat request
BICM	bit interleaved coded modulation
BLER	block error rate
BS	base station
CAI	co-antenna interference
CCI	co-channel interference
CDMA	code division multiple access
CFR	channel frequency response
CP	cyclic prefix
CSI	channel state information
DF	decode-and-forward
DFT	discrete Fourier transform
FER	frame error rate
IBI	inter-block interference
IC	interference cancellation
ID	iterative decoding
i.i.d.	independent and identically distributed
IDFT	inverse discrete Fourier transform
IEQ	integrated equalization
IR	incremental redundancy
ISI	inter-symbol interference
LLR	Log-Likelihood Ratio
MAP	maximum a posteriori
MFB	matched filter bound
MIMO	multiple-input–multiple-output
ML	maximum likelihood
MMSE	minimum mean square error
MRC	maximum ratio combining
MUD	multi-user detection
MUI	multi-user interference
NACK	negative acknowledgment
OFDM	orthogonal frequency division multiplexing
SC	single carrier
SDMA	space division multiple access
SISO	soft-input–soft-output
SIR	signal-to-interference ratio
SNR	signal-to-noise ratio
ST	space-time
STC	space–time code
ZF	zero forcing

Contents

Acknowledgments **i**

Abstract **iii**

Résumé **v**

List of Notations and Acronyms **vii**

Contents **xiii**

List of Figures **xvii**

List of Tables **xix**

1 Introduction **21**
1.1 Motivation and Background 21
1.2 Thesis Objective 22
1.3 Thesis Outline 23

2 Iterative Turbo Packet Combining for Single Carrier MIMO ARQ System **25**
2.1 Introduction 25
2.2 Background and System Model 27
2.2.1 SC–MIMO ARQ Transmission Scheme 27
2.2.2 Turbo Receiver with No Packet Combining for Single-Carrier Multi-Antenna ARQ Systems 29
2.3 Packet Combining scheme for SC-MIMO ARQ Systems 32
2.3.1 Soft MMSE-Based Turbo Combining 32
2.3.2 Complexity Issues 34
2.4 An Optimized Signal-Level Combining Strategy 34
2.4.1 Recursive Combining Strategy 35
2.4.2 Adaptive Combining Strategy 36

2.5 Computational Complexity and Memory Requirements 36
2.6 Numerical Results 38
2.6.1 Simulation Settings 38
2.6.2 Analysis 39
2.7 Conclusions 41

3 Turbo Packet Combining for Broadband Space–Time BICM Hybrid–ARQ Systems with Co–Channel Interference 43
3.1 Introduction 43
3.2 ARQ System Model 44
3.2.1 Communication Model in the Presence of CCI 44
3.2.2 Single-Round Communication Model 46
3.2.3 Multi-Round Communication Model 47
3.3 Frequency Domain Packet Combining in the Presence of CCI 48
3.3.1 General Description 48
3.3.2 Properties of CCI plus Noise Covariance 48
3.3.3 Proposed Combining Scheme 50
3.4 Peformance Evaluation 51
3.4.1 Asymptotic Performance Analysis 51
3.4.2 Numerical Results 53
3.5 Conclusions 56

4 Frequency Domain HARQ Chase Combining for Broadband MIMO CDMA Systems 59
4.1 Introduction 59
4.2 System Description 60
4.2.1 Multi-Code CP-CDMA MIMO ARQ Transmission Scheme 60
4.2.2 Communication Model 61
4.3 Iterative Receivers for Multi-Antenna Multi-Code CP-CDMA ARQ 63
4.3.1 Chip-Level Turbo Packet Combining 63
4.3.2 Symbol-Level Turbo Packet Combining 66
4.4 Complexity and Performance Analysis 67
4.4.1 Complexity Evaluation 67
4.4.2 Performance Evaluation 68
4.5 Conclusions 71

5 Turbo Packet Combining for Relaying Schemes over Multi-Antenna Broadband Channels 73
5.1 Introduction . . . 73
5.2 Relay System model . . . 75
5.2.1 Multi-Relay Transmission Scheme . . . 75
5.2.1.1 Decode-and-Forward Relaying . . . 77
5.2.1.2 Amplify-and-Forward Relaying . . . 79
5.2.2 Multi-Slot Block Communication Model . . . 81
5.3 Frequency Domain Turbo Packet Combining and Outage Analysis . . . 82
5.3.1 Iterative Receiver Scheme . . . 82
5.3.2 Outage Probability . . . 84
5.3.3 Outage Analysis . . . 85
5.4 MMSE-based Frequency Domain Turbo Packet Combining . . . 88
5.5 Performance Evaluation . . . 89
5.5.1 Simulation Settings . . . 89
5.5.2 Analysis . . . 89
5.6 Conclusion . . . 92

6 Conclusions 95
6.1 Summary of Contributions . . . 95
6.2 Future Research Directions . . . 96

A Proof of Theorem 1 99

B DF Schemes Outage Expressions 101

Bibliography 103

Publications List 111

List of Figures

2.1 Cyclic prefix single carrier ARQ communication scheme with k transmissions over k independent broadband MIMO channels. 29
2.2 SC-MIMO ARQ receiver at kth transmission with no packet combining. . . 32
2.3 SC-MIMO ARQ receiver at kth transmission with conventional signal-level combining. 34
2.4 SC-MIMO ARQ receiver at kth transmission with recursive combining strategy. 36
2.5 BLER performance for CC $(35, 23)_8$, QPSK, $N_T = 2$, $N_R = 2$, $L = 10$ equal power taps profile. 40
2.6 BLER performance for CC $(35, 23)_8$, QPSK, $N_T = 4$, $N_R = 2$, $L = 10$ equal power taps profile. 40
2.7 Throughput performance for CC $(35, 23)_8$, QPSK, $N_T = 3$, $N_R = 1$, $L = 10$ equal power taps profile, spectrum efficiency=3bit/channel use. 41

3.1 SC–MIMO ARQ communication scheme in the presence of CCI at ARQ round k. 45
3.2 Block diagram of the turbo combining receiver scheme at ARQ round k . . 49
3.3 BLER performance for CC $(35, 23)_8$, QPSK, $N_T = N_R = 2$, $L = L' = 2$ equal energy paths, and SIR = 3dB. 54
3.4 BLER performance for CC $(35, 23)_8$, QPSK, $N_T = N_R = 2$, $L = L' = 2$ equal energy paths, and SIR = 5dB. 55
3.5 BLER performance for CC $(35, 23)_8$, QPSK, $N_T = 4$, $N_R = 2$, $L = L' = 2$ equal energy paths, and SIR = 5dB. 56
3.6 BLER performance for CC $(35, 23)_8$, QPSK, $N_T = N_R = 2$, $L = 2$ equal energy paths, $N'_T = 1$, $L' = 1$, and $\rho_k = 1$, $k = 1, \cdots, K$, SIR = 3dB. 57
3.7 BLER performance for CC $(35, 23)_8$, QPSK, $N_T = N_R = 4$, $L = 2$ equal energy paths, and SIR = 1dB. Scenario 1: $N'_T = 4$, $L' = 4$, Scenario 2: $N'_T = 2$, $L' = 1$, and $\rho_k = 2$, $k = 1, \cdots, K$. 58

4.1 Multi-antenna multi-code Cyclic-prefix-CDMA transmitter with ARQ. . . . 62

4.2 Multi-antenna multi-code CP-CDMA receiver at kth transmission with chip-level packet combining and frequency domain MMSE-based turbo equalization 65
4.3 Multi-antenna multi-code CP-CDMA receiver at kth transmission with symbol-level packet combining and frequency domain MMSE-based turbo equalization. 67
4.4 BLER performance with $N_T = 2$, $N_R = 2$, $C = 16$, $L = 10$ equal power taps profile, spectrum efficiency = 32bits/channel use. 69
4.5 BLER performance with $N_T = 4$, $N_R = 4$, $C = 16$, $L = 10$ equal power taps profile, spectrum efficiency = 64bits/channel use. 70
4.6 BLER performance with $N_T = 2$, $N_R = 1$, $C = 16$, $L = 10$ equal power taps profile, spectrum efficiency = 32bits/channel use. 71
4.7 Throughput performance with $N_T = 2$, $N_R = 2$, $L = 10$ equal power taps profile. 72
4.8 Throughput performance with $N_T = 2$, $N_R = 1$, $L = 10$ equal power taps profile. 72

5.1 Block diagram of the considered multi-relay assisted systems. 76
5.2 The equivalent ST–BICM diagram for multi-rate multi-relay systems. . . . 81
5.3 The block diagram of the turbo packet combining receiver scheme at slot k. 83
5.4 Outage probability versus l_{SR} for $M_{\mathrm{S}} = M_{\mathrm{R}} = M_{\mathrm{D}} = 2$, $K = 2$, $L = 3$, and the path loss exponent $\kappa = 3$. 86
5.5 Outage probability versus $\mathrm{SNR}_{\mathrm{SD}}$ for $M_{\mathrm{S}} = M_{\mathrm{R}} = M_{\mathrm{D}} = 2$, $l_{SR} = 0.5$, $L = 3$, and the path loss exponent $\kappa = 3$. 86
5.6 Outage probability versus $\mathrm{SNR}_{\mathrm{SD}}$ for $M_{\mathrm{S}} = M_{\mathrm{R}} = 2$, $M_{\mathrm{D}} = 1$, $l_{SR} = 0.5$, $L = 3$, and the path loss exponent $\kappa = 3$. 87
5.7 BLER performance for CC $(35, 23)_8$, QPSK, $M_{\mathrm{S}} = M_{\mathrm{R}} = M_{\mathrm{D}} = 2$, $K = 3$, $L = 3$ equal energy paths, and the path loss exponent $\kappa = 3$. 90
5.8 AF relaying scheme BLER performance for CC $(35, 23)_8$, QPSK, $L = 3$ equal energy paths, $l_{SR} = 0.7$, and the path loss exponent $\kappa = 3$. 91
5.9 Selective DF relaying scheme BLER performance for CC $(35, 23)_8$, QPSK, $L = 3$ equal energy paths, $l_{SR} = 0.3$, and the path loss exponent $\kappa = 3$. . . 93
5.10 ACK/NACK DF relaying scheme BLER performance for CC $(35, 23)_8$, QPSK, $M_{\mathrm{S}} = 4$, $M_{\mathrm{R}} = M_{\mathrm{D}} = 2$, $L = 3$ equal energy paths, $l_{SR} = 0.3$ and the path loss exponent $\kappa = 3$. 94
5.11 ACK/NACK DF relaying scheme BLER performance for CC $(35, 23)_8$, QPSK, $M_{\mathrm{S}} = 4$, $M_{\mathrm{R}} = 2$, $M_{\mathrm{D}} = 1$, $L = 3$ equal energy paths, $l_{SR} = 0.3$ and the path loss exponent $\kappa = 3$. 94

List of Tables

2.1 Adaptive Turbo Packet Combining 37
2.2 Summary of Memory and Arithmetic Additions Required by the Proposed and LLR-Level Combining Schemes when $kN_R > N_T$ 38

4.1 Summary Of The Chip-Level Turbo Combining Algorithm 65
4.2 Summary Of The Symbol-Level Turbo Combining Algorithm 67
4.3 Summary of the Maximum Number of Arithmetic Additions, and Memory Size . . 68

Chapter 1

Introduction

1.1 Motivation and Background

Space–time (ST) multiplexing oriented multiple–input–multiple–output (MIMO) and hybrid–automatic repeat request (ARQ) protocols play a key role in the evolution of current wireless systems toward high data rate wireless broadband standards [1]. While ST multiplexing architectures allow the space and time diversities of the multi–antenna channel to be translated into diversity and/or multiplexing gains [2, 3], hybrid–ARQ mechanisms exploit the ARQ delay, i.e., the maximum number of ARQ transmission rounds, to reduce the frame error rate (FER) and therefore increase the system throughput [4, 5]. Depending on the retransmitted information, hybrid–ARQ can be classified into Chase–type ARQ where the data packet is entirely retransmitted, and incremental redundancy (IR) where retransmissions only carry portions of the data packet, this presents an efficient technique for increasing the system throughput while keeping the error performance acceptable. In this work, we focus on Chase–type ARQ. A comprehensive tutorial about IR–type ARQ can be found in [6].

In slow fading wireless environments, ARQ mechanisms generally have limited performance due to the long–term static dynamic of the ARQ fading channel where multiple ARQ rounds see the same channel realizations. To overcome this limitation, cooperative relay communication has been introduced [7]. It presents an efficient technique for building up a virtual short–term static ARQ channel where virtual ARQ rounds see independent channel realizations. This is achieved by using multiple relays which act as packet retransmitters. In ARQ cooperative relay communications, the source first broadcasts the information packet to the destination. In case of erroneous decoding, packet retransmission, i.e., ARQ, is performed with the aid of relays. This dramatically improves the diversity gain since the fading channels connecting the source and relays to the destination are independent. Cooperative relaying presents a potential alternative to classical ARQ and has recently received a lot of attention in the research community [8, 9].

In practical wireless MIMO systems employing single carrier (SC) transmission, the communication link suffers from inter–block interference (IBI) caused by frequency selective fading. Space–time–bit–interleaved coded modulation (ST–BICM) with iterative decoding is an attractive signaling scheme that offers high spectral efficiencies over MIMO broadband channels [10,11]. To combat IBI in SC–broadband ST–BICM transmission, frequency domain equalization, initially introduced for single antenna systems [12–15], has been proposed using iterative (turbo) processing [16]. It is a receiver scheme that allows high IBI cancellation capability at an affordable complexity cost. As with multi–carrier-based orthogonal frequency–division multiplexing (OFDM) [17,18], each transmitted block includes at its beginning a cyclic prefix (CP) long enough to cope with the maximum channel delay and therefore avoid any IBI. Zero-padding approach, also assuring IBI-free, can offer better performances than the CP approach adopted in this work but at the price of a much increased implementation cost [19].

To improve spatial diversity of MIMO transmission with ARQ, the erroneous data packets are kept in the receiver and used to detect/decode the retransmitted frame [20–25]. This technique is often referred to as *packet combining*. Recently, particular attention has been paid to the joint optimization of the packet combiner and the MIMO receiver which allows to reduce the number of transmissions required to correctly decode a packet. Symbol level packet combining using zero forcing (ZF) and minimum mean square error (MMSE) detection were investigated for a MIMO system operating over a flat fading channel [26]. Performance of hybrid ARQ techniques with iterative MMSE frequency domain equalization was evaluated for a turbo coded MIMO broadband transmission [27,28]. Signal level packet combining also known as transmission combining with integrated equalization (IEQ) was first proposed by Samra and Ding for single antenna systems operating over intersymbol interference (ISI) channels [29–32]. In particular, it was shown in [32] that, when concatenated with an outer code, IEQ performs better than the iterative combining scheme introduced by Doan and Narayanan [33]. In iterative combining, multiple copies of the same packet are independently interleaved and combining is performed by iterating between multiple equalizers before channel decoding. The IEQ concept was then extended to MIMO systems with flat fading to jointly perform co–antenna interference (CAI) cancellation and transmission combining [34, 35].

1.2 Thesis Objective

Motivated by the IEQ concept [32], we attempt to propose new low–complexity packet combining strategies for coded transmission with Chase–type ARQ operating over broadband MIMO channels. Our main objective is to reduce the number of ARQ rounds required to correctly decode a data packet while keeping the receiver complexity (computational load and memory requirements) affordable. In our design, packet combining is performed at each ARQ round by exchanging soft information in an iterative fashion between the soft

packet combiner and the soft–input–soft–output (SISO) decoder. In the proposed combining scheme, we exploit the fact that the same data packet is retransmitted at each ARQ round, i.e., Chase–type ARQ. This allows us to view each transmission as a group of virtual receive antennas, and build up a virtual MIMO channel that takes into account both multi–antenna and multi–round transmission. We also include the problem of unknown co–channel interference (CCI) caused by other transmitters (distant users and/or neighboring cells) who simultaneously use the same radio resource and analyze the asymptotic performance of the proposed combining scheme in the presence of CCI. The combining approach is then extended to broadband MIMO code division multiple access (CDMA) systems with ARQ and cooperative relay–assisted communications.

1.3 Thesis Outline

This thesis is organized as follows. In chapter 2, using *virtual antenna* concept, we introduce a new turbo combining technique for ARQ MIMO–ISI systems inspired by MMSE criterion. We focus on implementation issues and propose two optimized combining strategies. In chapter 3, we analyze the asymptotic performance of the proposed combining scheme over broadband MIMO channel with unknown CCI. The proposed turbo combining approach is then extended to CP–CDMA MIMO with Chase–type ARQ in chapter 4. A new turbo combining scheme is introduced where combining is performed at the level of the soft symbol demapper. We analyze both the implementation complexity and the performance of the proposed techniques and show that the choice of the best combining technique depends on the system configuration. In chapter 5, we focus on packet combining for multi–relay systems. We derive a communication model in such a way that the destination can see the received signals during the relaying slots as direct retransmissions from the source. We investigate the outage probability and extend the combining scheme proposed in chapter 2 to the case of cooperative multi–relay systems.

Chapter 2

Iterative Turbo Packet Combining for Single Carrier MIMO ARQ System

2.1 Introduction

ST multiplexing oriented MIMO and hybrid–ARQ are two major techniques that allow to improve the transmission rate and quality over the wireless link. While MIMO ST multiplexing schemes increase the spectrum efficiency [2], hybrid–ARQ mechanisms provide an important source of time diversity through the combination of channel coding and ARQ [36,37]. In hybrid–ARQ, erroneous data packets are saved in the receiver and used to help detect and/or decode the retransmitted frame. This is generally refereed to as *packet combining* [38]. In the literature, several packet combining strategies have been proposed. In [4], Chase has developed a maximum likelihood (ML)-based technique for combining multiple coded packets. In [38], the authors have introduced different diversity-based combining schemes for hybrid ARQ systems. Recently, particular attention has been paid to the design of packet combining algorithms for MIMO systems. In general, multi–antenna transmission techniques provide multiplexing and diversity gains. If an ARQ protocol is employed at the upper layer, retransmission of the same data packet increases the diversity gain, especially if the MIMO channel changes from one transmission to another. Moreover, the presence of ISI caused by frequency selective fading translates into additional diversity branches if an efficient equalization scheme is employed. Therefore, the maximum achievable diversity order of a multi–antenna transmission link with ARQ over a time varying MIMO–ISI fading channel is kLN_R, where k, L, and N_R are the numbers of transmissions, MIMO paths, and receive antennas, respectively.

In this chapter, we focus on efficient packet combining techniques for SC ARQ with ST–

BICM systems operating over a MIMO–ISI channel. Several contributions have confirmed the remarkable diversity gain of ST–BICM with iterative decoding over broadband multi–antenna fading channels [10, 11, 39]. Efficient low-complexity turbo equalization strategies for ST–BICM using soft interference cancellation (IC) techniques and MMSE filtering have been proposed in the last few years [40, 41]. CP-aided iterative equalization approaches relying on frequency domain processing have recently shown an attractive performance to complexity trade-off [16, 42]. In the framework of a ST–BICM transmission with ARQ and iterative decoding, the packet combining scheme has a great impact on the achievable diversity order and consequently the overall receiver performance. In the last few years, special interest has been paid to the joint design of the *packet combiner* and the signal processor receiver. The idea of merging soft equalization and transmission combining has been initially introduced in [32] for single antenna broadband systems using a *maximum a posteriori* (MAP) equalizer. Then, the principle was generalized to MIMO channels with flat fading using a sphere decoding-based scheme in order to jointly perform packet combining and signal detection [35]. Another approach, where multiple transmissions use different interleavers, and the combiner iterates over multiple equalizers before decoding the packet, was proposed in [33] for single antenna systems and is called iterative combining. In [32], the authors have shown that packet combining with integrated MAP-based equalization outperforms its iterative combining counterpart. Symbol-level transmission combining using ZF and MMSE detection techniques were investigated in [26] for MIMO flat fading channels. In this chapter, we introduce a new combining technique for ARQ MIMO-ISI systems where space-time MMSE-based turbo equalization is integrated into the packet combiner. The key idea of our receiver is to view a particular transmission k as an additional set of virtual N_R receive antennas. First, we describe the proposed MMSE-based turbo packet combiner. Then, we present a recursive implementation strategy and show that the complexity of this scheme is only cubic in terms of the number of transmit antennas and less sensitive to the number of transmission rounds. Finally, we introduce a low complexity adaptive packet combining algorithm.

The remainder of the chapter is organized as follow. In section 2.2, we introduce the system background and the MIMO ARQ communication model. We also present the architecture of a space-time turbo receiver with no packet combiner. This receiver will be used as a reference to evaluate the proposed packet combining approach in term of implementation cost. In section 2.3, we detail the proposed combining approach then focus on complexity issues. In section 2.4, we propose two optimized combining strategies adapted to the system configuration. Section 2.5 focuses on implementation cost of the proposed combining strategy. Numerical results are provided in section 2.6. The chapter is concluded is section 2.7.

2.2 Background and System Model

2.2.1 SC–MIMO ARQ Transmission Scheme

We consider a multi-antenna link operating over a frequency selective fading channel and using an ARQ protocol at the upper layer. The broadband MIMO channel is composed of L taps (index $l = 0, \cdots, L-1$). The transmitter and the receiver are equipped with N_T transmit (index $t = 1, \cdots, N_T$) and N_R receive (index $r = 1, \cdots, N_R$) antennas, respectively. Transmission of an information block includes channel coding using a rate-ρ encoder, interleaving with the aid of a semi-random interleaver Π, then bit to symbol mapping, and spatial multiplexing over N_T transmit antennas. This presents a typical ST–BICM scheme. The choice of ST–BICM is due to the simplicity of this coding scheme, and the efficiency of its iterative decoding (ID) receiver in achieving high diversity and coding gains over frequency selective MIMO channels [10, 43]. This work is still valid for other space–time codes (STCs). The resulting symbol vector, at the output of the ST–BICM encoder, is given by,

$$\mathbf{s} \triangleq \left[\mathbf{s}_0^\top, \cdots, \mathbf{s}_{T-1}^\top\right]^\top \in \mathcal{S}^{N_T T}, \tag{2.1}$$

where

$$\mathbf{s}_i \triangleq \left[s_{1,i}^\top, \cdots, s_{t,i}^\top, \cdots, s_{N_T,i}^\top\right]^\top \in \mathcal{S}^{N_T} \tag{2.2}$$

is the symbol vector at channel use $i = 0, \cdots, T-1$, and $\mathcal{S}$ is the symbol constellation set. We suppose that no channel state information (CSI) is available at the transmitter and assume infinitely deep interleaving. Hence, transmitted symbols are independent and have equal transmit power, i.e.,

$$\mathbb{E}\left[s_{t,i} s_{t',i'}^\star\right] = \delta_{t-t',i-i'}. \tag{2.3}$$

Moreover, CP-aided transmission is assumed. This prevents inter-block interference and allows us to use frequency domain processing at the receiver side. Therefore, before transmission, a CP symbol word of length T_{CP} ($\geq L$) is appended to the symbol vector $\mathbf{s}$ as,

$$\mathbf{s}^{(\mathrm{CP})} \triangleq \left[\mathbf{s}_{T-1-T_{CP}}^\top, \cdots, \mathbf{s}_{T-1}^\top, \mathbf{s}_0^\top, \cdots, \mathbf{s}_{T-1}^\top\right]^\top \in \mathcal{S}^{N_T T}. \tag{2.4}$$

At the upper layer, an ARQ protocol is used to help correct erroneous frames. An acknowledgment message is generated after the decoding of each information block. Therefore, when the decoding is successful, the receiver sends back a positive acknowledgment (ACK) to the transmitter, while the feedback of a negative acknowledgment (NACK) indicates that the decoding outcome is erroneous. Let K denote the ARQ delay, and $k = 1, \cdots, K$ denote the ARQ round index. When the transmitter receives an ACK feedback, it stops the transmission of the current block and moves on to the next information block. Recep-

tion of a NACK message incurs supplementary ARQ rounds until the packet is correctly decoded or the ARQ delay K is reached. We focus on Chase-type ARQ where the retransmitted packets go through the same ST–BICM transmitter. Puncturing and diversity mapping optimization are therefore out of the scope of this work. In addition, we suppose perfect packet error detection, and assume that the one bit ACK/NACK feedback is error-free.

The MIMO channel is frequency selective and is composed of L symbol-spaced taps (index $l = 0, \cdots, L-1$). The energy of each tap l is denoted σ_l^2, and the total energy is normalized to one, i.e., $\sum_{l=0}^{L-1} \sigma_l^2 = 1$. The broadband MIMO ARQ channel is assumed to be short-term static fading, i.e., the channel independently changes from round to round. Note that this channel dynamic applies to slow ARQ protocols where the delay between two consecutive ARQ rounds is larger than the channel coherence time. Let $\mathbf{H}_0^{(k)}, \cdots, \mathbf{H}_{L-1}^{(k)} \in \mathbb{C}^{N_R \times N_T}$ denote channel matrices at the kth ARQ round, and whose entries are i.i.d zero-mean circularly symmetric Gaussian, i.e., $h_{r,t,l}^{(k)} \sim \mathcal{CN}\left(0, \sigma_l^2\right)$, where $h_{r,t,l}^{(k)}$ denotes the fading channel connecting the tth transmit and the rth receive antennas of path l at the kth ARQ round. Therefore, the channel energy at each receive antenna r is

$$\sum_{l=0}^{L-1} \sum_{t=1}^{N_T} \mathbb{E}\left[\left|h_{r,t,l}^{(k)}\right|^2\right] = N_T. \tag{2.5}$$

The channel profile, i.e., power distribution $\sigma_0^2, \cdots, \sigma_{L-1}^2$ and number of taps L, is supposed to be identical for at least K consecutive rounds. This is a reasonable assumption because the channel profile dynamic mainly depends on the shadowing effect.

At the receiver side, after the CP removal, the $N_R \times 1$ received signal at channel use i and transmission k is expressed as,

$$\mathbf{y}_i^{(k)} = \sum_{l=0}^{L-1} \mathbf{H}_l^{(k)} \mathbf{s}_{(i-l) \bmod T} + \mathbf{n}_i^{(k)}. \tag{2.6}$$

where $\mathbf{n}_i^{(k)} \sim \mathcal{N}\left(\mathbf{0}_{N_R \times 1}, \sigma^2 \mathbf{I}_{N_R}\right)$ is the thermal noise at the receiver side. The block communication model, at transmission k, can be written as,

$$\mathbf{y}^{(k)} = \boldsymbol{\mathcal{H}}^{(k)} \mathbf{s} + \mathbf{n}^{(k)}, \tag{2.7}$$

where $\mathbf{y}^{(k)} \triangleq \left[\mathbf{y}_0^{(k)^\top}, \cdots, \mathbf{y}_{T-1}^{(k)^\top}\right]^\top$, $\mathbf{n}^{(k)} = \left[\mathbf{n}_0^{(k)^\top}, \cdots, \mathbf{n}_{T-1}^{(k)^\top}\right]^\top$ and $\boldsymbol{\mathcal{H}}^{(k)} \in \mathbb{C}^{TN_R \times TN_T}$ is a block circulant matrix whose first $TN_R \times N_T$ column matrix is

$$\left[\mathbf{H}_0^{(k)^\top}, \cdots, \mathbf{H}_{L-1}^{(k)^\top}, \mathbf{0}_{N_T \times (T-L)N_R}\right]^\top. \tag{2.8}$$

The cyclic prefix ARQ communication scheme is depicted in Fig. 2.1.

Note that the block circulant matrix $\boldsymbol{\mathcal{H}}^{(k)}$ can be block diagonalized in a Fourier basis

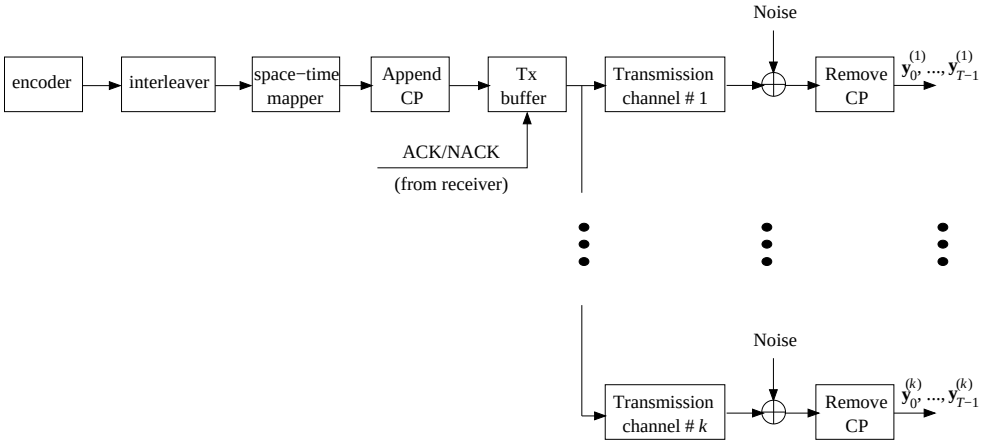

Figure 2.1: Cyclic prefix single carrier ARQ communication scheme with k transmissions over k independent broadband MIMO channels.

as

$$\boldsymbol{\mathcal{H}}^{(k)} = \mathbf{U}_{T,N_R}^{\mathrm{H}} \boldsymbol{\Lambda}^{(k)} \mathbf{U}_{T,N_T}. \tag{2.9}$$

Therefore, applying the discrete Fourier transform (DFT) to the block signal vector (5.22) yields the following frequency domain block communication model,

$$\mathbf{y}_f^{(k)} = \boldsymbol{\Lambda}^{(k)} \mathbf{s}_f + \mathbf{n}_f^{(k)}, \tag{2.10}$$

where

$$\begin{cases} \boldsymbol{\Lambda}^{(k)} \triangleq \mathrm{diag}\left\{ \boldsymbol{\Lambda}_0^{(k)}, \cdots, \boldsymbol{\Lambda}_{T-1}^{(k)} \right\}, \\ \boldsymbol{\Lambda}_i^{(k)} \triangleq \sum_{l=0}^{L-1} \mathbf{H}_l^{(k)} e^{-j(2\pi i l/T)}. \end{cases} \tag{2.11}$$

2.2.2 Turbo Receiver with No Packet Combining for Single-Carrier Multi-Antenna ARQ Systems

The conventional receiver for SC-MIMO ARQ system, presented in this subsection, makes use of ARQ principle with no packet combining at the receiver side. At transmission k, the receiver performs soft equalization and computes the extrinsic log-likelihood ratio (LLR) about coded and interleaved bits with the aid of the communication model (2.10), and the *a priori* information generated by the SISO decoder at the previous iteration. Interference cancellation is performed starting from the first iteration. In fact, this conventional receiver makes use of prior LLRs of coded and interleaved bits generated by the SISO decoder during the last iteration of previous transmission $k-1$. This idea was initially introduced in [44] in the context of single antenna coded systems with ARQ.

Let $\boldsymbol{\phi}_{t,i}$ denote the vector of *a priori* LLRs of bits corresponding to symbol $s_{t,i}$, and

available at a particular turbo iteration. Therefore,

$$\sigma_{t,i}^2 \triangleq \mathbb{E}\left[|s_{t,i}|^2 \mid \boldsymbol{\phi}_{t,i}\right] - \left\{\mathbb{E}\left[s_{t,i} \mid \boldsymbol{\phi}_{t,i}\right]\right\}^2 \tag{2.12}$$

is the conditional variance of $s_{t,i}$, and

$$\tilde{\mathbf{s}} \triangleq \mathbb{E}\left[\mathbf{s} \mid \boldsymbol{\phi}_{t,i} : \forall\,(t,i)\right] \tag{2.13}$$

is the conditional mean of $\mathbf{s}$. First, soft ISI is canceled from the received signal vector $\mathbf{y}^{(k)}$,

$$\overline{\mathbf{y}}^{(k)} = \mathbf{y}^{(k)} - \boldsymbol{\mathcal{H}}^{(k)}\tilde{\mathbf{s}}_{|t,i}, \tag{2.14}$$

where $\tilde{\mathbf{s}}_{|t,i}$ denotes the conditional mean of $\mathbf{s}$ with zero at the $(N_T i + t)$th position. Then, the resulting soft ISI-free signal $\overline{\mathbf{y}}^{(k)}$ enters an unconditional MMSE filter $\mathbf{F}_{t,i}^{(k)}$ corresponding to antenna t and channel use i at transmission k. This yields a statistic $z_{t,i}^{(k)}$ obtained as,

$$\begin{cases} z_{t,i}^{(k)} \triangleq \mathbf{F}_{t,i}^{(k)}\,\overline{\mathbf{y}}^{(k)}, \\ \mathbf{F}_{t,i}^{(k)} = \mathbf{e}_{t,i}^{\mathrm{H}}\boldsymbol{\mathcal{H}}^{(k)^{\mathrm{H}}}\mathbf{A}^{(k)^{-1}}, \\ \mathbf{A}^{(k)} \triangleq \sigma^2\mathbf{I}_{TN_R} + \boldsymbol{\mathcal{H}}^{(k)}\boldsymbol{\Theta}\boldsymbol{\mathcal{H}}^{(k)^{\mathrm{H}}}, \end{cases} \tag{2.15}$$

where $\mathbf{e}_{t,i}$ denotes the $(N_T i + t)$th vector of the canonical basis, and $\boldsymbol{\Theta} = \mathbf{I}_T \otimes \tilde{\boldsymbol{\Xi}}$, where $\tilde{\boldsymbol{\Xi}}$ is the time average of matrices

$$\boldsymbol{\Xi}_i \triangleq \mathrm{diag}\left\{\sigma_{1,i}^2, \cdots, \sigma_{N_T,i}^2\right\}. \tag{2.16}$$

Note that for transmission $k > 1$, extrinsic information produced during the last iteration of the previous transmission is used in the first iteration to perform soft interference cancellation.

By invoking (2.9) and (2.11), the $TN_R \times TN_R$ matrix $\mathbf{A}^{(k)}$ can be written as,

$$\mathbf{A}^{(k)} = \mathbf{U}_{T,N_R}^{\mathrm{H}}\mathbf{B}^{(k)}\mathbf{U}_{T,N_R}, \tag{2.17}$$

where

$$\begin{cases} \mathbf{B}^{(k)} = \mathrm{diag}\left\{\mathbf{B}_0^{(k)}, \cdots, \mathbf{B}_{T-1}^{(k)}\right\}, \\ \mathbf{B}_i^{(k)} \triangleq \sigma^2\mathbf{I}_{N_R} + \boldsymbol{\Lambda}_i^{(k)}\tilde{\boldsymbol{\Xi}}\boldsymbol{\Lambda}_i^{(k)^{\mathrm{H}}}. \end{cases} \tag{2.18}$$

Soft ISI cancellation and MMSE filtering can then be implemented in the frequency domain using the following forward and backward filtering structure as [16],

$$\mathbf{z}_f^{(k)} = \boldsymbol{\Phi}^{(k)}\mathbf{y}_f^{(k)} - \boldsymbol{\Psi}^{(k)}\tilde{\mathbf{s}}_f, \tag{2.19}$$

where $\mathbf{z}_f^{(k)}$ is the MMSE estimate on $\mathbf{s}_f$ at transmission k, $\tilde{\mathbf{s}}_f \in \mathbb{C}^{N_T T}$ denotes the DFT of $\tilde{\mathbf{s}}$, $\boldsymbol{\Phi}^{(k)} = \mathrm{diag}\left\{\boldsymbol{\Phi}_0^{(k)}, \cdots, \boldsymbol{\Phi}_{T-1}^{(k)}\right\}$ is the forward filter given by,

$$\mathbf{\Phi}_i^{(k)} \triangleq \mathbf{\Lambda}_i^{(k)^{\mathrm{H}}} \mathbf{B}_i^{(k)^{-1}}, \tag{2.20}$$

and $\mathbf{\Psi}^{(k)} = \mathrm{diag}\left\{\mathbf{\Psi}_0^{(k)}, \cdots, \mathbf{\Psi}_{T-1}^{(k)}\right\}$ is the backward filter given by,

$$\begin{cases} \mathbf{\Psi}_i^{(k)} \triangleq \mathbf{\Phi}_i^{(k)} \mathbf{\Lambda}_i^{(k)} - \mathbf{\Upsilon}^{(k)}, \\ \mathbf{\Upsilon}^{(k)} = \frac{1}{T} \sum_{i=0}^{T-1} \mathbf{\Phi}_i^{(k)} \mathbf{\Lambda}_i^{(k)}. \end{cases} \tag{2.21}$$

After computing (4.16), the inverse DFT (IDFT) is then applied to $\mathbf{z}_f^{(k)}$ to obtain the time domain equalized vector,

$$\mathbf{z}^{(k)} = \mathbf{U}_{T,N_T}^{\mathrm{H}} \mathbf{z}_f^{(k)}. \tag{2.22}$$

the MMSE estimate $z_{t,i}^{(k)}$ corresponding to antenna t and channel use i at transmission k can be simply extracted from $\mathbf{z}^{(k)}$ as

$$z_{t,i}^{(k)} = \mathbf{e}_{t,i}^{\mathrm{H}} \mathbf{z}^{(k)}. \tag{2.23}$$

The extrinsic LLRs values $\phi_{t,i,m,n}^{(e)}(k)$ corresponding to coded and interleaved bits $b_{t,i,m}$ at iteration n of round k are then produced by the demapper using the following expression,

$$\phi_{t,i,m,n}^{(e)}(k) = \log \frac{\sum_{s \in \mathcal{S}_1^m} \exp\left\{ -\frac{\left| z_{t,i}^{(k)} - g_{t,i} s \right|^2}{\theta_{t,i}^2} + \sum_{m' \neq m} \phi_{t,i,m',n}^{(a)}(k) \lambda_{m'}\{s\} \right\}}{\sum_{s \in \mathcal{S}_0^m} \exp\left\{ -\frac{\left| z_{t,i}^{(k)} - g_{t,i} s \right|^2}{\theta_{t,i}^2} + \sum_{m' \neq m} \phi_{t,i,m',n}^{(a)}(k) \lambda_{m'}\{s\} \right\}}, \tag{2.24}$$

where $g_{t,i}$ and $\theta_{t,i}$ denote, respectively, the equivalent channel gain at the equalizer output and the residual interference variance corresponding to channel use i, and transmit antenna t. $\phi_{t,i,m,n}^{(a)}(k)$ denotes the *a priori* LLR of coded bit $b_{t,i,m}$ available at the input of the demapper at iteration n of round k. $\mathcal{S}_\beta^m$ is the set of symbols having the mth bit set to β, i.e., $\mathcal{S}_\beta^m = \{s : \lambda_m\{s\} = \beta\}$. The calculated extrinsic LLRs are then desinterleaved and fed back to the SISO decoder. The block diagram of the conventional receiver at ARQ round k is depicted in Fig. 2.2.

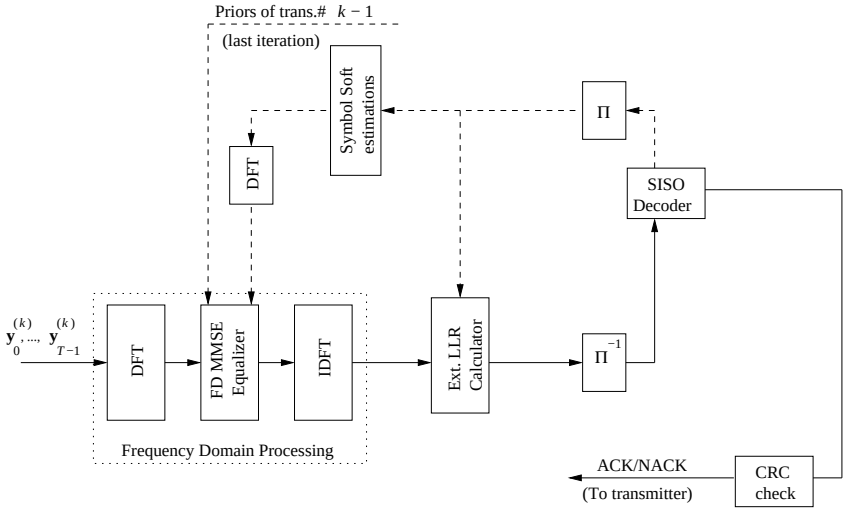

Figure 2.2: SC-MIMO ARQ receiver at kth transmission with no packet combining.

2.3 Packet Combining scheme for SC-MIMO ARQ Systems

In this section, we introduce MMSE-based packet combining strategy for SC-MIMO ARQ systems. First, we describe the proposed turbo packet combining strategy using the MMSE criterion. Then, we focus on complexity issues.

2.3.1 Soft MMSE-Based Turbo Combining

Let us suppose that, at round k, all received signals and channel matrices corresponding to previous rounds $k-1, \cdots, 1$ are available at the receiver side. To exploit the diversities available in received signals $\mathbf{y}_0^{(1)}, \cdots, \mathbf{y}_{T-1}^{(k)}$, we view each ARQ round k as an additional set of virtual N_R receive antennas. The MIMO ARQ system can therefore be considered as a point-to-point MIMO link with N_T transmit and kN_R receive antennas, where the $TkN_R \times 1$ virtual received signal vector $\underline{\mathbf{y}}^{(k)}$ is constructed as,

$$\underline{\mathbf{y}}^{(k)} \triangleq \left[\underline{\mathbf{y}}_0^{(k)^\top}, \cdots, \underline{\mathbf{y}}_{T-1}^{(k)^\top}\right]^\top \in \mathbb{C}^{kN_RT}, \tag{2.25}$$

with

$$\underline{\mathbf{y}}_i^{(k)} \triangleq \left[\ \mathbf{y}_i^{(1)^\top}, \cdots, \mathbf{y}_i^{(k)^\top}\ \right]^\top \in \mathbb{C}^{kN_R}, \tag{2.26}$$

is the virtual received signal at channel use i. The frequency domain communication model after k rounds is then given as,

$$\underline{\mathbf{y}}^{(k)} = \underline{\boldsymbol{\mathcal{H}}}^{(k)}\mathbf{s} + \underline{\mathbf{n}}^{(k)}, \tag{2.27}$$

where the vector

$$\underline{\mathbf{n}}^{(k)} = \left[\mathbf{n}_0^{(1)^\top}, \cdots, \mathbf{n}_0^{(k)^\top}, \cdots, \mathbf{n}_{T-1}^{(1)^\top}, \cdots, \mathbf{n}_{T-1}^{(k)^\top}\right]^\top \tag{2.28}$$

denotes the thermal noise present in the virtual MIMO system and $\underline{\boldsymbol{\mathcal{H}}}^{(k)} \in \mathbb{C}^{kN_RT \times N_TT}$ is a block circulant matrix whose first $kN_RT \times N_T$ block column matrix is

$$\left[\underline{\mathbf{H}}_0^{(\mathrm{k})^\top}, \cdots, \underline{\mathbf{H}}_{L-1}^{(\mathrm{k})^\top}, \mathbf{0}_{N_T \times (T-L)kN_R}\right]^\top, \tag{2.29}$$

with

$$\underline{\mathbf{H}}_l^{(k)} \triangleq \begin{bmatrix} \mathbf{H}_l^{(1)} \\ \vdots \\ \mathbf{H}_l^{(k)} \end{bmatrix} \in \mathbb{C}^{kN_R \times N_T} \tag{2.30}$$

correspond to the lth tap of the virtual MIMO channel. Applying the DFT $\mathbf{U}_{T,kN_R}$ to the block signal vector (2.27) yields the following frequency domain block communication model,

$$\underline{\mathbf{y}}_f^{(k)} = \underline{\boldsymbol{\Lambda}}^{(k)}\mathbf{s}_f + \underline{\mathbf{n}}_f^{(k)}, \tag{2.31}$$

where $\underline{\boldsymbol{\Lambda}}^{(k)} \triangleq \mathrm{diag}\left\{\underline{\boldsymbol{\Lambda}}_0^{(k)}, \cdots, \underline{\boldsymbol{\Lambda}}_{T-1}^{(k)}\right\} \in \mathbb{C}^{kN_RT \times N_TT}$ is the matrix gathering the channel frequency responses (CFRs) corresponding to all rounds with

$$\underline{\boldsymbol{\Lambda}}_i^{(k)} \triangleq \begin{bmatrix} \boldsymbol{\Lambda}_i^{(1)} \\ \vdots \\ \boldsymbol{\Lambda}_i^{(k)} \end{bmatrix} \in \mathbb{C}^{kN_R \times N_T}. \tag{2.32}$$

With the aid of the multi-round block communication model 2.31, soft ISI cancellation and MMSE filtering are jointly performed over all ARQ round. The MMSE estimate $\mathbf{z}_f^{(k)}$ on $\mathbf{s}_f$ at transmission k is expressed as ,

$$\mathbf{z}_f^{(k)} = \underline{\boldsymbol{\Phi}}^{(k)}\underline{\mathbf{y}}_f^{(k)} - \underline{\boldsymbol{\Psi}}^{(k)}\tilde{\mathbf{s}}_f, \tag{2.33}$$

where $\underline{\boldsymbol{\Phi}}^{(k)} = \mathrm{diag}\left\{\underline{\boldsymbol{\Phi}}_0^{(k)}, \cdots, \underline{\boldsymbol{\Phi}}_{T-1}^{(k)}\right\}$ is the multi-round forward filter given by,

$$\begin{cases} \underline{\boldsymbol{\Phi}}_i^{(k)} \triangleq \underline{\boldsymbol{\Lambda}}_i^{(k)^{\mathrm{H}}}\underline{\mathbf{B}}_i^{(k)^{-1}}, \\ \underline{\mathbf{B}}_i^{(k)} = \sigma^2\mathbf{I}_{kN_R} + \underline{\boldsymbol{\Lambda}}_i^{(k)}\tilde{\boldsymbol{\Xi}}\underline{\boldsymbol{\Lambda}}_i^{(k)^{\mathrm{H}}}, \end{cases} \tag{2.34}$$

and $\underline{\boldsymbol{\Psi}}^{(k)} = \mathrm{diag}\left\{\underline{\boldsymbol{\Psi}}_0^{(k)}, \cdots, \underline{\boldsymbol{\Psi}}_{T-1}^{(k)}\right\}$ is the multi-round backward filter given by,

$$\begin{cases} \underline{\boldsymbol{\Psi}}_i^{(k)} \triangleq \underline{\boldsymbol{\Phi}}_i^{(k)}\underline{\boldsymbol{\Lambda}}_i^{(k)} - \underline{\boldsymbol{\Upsilon}}^{(k)}, \\ \underline{\boldsymbol{\Upsilon}}^{(k)} = \frac{1}{T}\sum_{i=0}^{T-1}\underline{\boldsymbol{\Phi}}_i^{(k)}\underline{\boldsymbol{\Lambda}}_i^{(k)}. \end{cases} \tag{2.35}$$

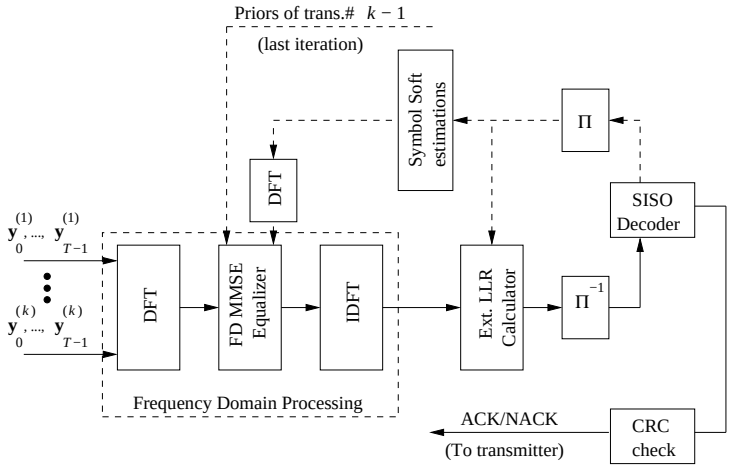

Figure 2.3: SC-MIMO ARQ receiver at kth transmission with conventional signal-level combining.

The IDFT $\mathbf{U}_{T,N_T}^{\mathrm{H}}$ is then applied to $\mathbf{z}_f^{(k)}$ to obtain the time domain equalized vector. the extrinsic LLR values $\phi_{t,i,m}^{(e)}$ are computed similarly to (2.24). The output of the demapper is then desinterleaved and fed to the SISO decoder. The block diagram of the proposed receiver at ARQ round k is depicted in Fig. 2.3. In the following, we call this combining scheme ***conventional signal-level combining***.

2.3.2 Complexity Issues

Note that in the conventional signal-level combining scheme, the receiver requires the computation of matrix inverses $\underline{\mathbf{B}}_0^{-1}, \cdots, \underline{\mathbf{B}}_{T-1}^{-1} \in \mathbb{C}^{kN_R \times kN_R}$ at each turbo iteration. This involves a complexity order cubic against kN_R. Furthermore, the signals received at slots $1, \cdots, k$ and their corresponding channel matrices have to be stored in the receiver. The implementation of such a combining scheme *could be feasible if the number of virtual receive antennas kN_R is less than the number of transmit antennas N_T, i.e., $kN_R \leq N_T$.* However, when $kN_R > N_T$, this approach requires a huge memory size that linearly increases with the increase in the number of retransmission rounds. It also involves a high computational complexity due to multiple inversions of large size matrices.

2.4 An Optimized Signal-Level Combining Strategy

In the following, we introduce an efficient recursive implementation strategy where both computational load and memory requirements are quite insensitive to the number of retransmission rounds. We also introduce an adaptive combining algorithm which takes advantage of both conventional and recursive combining.

2.4.1 Recursive Combining Strategy

To prevent the computation of $kN_R \times kN_R$ matrix inversions, we apply the matrix inversion lemma [45]. This allows us to express the inverse of $\underline{\mathbf{B}}_i^{-1}$ as

$$\underline{\mathbf{B}}_i^{-1} = \frac{1}{\sigma^2}\left\{\mathbf{I}_{kN_R} - \underline{\mathbf{\Lambda}}_i \mathbf{C}_i^{-1} \underline{\mathbf{\Lambda}}_i^{\mathrm{H}}\right\}, \tag{2.36}$$

where $\mathbf{C}_i = \sigma^2 \tilde{\mathbf{\Xi}}^{-1} + \underline{\mathbf{\Lambda}}_i^{\mathrm{H}} \underline{\mathbf{\Lambda}}_i \in \mathbb{C}^{N_T \times N_T}$. This reduces the implementation cost since the complexity order becomes cubic against N_T instead of kN_R. To relax the constraint put by the memory space required for storing received signals $\mathbf{y}_0^{(1)}, \cdots, \mathbf{y}_{T-1}^{(k)}$ and CFRs $\mathbf{\Lambda}_0^{(1)}, \cdots, \mathbf{\Lambda}_{T-1}^{(k)}$ corresponding to all rounds, we introduce the following frequency domain variables, $\underline{\tilde{\mathbf{y}}}_f^{(k)}$ and $\underline{\mathbf{D}}_i^{(k)}$. The first variable $\underline{\tilde{\mathbf{y}}}_f^{(k)}$ allows us to store received signals. It is calculated using the following recursion,

$$\begin{cases} \underline{\tilde{\mathbf{y}}}_f^{(k)} = \underline{\tilde{\mathbf{y}}}_f^{(k-1)} + \mathbf{\Lambda}^{(k)^{\mathrm{H}}} \mathbf{y}_f^{(k)}, \\ \underline{\tilde{\mathbf{y}}}_f^{(0)} = \mathbf{0}_{TN_T \times 1}. \end{cases} \tag{2.37}$$

The second variable $\underline{\mathbf{D}}_i^{(k)}$ is used to store CFRs. It is calculated as,

$$\begin{cases} \underline{\mathbf{D}}_i^{(k)} = \underline{\mathbf{D}}_i^{(k-1)} + \mathbf{\Lambda}_i^{(k)^{\mathrm{H}}} \mathbf{\Lambda}_i^{(k)}, \\ \underline{\mathbf{D}}_i^{(0)} = \mathbf{0}_{N_T \times N_T}. \end{cases} \tag{2.38}$$

Note that the storage requirements become linear in term of the number of transmit antennas, while they are insensitive to the number of receive antennas and the number of rounds. By using the matrix inversion lemma, we re-write the output of soft MMSE packet combiner as,

$$\mathbf{z}_f = \mathbf{\Gamma}^{(k)} \underline{\tilde{\mathbf{y}}}_f^{(k)} - \mathbf{\Omega}^{(k)} \tilde{\mathbf{s}}_f, \tag{2.39}$$

where $\mathbf{\Gamma}^{(k)} = \mathrm{diag}\left\{\mathbf{\Gamma}_0^{(k)}, \cdots, \mathbf{\Gamma}_{T-1}^{(k)}\right\} \in \mathbb{C}^{TN_T \times TN_T}$, and $\mathbf{\Omega}^{(k)} = \mathrm{diag}\left\{\mathbf{\Omega}_0^{(k)}, \cdots, \mathbf{\Omega}_{T-1}^{(k)}\right\} \in \mathbb{C}^{TN_T \times TN_T}$ denote the new multi-round forward and backward filters, respectively. They are given as

$$\begin{cases} \mathbf{\Gamma}_i^{(k)} \triangleq \frac{1}{\sigma^2}\left\{\mathbf{I}_{N_T} - \underline{\mathbf{D}}_i^{(k)} \mathbf{C}_i^{-1}\right\}, \\ \mathbf{C}_i = \sigma^2 \tilde{\mathbf{\Xi}}^{-1} + \underline{\mathbf{D}}_i^{(k)}, \end{cases} \tag{2.40}$$

$$\begin{cases} \mathbf{\Omega}_i^{(k)} \triangleq \mathbf{\Gamma}_i^{(k)} \underline{\mathbf{D}}_i^{(k)} - \mathbf{\Upsilon}, \\ \mathbf{\Upsilon} = \frac{1}{T} \sum_{i=0}^{T-1} \mathbf{\Gamma}_i^{(k)} \underline{\mathbf{D}}_i^{(k)}. \end{cases} \tag{2.41}$$

The block diagram of the proposed receiver with recursive combining strategy is depicted in Fig. 2.4.

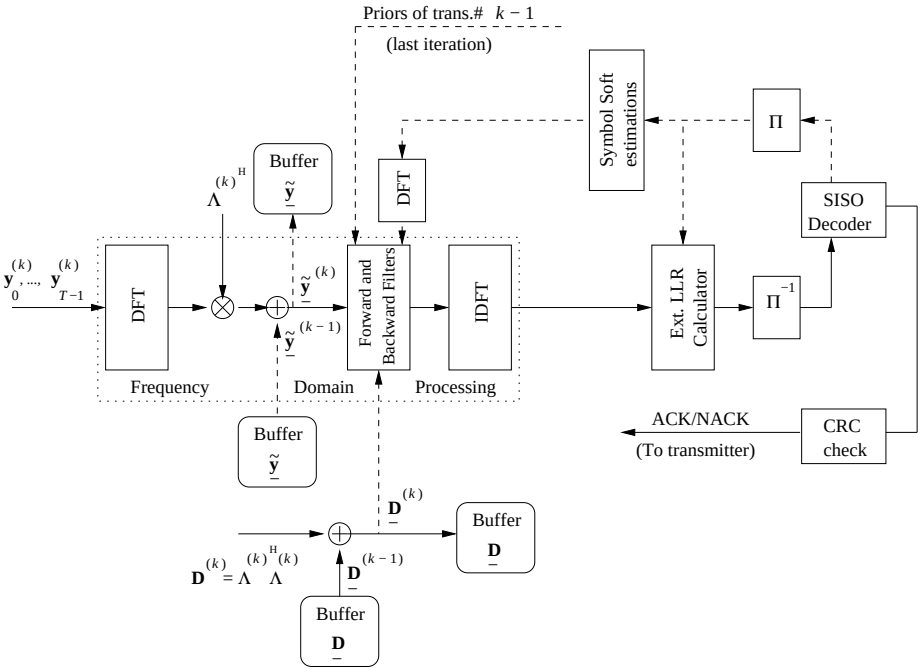

Figure 2.4: SC-MIMO ARQ receiver at kth transmission with recursive combining strategy.

2.4.2 Adaptive Combining Strategy

Note that in overloaded system configurations where the receiver has less antennas than the transmitter, i.e., $N_R < N_T$ the proposed recursive combining is not always the best solution to reduce the implementation cost. We therefore propose the following adaptive combining strategy.

The proposed adaptive combiner switches between conventional and recursive combining. Indeed, during the the first rounds when $kN_R \leq N_T$, the adaptive receiver uses conventional combining since the cost it involves for computing matrix inverses is less than that of recursive combining. In the course of retransmission rounds when the number of virtual receive antennas becomes greater than that of transmit antennas, i.e., $kN_R > N_T$, the receiver switches to recursive combining to reduce the computational complexity. The adaptive turbo combining algorithm is summarized in Tables 2.1.a and 2.1.b.

2.5 Computational Complexity and Memory Requirements

In the following, we analyze both the complexity and memory requirements of the proposed scheme, and compare them with those of the LLR-level combining technique [1].

[1] In this work, LLR-level combining refers to the iterative (turbo) packet combining and SISO decoding receiver, where transmissions corresponding to k ARQ rounds are separately turbo equalized using k

Table 2.1: Adaptive Turbo Packet Combining

(a) Case of $kN_R \leq N_T$

1. Construct $\underline{\mathbf{y}}_0^{(k)}, \cdots, \underline{\mathbf{y}}_{T-1}^{(k)}$ and $\underline{\mathbf{H}}_0^{(k)}, \cdots, \underline{\mathbf{H}}_{L-1}^{(k)}$ using (2.25) and (2.30), respectively.
2. Compute the DFT of the virtual received signal and the CFRs at slot k, i.e. $\underline{\mathbf{y}}_f^{(k)}$ and $\underline{\mathbf{\Lambda}}^{(k)}$, respectively.
3. For each iteration,
  3.1. Compute the forward and backward filters using (2.34) and (2.35).
  3.2. Compute the MMSE estimate of $\mathbf{s}_f$ using (2.33).
  3.3. Compute the extrinsic LLRs.
  3.4. Perform SISO decoding.
4. end **3.**
5. If "correct frame" then send "ACK" and empty the memory buffers.
Otherwise, send "NACK" and compare $(k+1)N_R$ and N_T.
If $(k+1)N_R > N_T$, compute $\tilde{\underline{\mathbf{y}}}_f^{(k)} = \underline{\mathbf{\Lambda}}^{(k)^{\mathrm{H}}} \underline{\mathbf{y}}_f^{(k)}$ and $\underline{\mathbf{D}}^{(k)} = \underline{\mathbf{\Lambda}}^{(k)^{\mathrm{H}}} \underline{\mathbf{\Lambda}}^{(k)}$, empty the memory buffers of the old setting, and replace it by $\tilde{\underline{\mathbf{y}}}_f^{(k)}$ and $\underline{\mathbf{D}}^{(k)}$.

(b) Case of $kN_R > N_T$

1. Update $\tilde{\underline{\mathbf{y}}}_f^{(k)}$ and $\underline{\mathbf{D}}^{(k)}$using recursions (2.37) and (2.38), respectively.
2. For each iteration,
  2.1. Compute the forward and backward filters using (2.40) and (2.41).
  2.2. Compute the MMSE estimate of $\mathbf{s}_f$ using (2.39).
  2.3. Compute the extrinsic LLRs.
  2.4. Perform SISO decoding.
3. end **2.**
4. If "correct frame" then send "ACK" and empty the memory buffers.
Otherwise, send "NACK".

LLR-level packet combining performs the combination of extrinsic LLR values generated by frequency domain soft equalizers at multiple ARQ rounds. Therefore, a storage capacity of $TN_T \log_2 |\mathcal{S}|$ real values is required to store accumulated LLR values corresponding to all ARQ rounds. In the proposed conventional signal-level combining, a storage capacity of $2TkN_R\,(kN_R + 1)$ real values is required to store both received signals and CFRs corresponding to all rounds. While in recursive combining, multiple transmissions at the signal level are combined using signals and CFRs corresponding to all ARQ rounds, without being required to be explicitly stored in the receiver. This is performed with the aid of the two variables $\underline{\mathbf{D}}^{(k)}$ and $\tilde{\underline{\mathbf{y}}}_f^{(k)}$ in recursions (2.38) and (2.37), respectively. This translates into a memory size of $2TN_T\,(N_T + 1)$ real values. Therefore, the computational complexity and storage requirements are less sensitive to the ARQ delay. In the adaptive combiner, the memory space is used by both combining schemes (i.e., by the conventional scheme when $kN_R < N_T$ and the recursive scheme when $kN_R > N_T$). We therefore choose a fixed memory space of size $2TN_T\,(N_T + 1)$ that suits both schemes.

For overloaded configurations where $kN_R < N_T$, our proposed combining strategy

frequency domain MMSE soft equalizers. To perform packet combining at each iteration of ARQ round k, extrinsic LLR values generated by the soft MMSE equalizer at round k and those obtained at the last iteration of previous rounds $1, \cdots, k-1$ are added together, then SISO decoding is performed.

is mainly limited by the computation of multi-round MMSE filters in (2.34) and (2.35). This involves T inversions of $kN_R \times kN_R$ matrices at each transmission k. While LLR-level combining involves only T inversions of $N_R \times N_R$ matrices at each transmission k. Therefore, transmission combining using integrated equalization is consequently cubic in k, while the LLR-level combining approach is only linear in the number of transmissions. This complexity impairment is motivated in the simulation section by the dramatic diversity order the proposed combining approach can achieve.

For system configurations where $kN_R > N_T$, the implementation of both combining schemes, i.e., LLR-level combining and proposed recursive combining, in the conventional receiver involves similar computational complexities. In fact, both schemes requires T inversions of $N_T \times N_T$ matrices to perform frequency domain MMSE equalization at each ARQ round. The only difference comes from number of arithmetic additions needed to perform packet combining. Let N_{it} denote the number of turbo iterations at each ARQ round. In the case of proposed combining scheme at most $C^{+}_{new\,scheme} = 2TN_T\left(K-1\right)\left(N_T+1\right)$ arithmetic additions is required to update (2.37) and (2.38), while $C^{+}_{LLR-level} = TN_TN_{it}\left(K-1\right)\log_2\left|\mathcal{S}\right|$ arithmetic additions are required to combine LLRs corresponding to multiple rounds. Note that the LLR-level combining is mainly limited by the number of iteration. In fact, the packet combining is performed at each iteration in LLR-level combining while it is performed only one time during the first iteration in the proposed combining. Table 2.2 summarizes implementation requirements for system configurations where $kN_R > N_T$.

Table 2.2: Summary of Memory and Arithmetic Additions Required by the Proposed and LLR-Level Combining Schemes when $kN_R > N_T$

Combining scheme	**Memory**	**Arithmetic Additions**
LLR-Level	$TN_T\log_2\left\|\mathcal{S}\right\|$	$TN_TN_{it}\left(K-1\right)\log_2\left\|\mathcal{S}\right\|$
Proposed	$2TN_T\left(N_T+1\right)$	$2TN_T\left(K-1\right)\left(N_T+1\right)$

2.6 Numerical Results

In this section, we provide simulated block error rate (BLER) and throughput performance for the proposed turbo packet combining strategy. Considering some representative MIMO configurations, our main focus is to demonstrate that the signal-level turbo combining approach has better ISI cancellation capability and diversity gain than the LLR-level combining.

2.6.1 Simulation Settings

In all simulations, we consider an ST-BICM scheme with QPSK modulation, 16 state convolutional encoder with polynomial generators $(35, 23)_8$. The length of the coded frame

is 1032 bits including tails. The MIMO channel has $L = 10$ paths with equally distributed power. The CP length is $T_{CP} = 10$. For SISO decoding, we use the max-log-MAP version of the MAP decoding algorithm [46]. The iterative receiver runs three turbo iterations for each transmission. The E_b/N_0 ratio appearing in all figures is the signal-to-noise ratio (SNR) per useful bit per receive antenna per ARQ round.

Note that the benefits of an ARQ mechanism appear in the region of low to moderate SNR, where multiple transmissions are required to help correct packets erroneously received after the first round. For high SNR values, ARQ may not be needed because most packets are correct after the first transmission. Therefore, we focus our analysis on the SNR region where BLER values, after the first round, are between 1 and 10^{-1}. In this region, an ARQ protocol is essential to have reliable communication. Our main goal is to analyze the ISI cancellation capability and the achieved diversity order for the proposed turbo combining scheme. We, therefore, evaluate the BLER performance per ARQ round. We also evaluate the proposed receiver in term of the throughput performance. Following [47], we define the throughput as $\eta = \frac{\mathbb{E}[\mathcal{R}]}{\mathbb{E}[\mathcal{K}]}$, where $\mathcal{R}$ is a random variable (RV) that takes R when the packet is correctly received or zero when the packet is erroneous after K ARQ rounds. $\mathcal{K}$ is a RV that denotes the number of rounds used for transmitting one data packet. We use Monte Carlo simulations for evaluating η. We compare the resulting performance with LLR-level combining and matched filter bound (MFB). The MFB curves are obtained for each transmission assuming perfect ISI cancellation and maximum ratio combining (MRC) of all time, space, multipath, and delay diversity branches.

2.6.2 Analysis

First, we consider a balanced configuration where the transmitter and the receiver have the same number of antennas, i.e., $N_T = N_R = 2$. For this configuration, the implementation of the proposed combining scheme in the conventional receiver requires a memory capacity 3 times greater than the memory capacity required by LLR-level combining. However, both combining schemes have the same computational complexity, i.e., $12T(K-1)$ arithmetic additions. Fig. 2.5 compares the BLER performance for the studied combining schemes with the MFB. For the proposed combining, the performance improvement after the second ARQ round is very significant compared with LLR-level combining. Moreover, the proposed combining approach is shown to achieve the MFB while the LLR-level combining presents approximately a gap of 1.73dB at $3 * 10^{-2}$BLER compared with the MFB. This means that signal-level combining has higher ISI cancellation capability than LLR-level combining. This result is due to the fact that in signal-level combining, each ARQ round is considered as a set of virtual N_R receive antennas. This allows the ARQ delay diversity to be efficiently exploited. In Fig. 2.6, we examine the BLER performance of an overloaded configuration where the number of transmit antennas is greater than the number of receive antennas, i.e., $N_T = 4$ and $N_R = 2$. We observe that the proposed com-

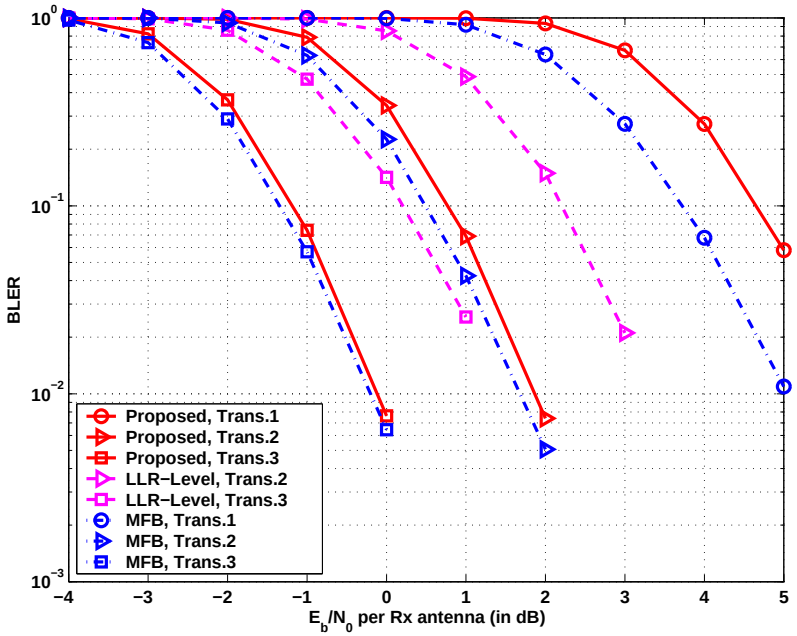

Figure 2.5: BLER performance for CC $(35, 23)_8$, QPSK, $N_T = 2$, $N_R = 2$, $L = 10$ equal power taps profile.

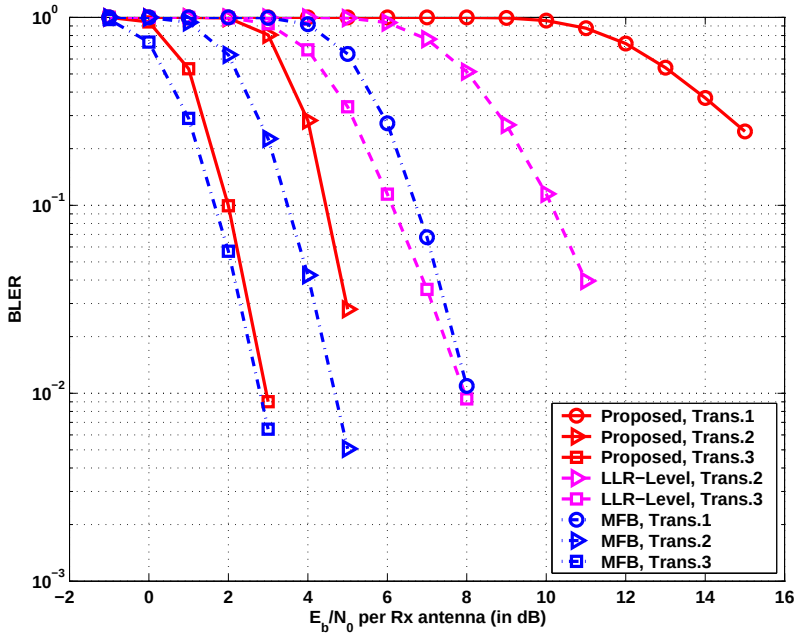

Figure 2.6: BLER performance for CC $(35, 23)_8$, QPSK, $N_T = 4$, $N_R = 2$, $L = 10$ equal power taps profile.

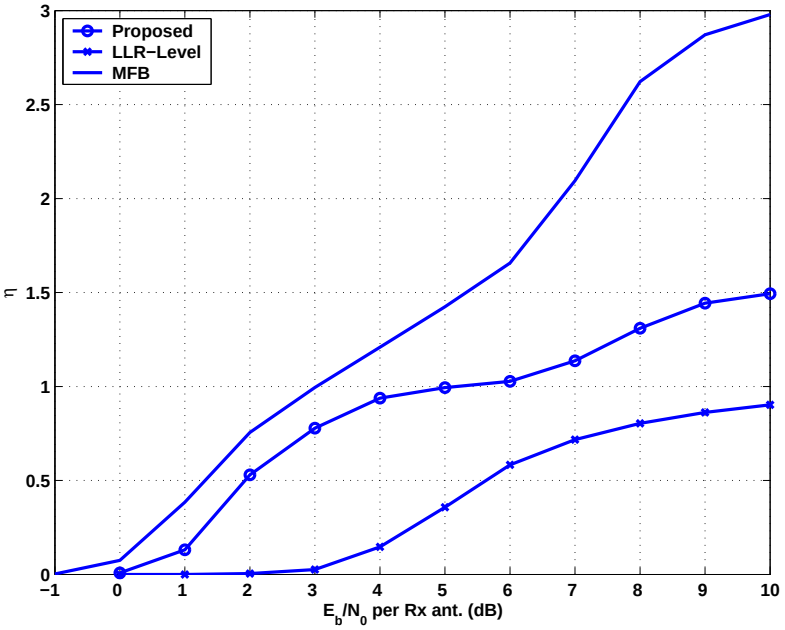

Figure 2.7: Throughput performance for CC $(35, 23)_8$, QPSK, $N_T = 3$, $N_R = 1$, $L = 10$ equal power taps profile, spectrum efficiency=3bit/channel use.

bining achieve BLER performance close to the MFB (the gap is less than 0.3dB), while the LLR-level combining has a degraded performance (the gap between the LLR-level combining and the MFB is more than 5dB at $3*10^{-2}$BLER). It is also important to note that signal-level combining manifests itself in almost achieving the diversity gain while it is shown that LLR-level combining fails to do so. This is mainly due to the fact that, at the second ARQ round, the signal-level scheme constructs a 4×4 virtual MIMO-ISI channel, while the MIMO configuration remains unbalanced in the case of LLR-level combining. In Fig. 2.7, we compare the throughput performance of the two combining scheme for an overloaded configuration where $N_T = 3$ and $N_R = 1$. The maximum number of transmissions is set to $K = 4$. It is shown that signal-level combining offers higher throughput. Also, note that while the MFB achieves the maximum throughput of 3bit/s/Hz, the proposed technique saturate around 1.5bit/s/Hz because most of the packets received in the first ARQ round are erroneous.

2.7 Conclusions

In this chapter, we considered the design of efficient turbo packet combiner for SC-MIMO ARQ systems operating over broadband channels. First, we introduced a signal-level turbo packet combiner that exploits the delay diversity to perform transmission combining. The proposed combining scheme considers an ARQ round as a set of virtual receive

antennas and performs packet combining jointly with ISI cancellation. Then, we provided an efficient recursive implementation for the proposed scheme, and showed that both its computational complexity and memory requirements are quite insensitive to the number of ARQ rounds. We also introduced an adaptive packet combining algorithm that enable to reduce the receiver implementation cost for overloaded configurations. Finally, we presented simulation results that demonstrated that signal-level combining provides better BLER and throughput performance than that of LLR-level combining.

Chapter 3

Turbo Packet Combining for Broadband Space–Time BICM Hybrid–ARQ Systems with Co–Channel Interference

3.1 Introduction

In practical systems, unknown CCI caused by other transmitters (distant users and/or neighboring cells) who simultaneously use the same radio resource can dramatically degrade the link performance. This limitation can be overcome by using the so-called hybrid–ARQ protocols, where channel coding is combined with ARQ . In [47], an elegant information-theoretic framework has been introduced to analyze the throughput and delay of hybrid–ARQ under random user behavior. Interestingly, the authors have shown that hybrid–ARQ systems are not interference limited, i.e., arbitrarily high throughput can be achieved by simply increasing the transmit power of all users even when multi-user detection (MUD) techniques are not used at the receiver. Motivated by the above considerations, we investigate turbo packet combining for SC broadband ST–BICM signaling with hybrid–ARQ operating over CCI-limited MIMO channels.

The powerful diversity–multiplexing tradeoff tool, initially introduced by Zheng and Tse for coherent delay-limited, i.e., quasi-static, MIMO channels [48], has been elegantly extended by El Gamal *et al.* to MIMO ARQ channels with flat fading, and referred to as diversity–multiplexing–delay tradeoff [49]. The authors have proved that the ARQ delay, i.e., maximum number of ARQ protocol rounds, improves the outage probabil-

ity[1] performance for large classes of MIMO ARQ channels [49]. In particular, they have demonstrated that the diversity order can be increased due to ARQ even when the MIMO ARQ channel is long-term static, i.e., the MIMO channel is random but fixed for all ARQ rounds. The diversity–multiplexing–delay tradeoff has then been characterized in the case of block-fading MIMO ARQ channels, i.e., multiple fading blocks are allowed within the same ARQ round [51]. In [52], the outage probability of MIMO-ISI ARQ channels has been evaluated under the assumptions of short-term static channel dynamic [2], and Chase-type ARQ, i.e., the data packet is entirely retransmitted. It has been shown that, as in the flat fading case, ARQ presents an important source of diversity, but its influence becomes only minimal when the ARQ delay is increased. This observation suggests that the design of practical packet combining schemes should target a high diversity order for early ARQ rounds. Supplementary retransmissions are then used to correct rare erroneous data packets, when they occur.

In this chapter, we extend the signal-level turbo combining strategy we have introduced in chapter 2, to the case of broadband MIMO channel with unknown CCI. The proposed frequency domain soft MMSE packet combiner performs soft ISI cancellation and retransmission combining in the presence of CCI jointly over all received signal blocks. We also analyze the asymptotic performance of the proposed combining scheme. Interestingly, we show that under a rank-condition on the MIMO ARQ channel corresponding to CCI, the proposed combining scheme is not interference-limited, i.e., CCI can be completely removed. Finally, we provide numerical simulation results for some scenarios to validate our findings.

The remainder of the chapter is organized as follows. In section 3.2, we describe the ARQ system under consideration, along with the communication model in the presence of CCI. In section 3.3, we briefly describe the frequency domain turbo packet combining scheme we propose in this chapter. In section 3.4, we carry out the asymptotic performance analysis, and provide representative numerical results that demonstrate the gains achieved by the proposed scheme. Finally, we point out conclusions in section 3.5.

3.2 ARQ System Model

3.2.1 Communication Model in the Presence of CCI

We consider an SC multi-antenna-aided transmission scheme where the transmitter and the receiver are equipped with N_T transmit (index $t = 1, \cdots, N_T$) and N_R receive (index

[1] In non-ergodic, i.e., block fading quasi-static channels, the outage probability is a meaningful measure that provides a lower bound on the block error probability. It is defined as the probability that the mutual information, as a function of the channel realization and the average SNR, is below the transmission rate [50].

[2] In the case of short-term static dynamic, the ARQ channel realizations are independent from round to round. This dynamic applies to slow ARQ protocols where the delay between two rounds is larger than the channel coherence time.

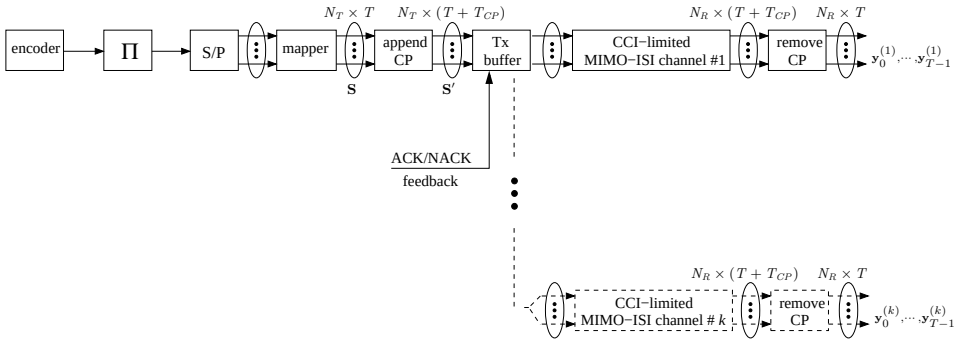

Figure 3.1: SC–MIMO ARQ communication scheme in the presence of CCI at ARQ round k.

$r = 1, \cdots, N_R$) antennas, respectively. The MIMO channel is frequency selective and is composed of L symbol-spaced taps (index $l = 0, \cdots, L-1$). The energy of each tap l is denoted σ_l^2, and the total energy is normalized to one, i.e., $\sum_{l=0}^{L-1} \sigma_l^2 = 1$.

Each information block is initially encoded then interleaved with the aid of a semi-random interleaver Π. The resulting frame is *serial to parallel* converted and mapped over the elements of the constellation set $\mathcal{S}$ to produce symbol matrix $\mathbf{S} \in \mathcal{S}^{N_T \times T}$, where T is the number of channel use. A CP word, whose length is $T_{CP} \geq L-1$, is then appended to $\mathbf{S}$, thereby yielding matrix $\mathbf{S}' \in \mathcal{S}^{N_T \times (T+T_{CP})}$. We suppose that no CSI is available at the transmitter and assume infinitely deep interleaving. Therefore, transmitted symbols verify the independence/energy-normalization condition as follow,

$$\mathbb{E}\left[s_{t,i} s_{t',i'}^{\star}\right] = \delta_{t-t',i-i'}. \tag{3.1}$$

At the upper layer, an ARQ protocol is used to help correct erroneous frames. An acknowledgment message is then generated after the decoding of each information block. Let K denote the ARQ delay, and $k = 1, \cdots, K$ denote the ARQ round index. We focus on Chase-type ARQ, i.e., the symbol matrix $\mathbf{S}'$ is completely retransmitted. In addition, we suppose perfect packet error detection, and assume that the one bit ACK/NACK feedback is error-free.

The broadband MIMO ARQ channel is assumed to be short-term static fading. Let $\mathbf{H}_0^{(k)}, \cdots, \mathbf{H}_{L-1}^{(k)} \in \mathbb{C}^{N_R \times N_T}$ denote channel matrices at the kth ARQ round, and whose entries are i.i.d. zero-mean circularly symmetric Gaussian, i.e., $h_{r,t,l}^{(k)} \sim \mathcal{CN}\left(0, \sigma_l^2\right)$. The channel profile, i.e., power distribution $\sigma_0^2, \cdots, \sigma_{L-1}^2$ and number of taps L, is supposed

to be identical for at least K consecutive rounds.

We suppose that transmitted blocks are corrupted by an *undesired* CCI signal caused by a co–channel transmission that uses $N_T^{'}$ transmit antennas (index $t' = 1, \cdots, N_T^{'}$) and T channel uses. The link between the interferer transmitter and the receiver is composed of L' taps, where the channel matrix of each tap $l' = 0, \cdots, L'-1$ at round k is $\mathbf{H}_{l'}^{\mathrm{CCI}^{(k)}} \in \mathbb{C}^{N_R \times N_T'}$ and its energy is $\sigma_{u_{l'}}^2$ [3]. We suppose that the receiver has no knowledge either about the interferer CSI or about its channel profile and number of transmit antennas (i,.e., parameters $N_T^{'}$, L', $\mathbf{H}_{l'}^{\mathrm{CCI}^{(k)}}$, and $\sigma_{u_{l'}}^2$ are completely unknown at the receiver). As the desired user, the interferer employs a CP-aided transmission strategy. Its transmitted symbols $s_{t',i}^{\mathrm{CCI}^{(k)}}$at each round k verify the independence/energy-normalization condition (3.1) as useful symbols. Therefore, the signal-to-interference ratio (SIR) at each receive antenna is given as

$$\mathrm{SIR} = \frac{N_T}{N_T' \sum_{l'=0}^{L'-1} \sigma_{u_{l'}}^2}. \tag{3.2}$$

We assume perfect frame synchronization between the interferer and the desired user. They can differ in terms of the CP word length, which depends on the delay of the multipath channel, but are synchronized in terms of the useful symbol frames. Under this assumption, CP deletion yields the following baseband received $N_R \times 1$ signal at round k and channel use i is given as

$$\mathbf{y}_i^{(k)} = \sum_{l=0}^{L-1} \mathbf{H}_l^{(k)} \mathbf{s}_{(i-l) \bmod T} + \underbrace{\sum_{l'=0}^{L'-1} \mathbf{H}_{l'}^{\mathrm{CCI}^{(k)}} \mathbf{s}_{(i-l') \bmod T}^{\mathrm{CCI}^{(k)}} + \mathbf{n}_i^{(k)}}_{\mathbf{w}_i^{(k)} = \mathrm{CCI+noise}}, \tag{3.3}$$

where $\mathbf{n}_i^{(k)} \sim \mathcal{CN}\left(\mathbf{0}_{N_R \times 1}, \sigma^2 \mathbf{I}_{N_R}\right)$ denotes the receiver thermal noise. The SC–MIMO ARQ communication scheme at round k is depicted in Fig. 3.1. In the following, we assume perfect channel estimation at each ARQ round k (i.e., $\mathbf{H}_l^{(k)}$ $\forall l$ are perfectly known) while CCI channel matrices $\mathbf{H}_{l'}^{\mathrm{CCI}^{(k)}}$ $\forall l'$, k are completely unknown at the receiver side.

3.2.2 Single-Round Communication Model

To derive the block communication model corresponding to ARQ round k, we consider the following block signal vector,

$$\mathbf{y}^{(k)} \triangleq \left[{\mathbf{y}_0^{(k)}}^{\top}, \cdots, {\mathbf{y}_{T-1}^{(k)}}^{\top} \right]^{\top} \in \mathbb{C}^{N_R T}, \tag{3.4}$$

[3] The ARQ processes corresponding to the desired user and the interferer are not necessarily synchronized. Therefore, the round index k appearing in the CCI channel matrices only refers to the index of a realization of the interferer channel at ARQ round k. The same remark holds for CCI symbols in (3.3). Also, note that $\sum_{l'=0}^{L'-1} \sigma_{u_{l'}}^2 \neq 1$ in order to account for the path-loss between the interferer and the receiver.

that groups signals corresponding to the entire symbol frame. Vector $\mathbf{y}^{(k)}$ can be expressed as,

$$\mathbf{y}^{(k)} = \boldsymbol{\mathcal{H}}^{(k)}\mathbf{s} + \mathbf{w}^{(k)}, \tag{3.5}$$

where $\mathbf{s} \triangleq \left[\mathbf{s}_0^\top, \cdots, \mathbf{s}_{T-1}^\top\right]^\top \in \mathcal{S}^{N_T T}$ is the transmitted symbol vector, the vector

$$\mathbf{w}^{(k)} \triangleq \left[\mathbf{w}_0^{(k)^\top}, \cdots, \mathbf{w}_{T-1}^{(k)^\top}\right]^\top \in \mathbb{C}^{N_R T} \tag{3.6}$$

is the CCI plus noise single-round block vector , and $\boldsymbol{\mathcal{H}}^{(k)} \in \mathbb{C}^{TN_R \times TN_T}$ is a block circulant matrix whose first $TN_R \times N_T$ column matrix is $\left[\mathbf{H}_0^{(k)^\top}, \cdots, \mathbf{H}_{L-1}^{(k)^\top}, \mathbf{0}_{N_T \times (T-L)N_R}\right]^\top$. Applying the DFT $\mathbf{U}_{T,N_R}$ on signal vector $\mathbf{y}^{(k)}$ yields the single-round frequency domain communication model

$$\mathbf{y}_f^{(k)} = \boldsymbol{\Lambda}^{(k)}\mathbf{s}_f + \mathbf{w}_f^{(k)}, \tag{3.7}$$

where $\boldsymbol{\Lambda}^{(k)}$ is the CFR corresponding to round k defined as

$$\begin{cases} \boldsymbol{\Lambda}^{(k)} \triangleq \operatorname{diag}\left\{\boldsymbol{\Lambda}_0^{(k)}, \cdots, \boldsymbol{\Lambda}_{T-1}^{(k)}\right\}, \\ \boldsymbol{\Lambda}_i^{(k)} \triangleq \sum_{l=0}^{L-1} \mathbf{H}_l^{(k)} e^{-j(2\pi il/T)}. \end{cases} \tag{3.8}$$

3.2.3 Multi-Round Communication Model

Let us suppose that received signals and channel matrices corresponding to ARQ rounds $1, \cdots, k$ are available at the receiver. The block communication model that serves for jointly performing, at ARQ round k, packet combining and equalization in the presence of CCI is then given as,

$$\underline{\mathbf{y}}^{(k)} = \underline{\boldsymbol{\mathcal{H}}}^{(k)}\mathbf{s} + \underline{\mathbf{w}}^{(k)}, \tag{3.9}$$

where $\underline{\mathbf{y}}^{(k)}$ is the multi-round block signal vector given as

$$\underline{\mathbf{y}}^{(k)} \triangleq \left[\underline{\mathbf{y}}_0^{(k)^\top}, \cdots, \underline{\mathbf{y}}_{T-1}^{(k)^\top}\right]^\top \in \mathbb{C}^{kN_R T}, \tag{3.10}$$

with

$$\underline{\mathbf{y}}_i^{(k)} \triangleq \left[\mathbf{y}_i^{(1)^\top}, \cdots, \mathbf{y}_i^{(k)^\top}\right]^\top \in \mathbb{C}^{kN_R}, \tag{3.11}$$

the vector

$$\underline{\mathbf{w}}^{(k)} \triangleq \left[\underline{\mathbf{w}}_0^{(k)^\top}, \cdots, \underline{\mathbf{w}}_{T-1}^{(k)^\top}\right]^\top \in \mathbb{C}^{kN_R T}, \tag{3.12}$$

is the CCI plus noise multi-round block vector with

$$\underline{\mathbf{w}}_i^{(k)} \triangleq \left[\mathbf{w}_i^{(1)^\top}, \cdots, \mathbf{w}_i^{(k)^\top}\right]^\top \in \mathbb{C}^{kN_R}. \tag{3.13}$$

and $\underline{\boldsymbol{\mathcal{H}}}^{(k)} \in \mathbb{C}^{kN_RT \times N_TT}$ is a block circulant matrix whose first $kN_RT \times N_T$ block column is

$$\left[\mathbf{H}_0^{(1)^\top}, \cdots, \mathbf{H}_0^{(k)^\top}, \cdots, \mathbf{H}_{L-1}^{(1)^\top}, \cdots, \mathbf{H}_{L-1}^{(k)^\top}, \mathbf{0}_{N_T \times (T-L)kN_R}\right]^\top. \tag{3.14}$$

Applying the DFT $\mathbf{U}_{T,kN_R}$ on signal vector $\underline{\mathbf{y}}^{(k)}$ yields the multiple ARQ rounds frequency domain packet combining and equalization block communication model, at ARQ round k,

$$\underline{\mathbf{y}}_f^{(k)} = \underline{\boldsymbol{\Lambda}}^{(k)}\mathbf{s}_f + \underline{\mathbf{w}}_f^{(k)}, \tag{3.15}$$

where

$$\begin{cases} \underline{\boldsymbol{\Lambda}}^{(k)} \triangleq \operatorname{diag}\left\{\underline{\boldsymbol{\Lambda}}_0^{(k)}, \cdots, \underline{\boldsymbol{\Lambda}}_{T-1}^{(k)}\right\} \in \mathbb{C}^{kN_RT \times N_TT}, \\ \underline{\boldsymbol{\Lambda}}_i^{(k)} \triangleq \left[\underline{\boldsymbol{\Lambda}}_i^{(1)^\top}, \cdots, \underline{\boldsymbol{\Lambda}}_i^{(k)^\top}\right]^\top \in \mathbb{C}^{kN_R \times N_T}. \end{cases} \tag{3.16}$$

3.3 Frequency Domain Packet Combining in the Presence of CCI

3.3.1 General Description

At each ARQ round, the decoding of a data packet is performed by iteratively exchanging soft information in the form of LLR values between the *soft packet combiner* and the SISO decoder. Let us suppose that, at ARQ round k, all received signals and channel matrices corresponding to previous rounds $k-1, \cdots, 1$ are available at the receiver. The block diagram of the frequency domain turbo packet combining receiver at ARQ round k is depicted in Fig. 3.2. First, the multiple ARQ rounds frequency domain block signal vector $\underline{\mathbf{y}}_f^{(k)} \triangleq \mathbf{U}_{T,kN_R}\underline{\mathbf{y}}^{(k)}$ and its corresponding CFR $\underline{\boldsymbol{\Lambda}}^{(k)}$ are constructed. Second, the soft packet combining with CCI module estimates the covariance of CCI plus noise, and computes the multi-round MMSE filter. These two elements are then used with *a priori* information to compute extrinsic LLRs corresponding to coded and interleaved bits. The generated soft information is transferred to the SISO decoder to compute *a posteriori* LLRs about both coded and useful bits. Only extrinsic information is fed back to the soft packet combiner to help perform transmission combining and equalization in the next turbo iteration. The iterative soft packet combining and decoding process is stopped after a preset number of turbo iterations and decision about the data packet is performed. The ACK/NACK message is then sent back to the transmitter depending on the decoding outcome. Note that during the first iteration *a priori* LLR values are the output of the SISO decoder obtained at the last iteration of previous round $k-1$.

3.3.2 Properties of CCI plus Noise Covariance

In this subsection, we focus on covariance properties of CCI plus noise present in both the single-round and multi-round communication models given by (3.5) and (3.9), respectively.

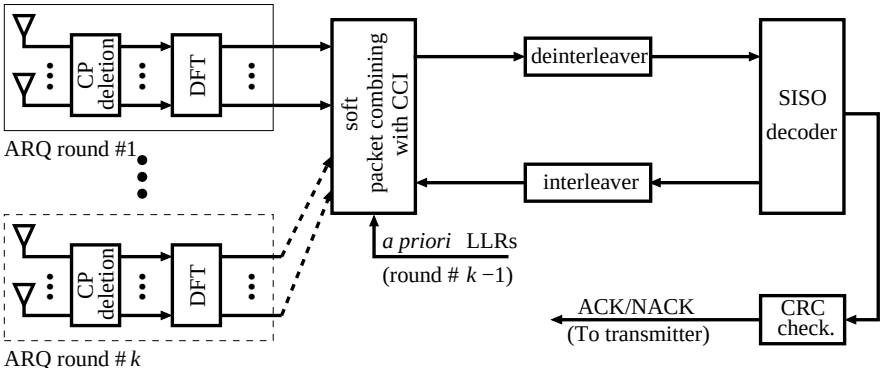

Figure 3.2: Block diagram of the turbo combining receiver scheme at ARQ round k

These properties present an important ingredient in the turbo packet combining algorithm we introduce in subsection 3.3.3.

Let $\mathbf{\Theta}_k$ denote the covariance of CCI plus noise $\mathbf{w}_i^{(k)}$ present in received signal (3.3) at round k,

$$\mathbf{\Theta}_k \triangleq \mathbb{E}\left[\mathbf{w}_i^{(k)}\mathbf{w}_i^{(k)^{\mathrm{H}}}\right] \in \mathbb{C}^{N_R \times N_R}. \tag{3.17}$$

Let us group covariance matrices corresponding to rounds $1, \cdots, k$ in the block diagonal matrix

$$\mathbf{\Sigma}_k \triangleq \mathrm{diag}\left\{\mathbf{\Theta}_1, \cdots, \mathbf{\Theta}_k\right\} \in \mathbb{C}^{kN_R \times kN_R}. \tag{3.18}$$

Proposition 1: The covariance $\underline{\mathbf{\Sigma}}_k \triangleq \mathbb{E}\left[\underline{\mathbf{w}}^{(k)}\underline{\mathbf{w}}^{(k)^{\mathrm{H}}}\right]$ of the CCI plus noise block vector $\underline{\mathbf{w}}^{(k)}$present in the multi-round communication model (3.9) after k rounds is expressed as

$$\underline{\mathbf{\Sigma}}_k = \mathbf{I}_T \otimes \mathbf{\Sigma}_k \in \mathbb{C}^{TkN_R \times TkN_R}. \tag{3.19}$$

Proof: The expression in (3.19) is easily obtained by calculating the mathematical expectation of $\underline{\mathbf{w}}^{(k)}\underline{\mathbf{w}}^{(k)^{\mathrm{H}}}$. In the derivation, we only exploit the independence between the entries of $\mathbf{H}_l^{\mathrm{CCI}^{(k)}}$ and $\mathbf{H}_{l'}^{\mathrm{CCI}^{(k')}}$ $\forall l, l', k$, and k' (i.e., short-term static block fading dynamic of the CCI MIMO ARQ channel), and the fact that CCI symbols satisfy (3.1). No assumption on the structure of the CCI block matrix is used. A detailed proof of (3.19) in the case of sliding-window aided time-domain detection can be found in [53].

Proposition 2: The covariance $\underline{\mathbf{\Theta}}_k \triangleq \mathbb{E}\left[\mathbf{w}^{(k)}\mathbf{w}^{(k)^{\mathrm{H}}}\right]$ of the single-round CCI plus noise block vector $\mathbf{w}^{(k)}$ at ARQ round k is

$$\underline{\mathbf{\Theta}}_k = \mathbf{I}_T \otimes \mathbf{\Theta}_k. \tag{3.20}$$

Proof: The proof follows by simply invoking Proposition 1 for one round.

Proposition 3: Covariance matrices of frequency domain CCI plus noise vectors $\underline{\mathbf{w}}_f^{(k)}$ and $\mathbf{w}_f^{(k)}$ (corresponding to the DFTs of $\underline{\mathbf{w}}^{(k)}$ and $\mathbf{w}^{(k)}$, respectively) are $\underline{\boldsymbol{\Sigma}}_k$ and $\underline{\boldsymbol{\Theta}}_k$, respectively.

Proof:The proof of Proposition 3 follows from the fact that $\underline{\boldsymbol{\Sigma}}_k$ and $\underline{\boldsymbol{\Theta}}_k$ are block circulant and block diagonal matrices.

3.3.3 Proposed Combining Scheme

In this subsection, we derive the frequency domain MMSE-based soft packet combiner that cancels ISI jointly over multiple ARQ rounds in the presence of unknown CCI.

At each turbo iteration of ARQ round k, the MMSE-based soft packet combiner produces a complex scalar decision $z_{t,i}^{(k)}$ that serves for computing extrinsic LLR values corresponding to coded and interleaved bits mapped over symbol $s_{t,i}$. Soft ISI cancellation and MMSE-based packet combining at round k is performed in the frequency domain as,

$$\mathbf{z}_f^{(k)} = \underline{\boldsymbol{\Phi}}^{(k)} \underline{\mathbf{y}}_f^{(k)} - \underline{\boldsymbol{\Psi}}^{(k)} \tilde{\mathbf{s}}_f, \tag{3.21}$$

where $\tilde{\mathbf{s}}_f \in \mathbb{C}^{N_T T}$ denotes the DFT of the conditional expectation (i.e., computed based on *a priori* LLRs) of $\mathbf{s}$, and the multi-round forward filter $\underline{\boldsymbol{\Phi}}^{(k)} = \mathrm{diag}\left\{\underline{\boldsymbol{\Phi}}_0^{(k)}, \cdots, \underline{\boldsymbol{\Phi}}_{T-1}^{(k)}\right\}$ and multi-round backward filter $\underline{\boldsymbol{\Psi}}^{(k)} = \mathrm{diag}\left\{\underline{\boldsymbol{\Psi}}_0^{(k)}, \cdots, \underline{\boldsymbol{\Psi}}_{T-1}^{(k)}\right\}$ are given by,

$$\begin{cases} \underline{\boldsymbol{\Phi}}_i^{(k)} & \triangleq \underline{\boldsymbol{\Lambda}}_i^{(k)^{\mathrm{H}}} \underline{\mathbf{B}}_i^{(k)^{-1}}, \\ \underline{\boldsymbol{\Psi}}_i^{(k)} & \triangleq \underline{\boldsymbol{\Phi}}_i^{(k)} \underline{\boldsymbol{\Lambda}}_i^{(k)} - \frac{1}{T} \sum_{i=0}^{T-1} \underline{\boldsymbol{\Phi}}_i^{(k)} \underline{\boldsymbol{\Lambda}}_i^{(k)}, \end{cases} \tag{3.22}$$

with

$$\begin{cases} \underline{\mathbf{B}}_i^{(k)} & = \underline{\boldsymbol{\Lambda}}_i^{(k)} \tilde{\boldsymbol{\Xi}}\, \underline{\boldsymbol{\Lambda}}_i^{(k)^{\mathrm{H}}} + \boldsymbol{\Sigma}_k, \\ \tilde{\boldsymbol{\Xi}} & \triangleq \frac{1}{T} \sum_{i=0}^{T-1} \boldsymbol{\Xi}_i, \\ \boldsymbol{\Xi}_i & \triangleq \mathrm{diag}\left\{\sigma_{1,i}^2, \cdots, \sigma_{N_T,i}^2\right\} \in \mathbb{R}^{N_T \times N_T}, \end{cases} \tag{3.23}$$

where $\sigma_{t,i}^2$ is the conditional variance of symbol $s_{t,i}$. Extrinsic LLRs of coded bits mapped over symbol $s_{t,i}$ are then computed using the time domain output $z_{t,i}^{(k)} = \mathbf{e}_{t,i}^{\top} \mathbf{U}_{T,N_T}^{\mathrm{H}} \mathbf{z}_f^{(k)}$. As it can be seen from the forward–backward filtering structure in (3.21), the frequency domain MMSE filter explicitly cancels soft ISI while it only requires the covariance of unknown CCI plus noise. Note that both Propositions 1 and 2 are used to derive (3.21).

To obtain estimates of unknown CCI plus noise covariance matrices $1, \cdots, k$, required by (3.23), let us consider the single-round frequency domain communication model (3.7). Proposition 3 indicates that the covariance of $\mathbf{w}_f^{(k)}$ is $\underline{\boldsymbol{\Theta}}_k = \mathbf{I}_T \otimes \boldsymbol{\Theta}_k$. Therefore, with respect to the block diagonal structure of (3.7), unknown CCI plus noise covariance $\boldsymbol{\Theta}_k$ can directly be estimated in the frequency domain at each turbo iteration, with the aid of

a priori LLRs, according to the following average,

$$\mathbf{\Theta}_k = \frac{1}{T}\sum_{i=0}^{T-1}\left\{\mathbf{y}_{f_i}^{(k)} - \mathbf{\Lambda}_i^{(k)}\tilde{\mathbf{s}}_{f_i}\right\}\left\{\mathbf{y}_{f_i}^{(k)} - \mathbf{\Lambda}_i^{(k)}\tilde{\mathbf{s}}_{f_i}\right\}^H, \tag{3.24}$$

where $\mathbf{y}_{f_i}^{(k)}$ and $\tilde{\mathbf{s}}_{f_i}$ denote the DFTs of $\mathbf{y}^{(k)}$ and $\tilde{\mathbf{s}}$ at frequency bin i, respectively, i.e., $\mathbf{y}_{f_i}^{(k)} = \mathbf{E}_{i,N_R}\mathbf{y}_f^{(k)}$ and $\tilde{\mathbf{s}}_{f_i} = \mathbf{E}_{i,N_T}\tilde{\mathbf{s}}_f$, where $\mathbf{E}_{i,N}$ is a $N \times NT$ zero matrix where the ith $N \times N$ block is equal to $\mathbf{I}_N$. Covariances matrices $\mathbf{\Theta}_1, \cdots, \mathbf{\Theta}_{k-1}$ are similarly estimated at ARQ rounds $1, \cdots, k-1$, respectively, and correspond to estimates obtained at the last turbo iteration. In other words, when the decoding outcome is erroneous, a NACK message is fed back to the transmitter, and the unknown CCI plus noise covariance estimate obtained at the last iteration is saved in the receiver to help perform packet combining at the next ARQ round.

Note that the proposed technique has a complexity order cubic against the product of the number of receive antennas and ARQ delay. This limitation can be overcome by an optimized recursive implementation algorithm similar to the algorithm presented in the previous chapter. Therefore, the complexity will be only cubic in term of the number of transmit antennas.

3.4 Peformance Evaluation

3.4.1 Asymptotic Performance Analysis

In the following, we provide a frame-basis analysis where we derive system conditions under which perfect CCI cancellation holds. We suppose that the interferer CSI is perfectly known, and investigate the influence of its channel properties on the interference cancellation capability of the proposed packet combining scheme in the high SNR regime.

Theorem 1: We consider a CCI-limited MIMO ARQ system with N_T transmit and N_R receive antennas, and ARQ delay K. Let $\mathbf{\Theta}_k^{\mathrm{CCI}}$ denote the CCI covariance at ARQ round $k = 1, \cdots, K$, i.e., the covariance of the global noise at the receiver is $\mathbf{\Theta}_k = \mathbf{\Theta}_k^{\mathrm{CCI}} + \sigma^2\mathbf{I}_{N_R}$, and ρ_k be the rank of $\mathbf{\Theta}_k^{\mathrm{CCI}}$. We assume perfect LLR feedback from the SISO decoder. As explained in detail in the Appendix A, the frequency domain soft MMSE packet combiner provides perfect CCI suppression for asymptotically high SNR if

$$\sum_{u=1}^{k}\rho_u < kN_R - N_T. \tag{3.25}$$

We now proceed to derive an upper bound on ρ_k, where we incorporate the rank of the CCI fading channel. Under the assumption that CCI symbols verify (3.1), i.e., infinitely

deep interleaving, we get

$$\mathbf{\Theta}_k^{\mathrm{CCI}} = \sum_{l'=0}^{L'-1} \mathbf{H}_{l'}^{\mathrm{CCI}^{(k)}} \mathbf{H}_{l'}^{\mathrm{CCI}^{(k)^H}}. \tag{3.26}$$

Let us write each CCI channel matrix as

$$\mathbf{H}_{l'}^{\mathrm{CCI}^{(k)}} = \mathbf{R}_{N_R}^{1/2} \mathbf{A}_{l'}^{\mathrm{CCI}^{(k)}} \mathbf{R}_{N_T'}^{1/2} \quad \forall l', \tag{3.27}$$

where $\mathbf{A}_{l'}^{\mathrm{CCI}^{(k)}} \in \mathbb{C}^{N_R \times N_T'}$ characterizes the scattering environment between the CCI transmitter and receiver [54], and $\mathbf{R}_{N_R}$ and $\mathbf{R}_{N_T'}$ are the correlation matrices controlling the receive and transmit antenna arrays, and in general,

$$\mathbf{R}_{N_R} = \begin{bmatrix} 1 & & \delta_{\mathrm{Rx}} \\ & \ddots & \\ \delta_{\mathrm{Rx}} & & 1 \end{bmatrix}_{N_R \times N_R}, \quad \mathbf{R}_{N_T'} = \begin{bmatrix} 1 & & \delta_{\mathrm{Tx}} \\ & \ddots & \\ \delta_{\mathrm{Tx}} & & 1 \end{bmatrix}_{N_T' \times N_T'}, \tag{3.28}$$

where $0 \leq \delta_{\mathrm{Rx}}, \delta_{\mathrm{Tx}} < 1$ [55]. Note that (3.27) corresponds to a general model of correlated fading MIMO channels, where the scattering radii at transmitter and receiver sides is taken into account, and $\mathbf{A}_{l'}^{\mathrm{CCI}^{(k)}}$ is not necessarily a full rank matrix, i.e., $\mathrm{rank}\left\{\mathbf{A}_{l'}^{\mathrm{CCI}^{(k)}}\right\} \leq \min\left(N_T', N_R\right)$ [54]. Noting that $\mathbf{R}_{N_R}$ and $\mathbf{R}_{N_T'}$ are full rank matrices, and with respect to the fact that CCI tap channel matrices are independent, and using (3.26) and (3.27), we get

$$\begin{aligned} \rho_k &\leq \min\left\{ N_R, \sum_{l'=0}^{L'-1} \mathrm{rank}\left\{ \mathbf{H}_{l'}^{\mathrm{CCI}^{(k)}} \mathbf{H}_{l'}^{\mathrm{CCI}^{(k)^H}} \right\} \right\} \\ &= \min\left\{ N_R, \sum_{l'=0}^{L'-1} \mathrm{rank}\left\{ \mathbf{A}_{l'}^{\mathrm{CCI}^{(k)}} \mathbf{R}_{N_T'} \mathbf{A}_{l'}^{\mathrm{CCI}^{(k)^H}} \right\} \right\} \\ &\leq \min\left\{ N_R, \sum_{l'=0}^{L'-1} \mathrm{rank}\left\{ \mathbf{A}_{l'}^{\mathrm{CCI}^{(k)}} \right\} \right\}. \end{aligned} \tag{3.29}$$

A closer look at Theorem 3.4.1 and upper bound (3.29) provides interesting system interpretations.

- **Impact of CCI Fading Channel:** First, note that the CCI cancellation capability of the frequency domain MMSE packet combiner is related to the CCI channel rank. When the interferer has a rank-deficient channel matrix at a certain ARQ round, interference can completely be removed (at subsequent rounds) if the sum-rank condition in Theorem 3.4.1 is satisfied. In practice, the channel rank can

dramatically drop in the case of the so-called pinhole channel, where the transmitter and receiver are largely separated and are surrounded by multiple scatterers [54]. In this scenario, the channel can even prevent multipath from building up since the thin air pipe connecting transmitter and receiver scatterers is very long. For instance, in a system with $N_R = 3$ receive and $N_T = 2$ transmit antennas, and an unknown interferer who is experiencing one path ($L' = 1$) channel realizations with rank equal to two, CCI can be removed at the second ARQ round because the sum-rank condition (3.25) holds for $k \geq 2$.

- **Impact of the Number of Transmit Antennas and ARQ Delay:** Condition (3.25) suggests how, for a given CCI channel profile, the number of transmit antennas N_T and ARQ rounds K are chosen to achieve perfect CCI cancellation. For instance, if transmission is corrupted by CCI with quasi-static channel rank [4], and if the ARQ delay allowed by the upper layer is K, then only $N_T < K\,(N_R - \rho_0)$ transmit antennas can be allocated to the user of interest to achieve interference suppression at the latest at ARQ round K, where ρ_0 is the rank of $\mathbf{\Theta}_k^{\mathrm{CCI}}$, i.e., $\rho_k = \rho_0\ \forall k$. Increasing the ARQ delay will relax the condition on the number of transmit antennas and therefore allow for an increase in the diversity and/or multiplexing gains depending on the diversity-multiplexing-delay trade-off operating point [76]. Note that when $N_T^{'} \ll N_T$, the CCI channel rank dramatically drops, and therefore CCI suppression is achieved even when a short ARQ delay K is required.

- **Interaction with the Scheduling Mechanism:** In the case of opportunistic communications, interference with co-channel users who have high channel ranks can be prevented. For instance, when a retransmission is required on the reverse link, the base station (BS) can choose the timing of the next ARQ round in such a way that transmission simultaneously occurs with that of a user with low channel rank. This is feasible since the BS has complete knowledge about user CSIs in the reverse link. The same scheduling mechanism can be used in the forward link if all users provide the BS with feedback information about their channel ranks. When the system suffers from CCI caused by neighboring cells, the sum-rank condition (3.25) can be achieved by simply increasing the number of ARQ rounds because the CCI channel rank tends to be constant over time.

3.4.2 Numerical Results

In this sub-subsection, we provide BLER performance results for the proposed combining technique. Our focus is to demonstrate the superior performance of the introduced scheme compared to the conventional LLR-level combining. We also evaluate BLER performance

[4] In this case, CCI with quasi-static channel rank refers to an interferer whose channel rank is constant over multiple ARQ rounds.

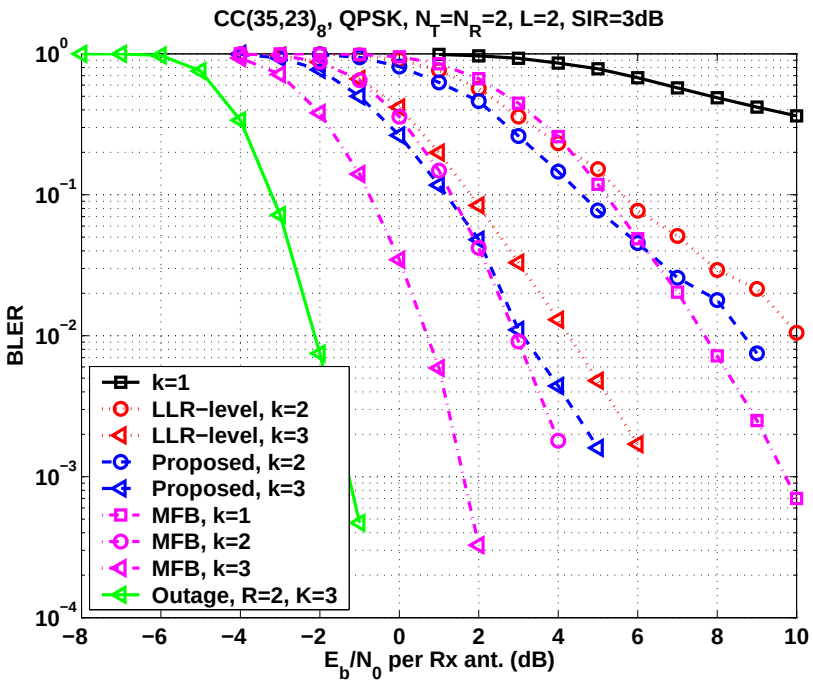

Figure 3.3: BLER performance for CC $(35, 23)_8$, QPSK, $N_T = N_R = 2$, $L = L' = 2$ equal energy paths, and SIR = 3dB.

for scenarios where the interferer has rank deficient channel matrices to corroborate the theoretical analysis in Subsection 3.4.1.

In all simulations, we consider a BICM scheme where the encoder is a 16 state convolutional code with polynomial generators $(35, 23)_8$, and the modulation scheme is QPSK. The length of the code bit frame is 1032 bits including tails. The ARQ delay is $K = 3$, and the E_b/N_0 ratio appearing in all figures is the SNR per useful bit per receive antenna. We consider a $L = 2$ path MIMO-ISI channel profile where $\sigma_0^2 = \sigma_1^2 = \frac{1}{2}$. We use both the MFB per ARQ round and the outage probability [52] of the CCI-free MIMO-ISI channel as absolute performance bounds to evaluate the CCI cancellation capability and diversity order achieved by the proposed combining scheme. The number of turbo iterations is set to five and the Max-Log-MAP algorithm is used for SISO decoding.

We first investigate performance for scenarios where the user of interest and the interferer have the same number of transmit antennas ($N_T = N_T'$) and identical channel profiles, i.e., $L = L'$, equal power taps, and CCI fading channel coefficients are i.i.d. In Fig. 3.3, we compare the BLER performance of the proposed scheme with that of LLR-level combining for a ST–BICM code with rate $R = 2$, i.e., $N_T = 2$. The number of receive antennas is $N_R = 2$, and SIR = 3dB. We observe that the proposed scheme significantly outperforms LLR-level combining. The performance gap at ARQ round $k = 3$ is about 1dB for BLER $\leq 10^{-2}$. Note that both combining schemes fail to perfectly cancel

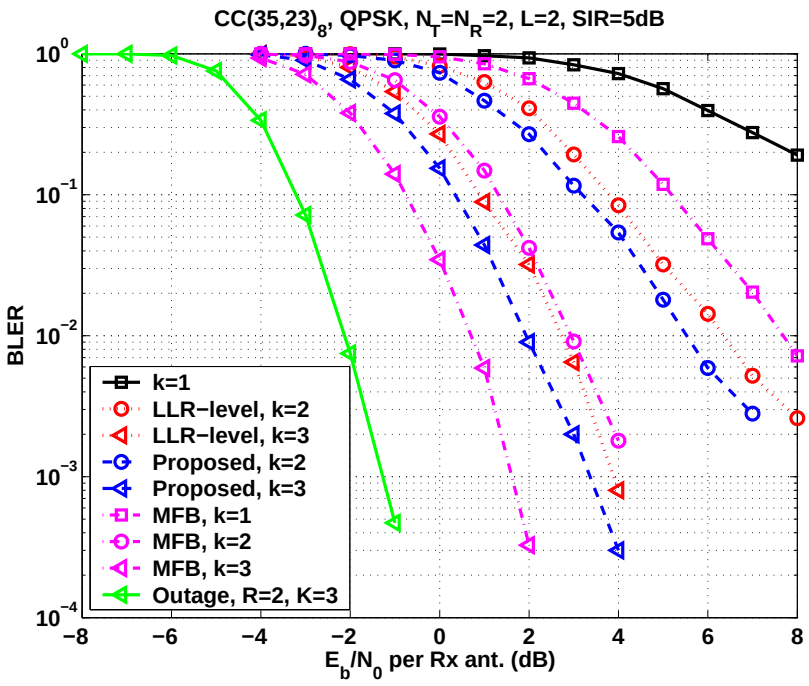

Figure 3.4: BLER performance for CC $(35, 23)_8$, QPSK, $N_T = N_R = 2$, $L = L' = 2$ equal energy paths, and SIR = 5dB.

CCI since performance curves tend to saturate for high E_b/N_0 values. Fig. 3.4 reports performance of both techniques when SIR is increased to SIR = 5dB. In this case, the performance gap between the two schemes is reduced. The CCI cancellation capability is also improved as can be seen from the steeper slopes of BLER curves. In Fig. 3.5, we evaluate the performance for a high rate ST–BICM code where $R = 4$, i.e., $N_T = 4$. Only $N_R = 2$ receive antennas are considered, and SIR = 5dB. The proposed scheme dramatically outperforms LLR-level combining, i.e., the performance gap at ARQ round $k = 3$ is about 4dB at $7 * 10^{-3}$ BLER. The proposed scheme also offers higher cancellation capability and diversity order than LLR-level combining.

We now turn to scenarios where the interferer has a rank-deficient uncorrelated MIMO channel, i.e., rank $\left\{ \mathbf{A}_{l'}^{\mathrm{CCI}^{(k)}} \right\} < \min\left(N_T^{'}, N_R\right)$ $\forall l'$, $\delta_{\mathrm{Tx}} = \delta_{\mathrm{Rx}} = 0$, and assume that the rank is constant over all ARQ rounds. In Fig. 3.6, we report the BLER performance of the proposed scheme for a CCI-limited MIMO system with settings similar to Fig. 3.3, i.e., $N_T = N_R = 2$, and SIR = 3dB. The interferer experiences flat fading, i.e., $L' = 1$, and only has $N_T^{'} = 1$ transmit antenna. Therefore, with respect to (3.29), $\rho_k = 1$ $\forall k$. Note that in this interference scenario, the perfect CCI cancellation condition (3.25) holds for $k > 2$. We observe that both the CCI cancellation capability and the diversity order of the proposed scheme are improved. The performance gain with respect to the case of $N_T^{'} = 2$ and $L' = 2$ is about 1.5dB at $3 * 10^{-3}$ BLER and round $k = 3$, and the

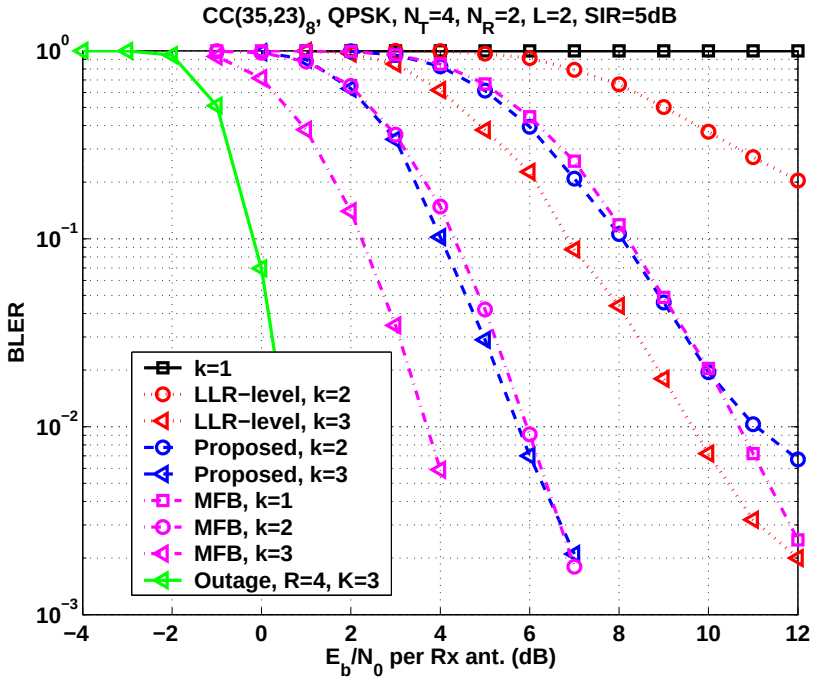

Figure 3.5: BLER performance for CC $(35,23)_8$, QPSK, $N_T = 4$, $N_R = 2$, $L = L' = 2$ equal energy paths, and SIR = 5dB.

slope of the BLER curve at round $k = 3$ is similar to that of the MFB curve. Fig. 3.7 compares the performance of the proposed scheme for two scenarios with heavy CCI, i.e., SIR = 1dB. The ST–BICM code has rate $R = 4$, i.e., $N_T = 4$, and the number of receive antennas is set to $N_R = 4$. In the first scenario (Scenario 1), the interferer has $N_T^{'} = 4$ transmit antennas, $L' = 2$ equal power taps, and i.i.d. fading coefficients, while in the second scenario (Scenario 2), $N_T^{'} = 2$, $L' = 1$, and the CCI channel rank is equal to two. Therefore, $\rho_k = 2\ \forall k$, and condition (3.25) holds for $k > 2$. It is clear that in the second scenario, better CCI cancellation capability is achieved for $k \geq 2$. For instance, the performance gap for $k = 3$ is more than 2dB at $2 * 10^{-2}$ BLER. Also, the diversity order of the CCI-free MIMO-ISI channel is almost achieved.

3.5 Conclusions

In this chapter, we investigated efficient iterative turbo packet combining for broadband ST–BICM transmission with hybrid ARQ over CCI-limited MIMO-ISI channels. We have presented a frequency domain turbo combining scheme where signals and CFRs corresponding to all ARQ rounds are combined in a MMSE fashion to decode the data packet at each round. The covariance of the overall (over all ARQ rounds) CCI plus noise required by the frequency domain MMSE soft packet combiner is constructed by separately com-

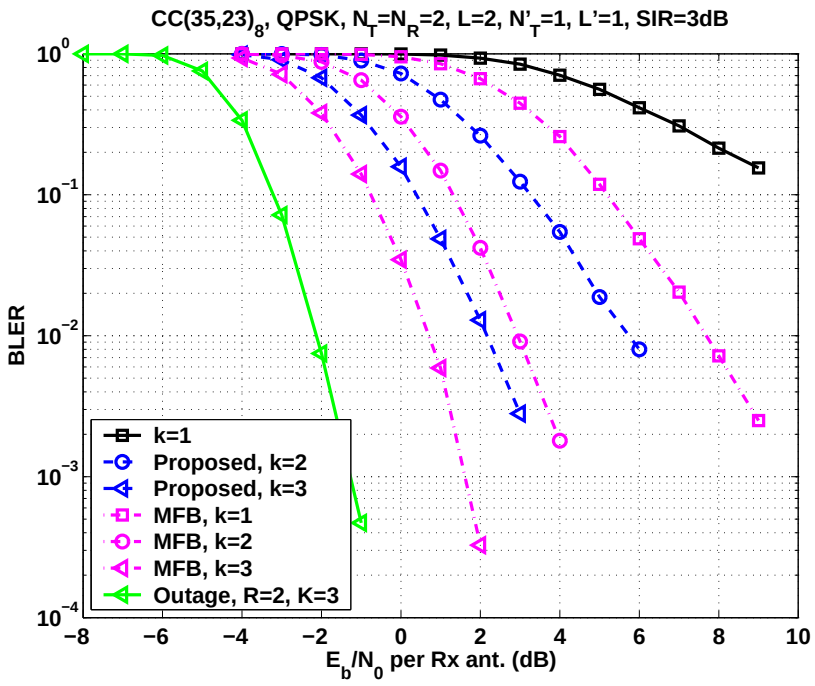

Figure 3.6: BLER performance for CC $(35, 23)_8$, QPSK, $N_T = N_R = 2$, $L = 2$ equal energy paths, $N'_T = 1$, $L' = 1$, and $\rho_k = 1$, $k = 1, \cdots, K$, SIR = 3dB.

puting the covariance related to each round. We analyzed the effect of CCI channel rank on performance. Interestingly, under a sum-rank condition, the frequency domain MMSE soft packet combiner can completely remove CCI for asymptotically high SNR. Finally, we provided simulation results where we showed that the proposed technique achieves BLER performance superior to LLR-level combining, and offers high CCI cancellation capability and diversity order for many interference scenarios.

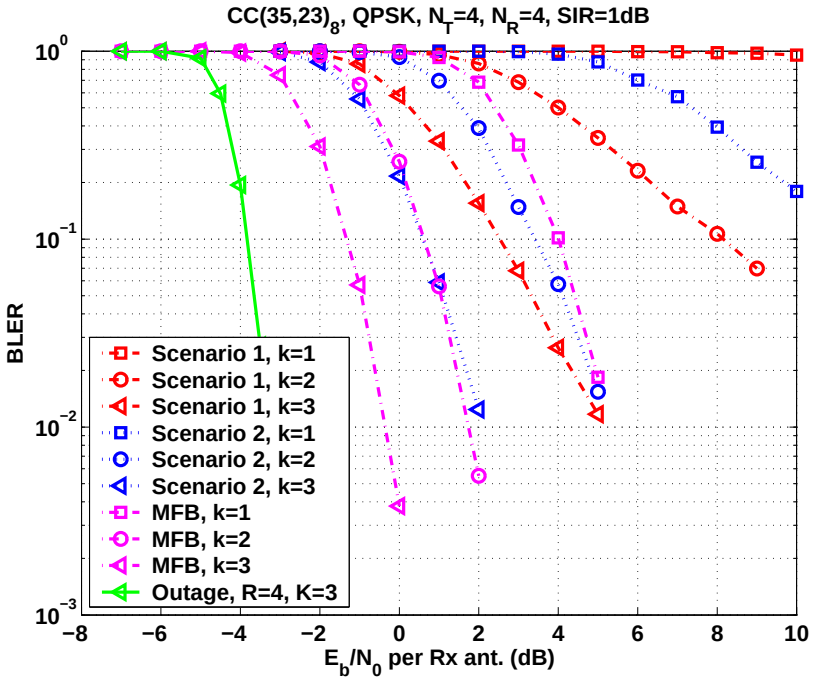

Figure 3.7: BLER performance for CC $(35, 23)_8$, QPSK, $N_T = N_R = 4$, $L = 2$ equal energy paths, and SIR = 1dB. Scenario 1: $N'_T = 4$, $L' = 4$, Scenario 2: $N'_T = 2$, $L' = 1$, and $\rho_k = 2$, $k = 1, \cdots, K$.

Chapter 4

Frequency Domain HARQ Chase Combining for Broadband MIMO CDMA Systems

4.1 Introduction

Multi-code CDMA is a simple technique for supporting users with heterogeneous data rates [56], i.e. a user who wishes to transmit at higher data rate is simply assigned additional orthogonal walsh codes. However, with high speed data transmission, multipath number could be increased, and causes inter-chip interference (ICI) and ISI, which destroy orthogonality property of the spreading code. Several authors studied time domain MMSE (TD-MMSE)-based chip equalizer as an efficient technique to restore a part of destroyed orthogonality of multi-code, so as to suppress the ISI [57–59]. However, the TD-MMSE-based equalizer, which implements a sliding-window detection approach, involves inversion of large matrices. The receiver complexity is generally cubic in terms of the MMSE filter length. Combining CP with single carrier multi-code CDMA enables frequency domain MMSE (FD-MMSE)-based equalization, which has the ability to restore a part of the spreading code orthogonality at an affordable complexity cost [60, 61]. However, even if FD-MMSE outperforms the conventional rake receiver [61], it can't overcome the error floor caused by ICI. In [62], frequency domain equalization for multi-code CDMA has been proposed using iterative (turbo) processing to support the multimedia services with high quality. Combined with MIMO multiplexing techniques, multi-code CDMA systems have the ability to provide very high spectral efficiency through the transmission of different

parallel substreams over multiple antennas [63]. To ensure highly reliable communication, hybrid-ARQ combined with channel coding is considered [64]. A multi-antenna CP-CDMA system with ARQ introduces more spatial and temporal diversities as the same block is transmitted over different and independent MIMO channels.

In this chapter, we investigate an efficient turbo receiver schemes for single user multi-code CDMA systems with chase-type ARQ operating over a broadband MIMO channel. We introduce two packet combining where all ARQ rounds are used jointly to decode the data packet. The first packet combining scheme, referred to as *chip-level packet combining scheme*, is an extension of the combining approach we have introduced in chapter 2 to the case of multi-antenna multi-code CDMA systems. The second scheme, referred to as *symbol-level packet combining scheme*, performs the transmission combining at the symbol level. In this scheme, frequency domain soft MMSE is performed separately for each transmission then the demapping is jointly performed with packet combining. First, we briefly describe the *chip-level packet combining scheme*. Then, we details the proposed *symbol-level packet combining scheme* and present a low complexity combining approach based on recursive implementation strategy. In this chapter, a comparative study, in term of implementation cost and performance evaluation, is presented. Using complexity analysis and BLER and throughput simulations, we demonstrate that the choice of the best combining technique depends on the system configuration.

The remaining of the chapter is organized as follow: Section 4.2 describes multi-code CP-CDMA system under consideration. The studied packet combining schemes are described in section 4.3. The complexity and performance evaluation is presented in section 4.4. The chapter is concluded in section 4.5.

4.2 System Description

4.2.1 Multi-Code CP-CDMA MIMO ARQ Transmission Scheme

We consider a single user multi-code CP-CDMA transmission scheme over a broadband MIMO channel and using an ARQ protocol at the upper layer where the ARQ delay is K (index $k = 1, \cdots, K$). An information block is first encoded using a ρ-rate encoder, then interleaved with the aid of a semi-random interleaver Π and spatially multiplexed over N_T transmit antennas (index $t = 1, \cdots, N_T$) to produce the coded and interleaved frame $\boldsymbol{b}$ which is *serial-to-parallel* converted to N_T sub-streams $\boldsymbol{b}_1, \ldots, \boldsymbol{b}_{N_T}$, where

$$\mathbf{b}_t \triangleq [b_{t,0,1}, \cdots, b_{t,j,m}, \cdots, b_{t,T_s-1,\mathcal{M}}] \in \{0,1\}^{\mathcal{M}T_S}, \tag{4.1}$$

with T_s (index $j = 0, \cdots, T_s - 1$) denotes the length of the symbol block transmitted over each antenna. Each sub-stream is then symbol mapped onto the elements of constellation $\mathcal{S}$ where $|\mathcal{S}| = 2^{\mathcal{M}}$. At each antenna the symbol block is then passed through a *serial-*

to-parallel converter and a spreading module which consists in C orthogonal codes. The same spreading matrix

$$\mathbf{W} \triangleq \left[\mathbf{w}_1^\top, \cdots, \mathbf{w}_C^\top\right] \in \left\{\pm 1/\sqrt{N}\right\}^{N \times C} \tag{4.2}$$

is used for each transmit antenna, where

$$\mathbf{w}_n \triangleq \left[w_{1,n}, \cdots, w_{N,n}\right], \; n = 1, \cdots, C \tag{4.3}$$

is a Walsh code of length N, and $C \leq N$ is the number of multiplexed codes. The rate of this space-time code is therefore $\mathcal{R} = \rho \mathcal{M} N_T C$. The C parallel chip-streams on each antenna are then added together to construct a block of $T_c = T_s \frac{N}{C}$ chips (index $i = 0, \cdots, T_c - 1$). The chips at the output of the N_T transmit antennas are arranged in the $N_T \times T_c$ matrix

$$\mathbf{X} \triangleq \begin{bmatrix} x_{1,0} & \cdots & x_{1,T_c-1} \\ \vdots & & \vdots \\ \underbrace{x_{N_T,0}}_{\mathbf{x}_0} & \cdots & \underbrace{x_{N_T,T_c-1}}_{\mathbf{x}_{T_c-1}} \end{bmatrix}, \tag{4.4}$$

where

$$x_{t,i} \triangleq \sum_{n=1}^{C} s_{t,n,i} w_{p,n}, \;\; p = i \bmod N + 1, \tag{4.5}$$

and $s_{t,n,i}$ denotes the symbol transmitted by antenna t at channel use i and using Walsh code $\mathbf{w}_n$. Transmitted chips are independent (infinitely deep interleaving assumption), and the chip-energy is normalized to one, i.e., $\mathbb{E}\left[|x_{t,i}|^2\right] = 1$. A CP chip-word of length T_{CP} is appended to $\mathbf{X}$ to construct the $N_T \times (T_c + T_{CP})$ chip matrix $\mathbf{X}'$ to be transmitted. We consider Chase-type ARQ: When the decoding outcome is erroneous at ARQ round k, the receiver feeds back a NACK message, then the transmitter completely retransmits chip-matrix $\mathbf{X}'$ in the next round. A successful decoding incurs the feed back of an ACK message. The transmitter then stops the transmission of the current frame and moves on to the next frame. Fig. 4.1 depicts the considered multi-code CP-CDMA MIMO transmission scheme with ACK/NACK.

4.2.2 Communication Model

The broadband MIMO propagation channel connecting the N_T transmit to the N_R receive antennas is composed of L chip-spaced taps (index $l = 0, \cdots, L - 1$). We assume a quasi-static block fading channel, i.e., the channel is constant over an information block and independently changes from frame to frame. The $N_R \times N_T$ channel matrix characterizing

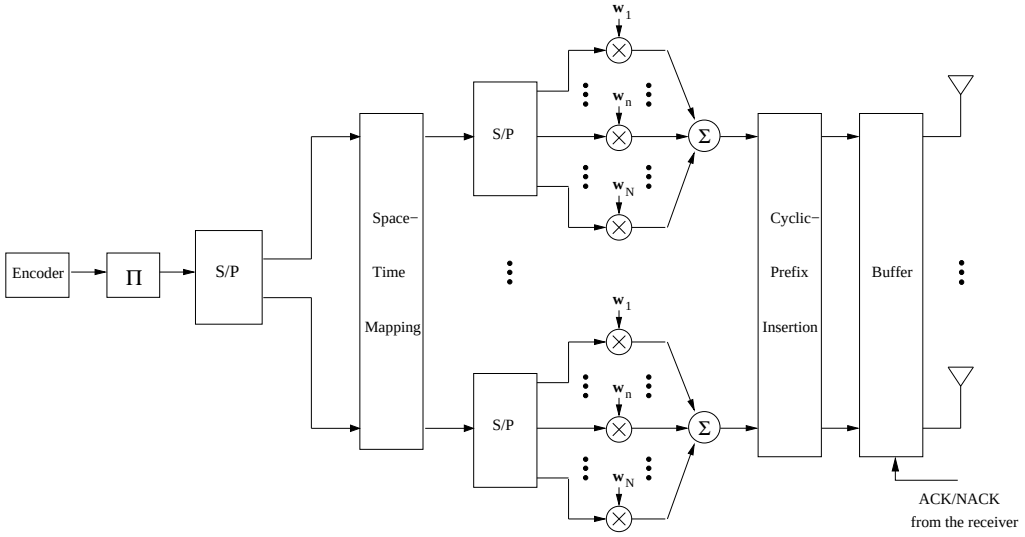

Figure 4.1: Multi-antenna multi-code Cyclic-prefix-CDMA transmitter with ARQ.

the lth discrete tap at ARQ round k is denoted $\mathbf{H}_l^{(k)}$, and is made of zero-mean circularly symmetric complex Gaussian random entries. The average channel energy per receive antenna is normalized as

$$\sum_{l=0}^{L-1}\sum_{t=1}^{N_T}\mathbb{E}\left[\left|h_{r,t,l}^{(k)}\right|^2\right]=N_T,\ r=1,\cdots,N_R. \tag{4.6}$$

At the receiver side, after removing the CP-word at ARQ round k, a DFT is applied on received signals. This yields T_c frequency domain components grouped in block

$$\mathbf{y}_f^{(k)}\triangleq\left[\mathbf{y}_{f_0}^{(k)^\top},\cdots,\mathbf{y}_{f_{T_c-1}}^{(k)^\top}\right]^\top, \tag{4.7}$$

which can be expressed as,

$$\mathbf{y}_f^{(k)}=\mathbf{\Lambda}^{(k)}\mathbf{x}_f+\mathbf{n}_f^{(k)}, \tag{4.8}$$

where vectors

$$\mathbf{x}_f\triangleq\left[\mathbf{x}_{f_0}^\top,\cdots,\mathbf{x}_{f_{T_c-1}}^\top\right]^\top\in\mathbb{C}^{T_cN_T\times 1}, \tag{4.9}$$

$$\mathbf{n}_f^{(k)}\triangleq\left[\mathbf{n}_{f_0}^{(k)^\top},\cdots,\mathbf{n}_{f_{T_c-1}}^{(k)^\top}\right]^\top, \tag{4.10}$$

group the DFTs of transmitted chips and thermal noise at round k, respectively, and $\mathbf{n}_f^{(k)}\sim\mathcal{N}\left(\mathbf{0},\sigma^2\mathbf{I}_{T_cN_R}\right)$. The CFR matrix $\mathbf{\Lambda}^{(k)}$ at ARQ round k is given by

$$\begin{cases}\mathbf{\Lambda}^{(k)}\triangleq\operatorname{diag}\left\{\mathbf{\Lambda}_0^{(k)},\cdots,\mathbf{\Lambda}_{T_c-1}^{(k)}\right\},\\ \mathbf{\Lambda}_i^{(k)}=\sum_{l=0}^{L-1}\mathbf{H}_l^{(k)}e^{-j(2\pi il/T_c)}.\end{cases} \tag{4.11}$$

4.3 Iterative Receivers for Multi-Antenna Multi-Code CP-CDMA ARQ

In this section, we present two efficient algorithms for performing turbo packet combining for CP-CDMA MIMO ARQ systems : i) chip-level turbo packet combining, and ii) symbol-level turbo packet combining. In both schemes, signals received over multiple ARQ rounds are processed using soft MMSE filtering. Transmitted data blocks are decoded, at each ARQ round, in an iterative fashion through the exchange of soft information, in the form of LLRs, between the *soft packet combiner*, i.e., soft–over ARQ rounds equalizer and demapper, and the SISO decoder.

4.3.1 Chip-Level Turbo Packet Combining

To exploit the diversities available in received signals $\mathbf{y}_{f_0}^{(1)}, \cdots, \mathbf{y}_{f_{T_c-1}}^{(k)}$, we view each ARQ round k as an additional set of virtual N_R receive antennas. The MIMO ARQ system can therefore be considered as a point-to-point MIMO link with N_T transmit and kN_R receive antennas, where the $T_c k N_R \times 1$ chip-level virtual received signal vector $\underline{\mathbf{y}}_f^{(k)}$ is constructed as,

$$\underline{\mathbf{y}}_f^{(k)} \triangleq \left[\mathbf{y}_{f_0}^{(1)^\top}, \cdots, \mathbf{y}_{f_0}^{(k)^\top}, \cdots, \mathbf{y}_{f_{T_c-1}}^{(1)^\top}, \cdots, \mathbf{y}_{f_{T_c-1}}^{(k)^\top} \right]^\top. \tag{4.12}$$

The frequency domain communication model after k rounds is then given as,

$$\underline{\mathbf{y}}_f^{(k)} = \underline{\mathbf{\Lambda}}^{(k)} \mathbf{x}_f + \underline{\mathbf{n}}_f^{(k)}, \tag{4.13}$$

where

$$\underline{\mathbf{\Lambda}}^{(k)} \triangleq \text{diag} \left\{ \begin{bmatrix} \mathbf{\Lambda}_0^{(1)} \\ \vdots \\ \mathbf{\Lambda}_0^{(k)} \end{bmatrix}, \cdots, \begin{bmatrix} \mathbf{\Lambda}_{T_c-1}^{(1)} \\ \vdots \\ \mathbf{\Lambda}_{T_c-1}^{(k)} \end{bmatrix} \right\} \in \mathbb{C}^{T_c k N_R \times T_c N_T} \tag{4.14}$$

and

$$\underline{\mathbf{n}}_f^{(k)} = \left[\mathbf{n}_{f_0}^{(1)^\top}, \cdots, \mathbf{n}_{f_0}^{(k)^\top}, \cdots, \mathbf{n}_{f_{T_c-1}}^{(1)^\top}, \cdots, \mathbf{n}_{f_{T_c-1}}^{(k)^\top} \right]^\top. \tag{4.15}$$

Soft ICI cancellation (and also soft ISI cancellation, in the case of $L \geq N+1$) and MMSE filtering are jointly performed over all ARQ round. We call this concept *chip-level turbo packet combining*. Similarly to signal-level combining scheme introduced in chapter 2, this requires a huge computational cost since the complexity of computing MMSE filters is cubic in the order of ARQ delay. In addition, the required receiver memory size linearly scales with the ARQ delay because all CFRs $\mathbf{\Lambda}_0^{(1)}, \cdots, \mathbf{\Lambda}_{T_c-1}^{(k)}$ and received signals $\mathbf{y}_{f_0}^{(1)}, \cdots, \mathbf{y}_{f_{T_c-1}}^{(k)}$ are required at round k. This limitation can be overcome by an optimized recursive implementation algorithm where both receiver complexity and memory requirements are quite insensitive to the ARQ delay. We introduce the recursive frequency

domain variables, $\underline{\tilde{\mathbf{y}}}_f^{(k)}$ and $\underline{\mathbf{D}}_i^{(k)}$ defined similarly to (2.37) and (2.38), respectively. In the following, we briefly present the turbo MMSE recursive implementation algorithm for chip-level combining. The soft MMSE estimate $\mathbf{z}_f^{(k)}$ on $\mathbf{x}_f$ at transmission k is expressed as ,

$$\mathbf{z}_f^{(k)} = \mathbf{\Gamma}^{(k)} \underline{\tilde{\mathbf{y}}}_f^{(k)} - \mathbf{\Omega}^{(k)} \tilde{\mathbf{x}}_f, \tag{4.16}$$

where $\tilde{\mathbf{x}}_f$ denotes the DFT of the conditional expectation (i.e., computed based on *a priori* LLRs) of $\mathbf{x}$, and $\mathbf{\Gamma}^{(k)} = \text{diag}\left\{\mathbf{\Gamma}_0^{(k)}, \cdots, \mathbf{\Gamma}_{T_c-1}^{(k)}\right\} \in \mathbb{C}^{T_c N_T \times T_c N_T}$ denotes the forward filter at ARQ round k and is defined similarly to (2.40) as,

$$\begin{cases} \mathbf{\Gamma}_i^{(k)} \triangleq \frac{1}{\sigma^2}\left\{\mathbf{I}_{N_T} - \underline{\mathbf{D}}_i^{(k)} \mathbf{C}_i^{(k)^{-1}}\right\}, \\ \mathbf{C}_i^{(k)} = \sigma^2 \tilde{\mathbf{\Xi}}^{-1} + \underline{\mathbf{D}}_i^{(k)}, \end{cases} \tag{4.17}$$

and $\mathbf{\Omega}^{(k)} = \text{diag}\left\{\mathbf{\Omega}_0^{(k)}, \cdots, \mathbf{\Omega}_{T_c-1}^{(k)}\right\} \in \mathbb{C}^{T_c N_T \times T_c N_T}$ denotes the backward filter at ARQ round k and is defined similarly to (2.41) as,

$$\begin{cases} \mathbf{\Omega}_i^{(k)} \triangleq \mathbf{\Gamma}_i^{(k)} \underline{\mathbf{D}}_i^{(k)} - \mathbf{\Upsilon}^{(k)}, \\ \mathbf{\Upsilon}^{(k)} = \frac{1}{T} \sum_{i=0}^{T-1} \mathbf{\Gamma}_i^{(k)} \underline{\mathbf{D}}_i^{(k)}. \end{cases} \tag{4.18}$$

The matrix $\tilde{\mathbf{\Xi}}$ is the $N_T \times N_T$ unconditional covariance of transmitted chips, and is computed as the time average of conditional covariance matrices $\mathbf{\Xi}_i \triangleq \text{diag}\left\{\sigma_{1,i}^2, \cdots, \sigma_{N_T,i}^2\right\}$ with $\sigma_{t,i}^2$ is the conditional variance of chip $x_{t,i}$. The inverse DFT is then applied to $\mathbf{z}_f^{(k)}$ to obtain the equalized time domain chip sequence. After despreading, extrinsic LLR values $\phi_{t,j,m,n}^{(e)}(k)$ corresponding to coded and interleaved bits $b_{t,j,m}$ $\forall\, t, j, m$ at iteration n of round k are computed as,

$$\phi_{t,j,m,n}^{(e)}(k) = \log \frac{\sum_{s \in \mathcal{S}_1^m} \exp\left\{\xi_{t,j}^{(k)}(s) + \sum_{m' \neq m} \phi_{t,j,m',n}^{(a)}(k) \lambda_{m'}\{s\}\right\}}{\sum_{s \in \mathcal{S}_0^m} \exp\left\{\xi_{t,j}^{(k)}(s) + \sum_{m' \neq m} \phi_{t,j,m',n}^{(a)}(k) \lambda_{m'}\{s\}\right\}}, \tag{4.19}$$

where

$$\xi_{t,j}^{(k)}(s) = \frac{\left|r_{t,j}^{(k)} - g_{t,j}^{(k)} s\right|^2}{\theta_{t,j}^{(k)^2}}, \tag{4.20}$$

with $r_{t,j}^{(k)}$, $g_{t,j}^{(k)}$, and $\theta_{t,j}^{(k)^2}$ are the despreading module output, the equivalent channel gain, and the residual interference variance, respectively. The obtained extrinsic LLR values are deinterleaved and fed to the SISO decoder. The recursive chip-level combining algorithm is summarized in Table 4.1 and the block diagram of the proposed receiver is depicted in Fig. 4.2.

Table 4.1: Summary Of The Chip-Level Turbo Combining Algorithm

0. Initialization
Initialize $\underline{\tilde{\mathbf{y}}}_f^{(0)}$ and $\underline{\mathbf{D}}_i^{(0)}$ with $\mathbf{0}_{T_c N_T \times 1}$ and $\mathbf{0}_{N_T \times N_T}$, respectively.

1. Combining at round k

1.1. Update $\underline{\tilde{\mathbf{y}}}_f^{(k)}$ and $\underline{\mathbf{D}}_i^{(k)}$ according to (2.37) and (2.38).

1.2. At each iteration,

1.2.1 Compute the forward and backward filters using (4.17) and (4.18).

1.2.2 Compute the MMSE estimate of $\mathbf{x}_f$ using (4.16).

1.2.3 Compute extrinsic LLRs $\phi_{t,j,m,n}^{(e)}(k)$ according to (4.19).

1.3. end **1.2.**

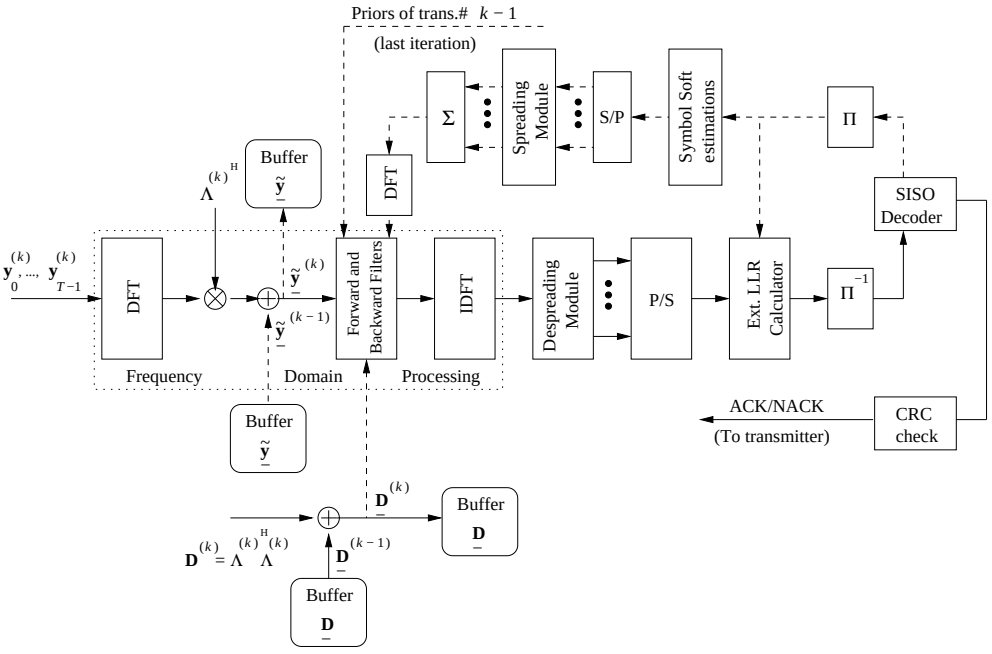

Figure 4.2: Multi-antenna multi-code CP-CDMA receiver at kth transmission with chip-level packet combining and frequency domain MMSE-based turbo equalization

4.3.2 Symbol-Level Turbo Packet Combining

In this combining scheme, the receiver performs chip-level space-time frequency domain equalization separately for each transmission then combines multiple transmissions at the level of the soft demapper. At each iteration of ARQ round k, soft ICI cancellation and MMSE filtering are performed similarly to (4.16) using communication model (4.8). The despreading module outputs at the current iteration of ARQ round k are then combined with those obtained at the last turbo iteration of previous rounds $k-1,\cdots,1$. Let $\mathbf{r}_{t,j}^{(k)} = \left[r_{t,j}^{(1)},\cdots,r_{t,j}^{(k)}\right]^{\top}$ denote the tth antenna despreading module outputs at discrete time j corresponding to transmissions $1,\cdots,k$. Assuming independence between the outputs of the despreading module of different transmissions $r_{t,j}^{(1)},\cdots,r_{t,j}^{(k)}$, the extrinsic LLR values $\phi_{t,j,m,n}^{(e)}(k)$ corresponding to coded and interleaved bits $b_{t,j,m}$ at iteration n of round k are expressed as,

$$\phi_{t,j,m,n}^{(e)}(k) = \log \frac{\sum\limits_{s\in\mathcal{S}_1^m} \exp\left\{ \boldsymbol{\xi}_{t,j}^{(k)}(s)^{\mathrm{H}} \boldsymbol{\xi}_{t,j}^{(k)}(s) + \sum\limits_{m'\neq m} \phi_{t,j,m',n}^{(a)}(k)\lambda_{m'}\{s\} \right\}}{\sum\limits_{s\in\mathcal{S}_0^m} \exp\left\{ \boldsymbol{\xi}_{t,j}^{(k)}(s)^{\mathrm{H}} \boldsymbol{\xi}_{t,j}^{(k)}(s) + \sum\limits_{m'\neq m} \phi_{t,j,m',n}^{(a)}(k)\lambda_{m'}\{s\} \right\}}, \tag{4.21}$$

where $\boldsymbol{\xi}_{t,j}^{(k)}(s) = \left|\mathbf{r}_{t,j}^{(k)} - \mathbf{g}_{t,j}^{(k)} s\right| \boldsymbol{\theta}_{t,j}^{(k)^{-1}}$, with $\mathbf{g}_{t,j}^{(k)} = \left[g_{t,j}^{(1)},\cdots,g_{t,j}^{(k)}\right]^{\mathrm{T}}$ is the equivalent channel gain and $\boldsymbol{\theta}_{t,j}^{(k)} = \mathrm{diag}\left\{\theta_{t,j}^{(1)},\cdots,\theta_{t,j}^{(k)}\right\}$ is the residual interference covariance matrix corresponding to transmissions $1,\cdots,k$.

Implementation Aspects: To relax the constraint put by the memory space required for storing the outputs of the despreading module of different transmissions, we introduce the new variable $\overline{\boldsymbol{\xi}}_{t,j}^{(k)}(s)$ computed according to the following recursion,

$$\begin{cases} \overline{\boldsymbol{\xi}}_{t,j}^{(k)}(s) = \overline{\boldsymbol{\xi}}_{t,j}^{(k-1)}(s) + \frac{\left|r_{t,j}^{(k)} - g_{t,j}^{(k)} s\right|^2}{\theta_{t,j}^{(k)^2}}, \\ \overline{\boldsymbol{\xi}}_{t,j}^{(0)}(s) = 0. \end{cases} \tag{4.22}$$

The extrinsic LLR $\phi_{t,j,m,n}^{(e)}(k)$ in (4.21) is then expressed as,

$$\phi_{t,j,m,n}^{(e)}(k) = \log \frac{\sum\limits_{s\in\mathcal{S}_1^m} \exp\left\{ \overline{\boldsymbol{\xi}}_{t,j}^{(k)}(s) + \sum\limits_{m'\neq m} \phi_{t,j,m',n}^{(a)}(k)\lambda_{m'}\{s\} \right\}}{\sum\limits_{s\in\mathcal{S}_0^m} \exp\left\{ \overline{\boldsymbol{\xi}}_{t,j}^{(k)}(s) + \sum\limits_{m'\neq m} \phi_{t,j,m',n}^{(a)}(k)\lambda_{m'}\{s\} \right\}}, \tag{4.23}$$

The recursions (4.22) presents the major ingredient in the proposed symbol-level combining

Table 4.2: Summary Of The Symbol-Level Turbo Combining Algorithm

0. Initialization:
Initialize $\overline{\boldsymbol{\xi}}_{t,j}^{(0)}(s)$ with 0.

1. Combining at round k

1.1. At each iteration,

1.1.1 Compute the forward and backward filters using (4.17) and (4.18) with $\underline{\mathbf{D}}_i^{(k)} = \boldsymbol{\Lambda}_i^{(k)^H} \boldsymbol{\Lambda}_i^{(k)}$.

1.1.2 Compute the MMSE estimate on $\mathbf{x}_f$ using (4.16) and $\underline{\tilde{\mathbf{y}}}_f^{(k)} = \boldsymbol{\Lambda}^{(k)^H} \mathbf{y}_f^{(k)}$.

1.1.3 Update $\overline{\boldsymbol{\xi}}_{t,j}^{(k)}(s)$ according to (4.22).

1.1.4 Compute extrinsic LLRs $\phi_{t,j,m,n}^{(e)}(k)$ using (4.23).

1.3. end **1.1.**

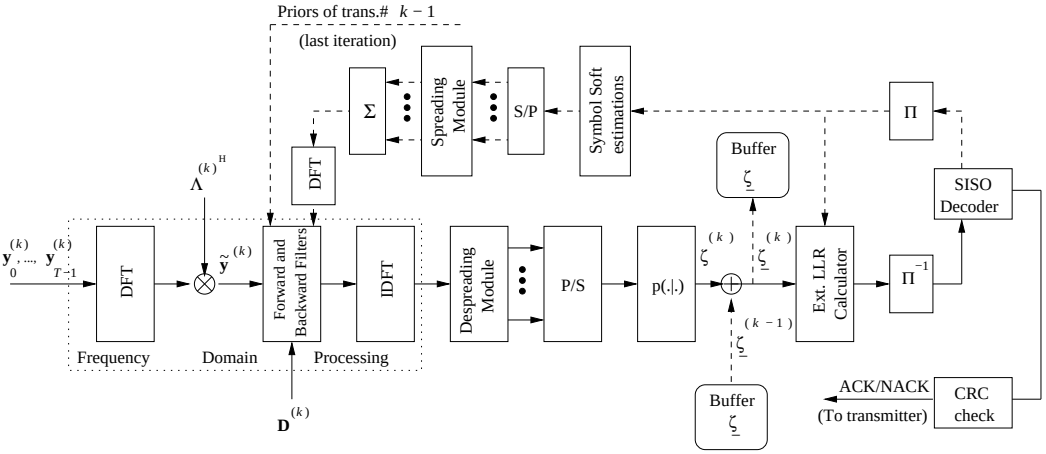

Figure 4.3: Multi-antenna multi-code CP-CDMA receiver at kth transmission with symbol-level packet combining and frequency domain MMSE-based turbo equalization.

algorithm since both complexity and memory requirements become quite insensitive to the ARQ delay. The proposed recursive algorithm is summarized in Table 4.2 and the block diagram is presented in Fig. 4.3.

4.4 Complexity and Performance Analysis

4.4.1 Complexity Evaluation

Herein, we briefly analyze both the computational cost and the memory requirements for the studied recursive combining schemes. First, note that other than updating $\underline{\tilde{\mathbf{y}}}_f^{(k)}$ and $\underline{\mathbf{D}}_i^{(k)}$ in Table 4.1, **1.1.** , and $\overline{\boldsymbol{\xi}}_{t,j}^{(k)}(s)$ in Table 4.2 , **1.1.3.**, both algorithms remain identical from one transmission to another. They have both similar computational complexities. The only implementation cost difference between both algorithms comes from the memory

Table 4.3: Summary of the Maximum Number of Arithmetic Additions, and Memory Size

	Chip-Level Combining	**Symbol-Level Combining**
Arithmetic Additions	$2T_s \frac{N}{C} N_T (K-1)(N_T+1)$	$T_s N_T (K-1) N_{\text{iter}} \lvert\mathcal{S}\rvert$
Memory	$2T_s \frac{N}{C} N_T (N_T+1)$	$T_s N_T \lvert\mathcal{S}\rvert$

requirements and arithmetic additions required to perform (2.37), (2.38), and (4.22).

The main idea in the proposed algorithms is to exploit the diversity among all transmissions without explicitly storing required 'data', i.e. signals, CFRs or filter outputs, corresponding to all ARQ rounds. This is performed with the aid of the recursions (2.37), (2.38), and (4.22), and translates into a memory size of $2T_c N_T (N_T+1)$ and $T_s N_T \lvert\mathcal{S}\rvert$ real values required to implement chip-level turbo combining algorithm and symbol-level turbo combining algorithm, respectively. Note that the memory requirements for both algorithms are insensitive to the number of rounds, which is very attractive particularly for mobile receivers. The number of rounds only influences the number of arithmetic additions required in the recursions. At each round k, the chip-level turbo combining algorithm involves $2T_c N_T$ and $2T_c N_T^2$ arithmetic additions to update $\underline{\tilde{\mathbf{y}}}_f^{(k)}$ and $\underline{\mathbf{D}}_i^{(k)}$, respectively. In the symbol-level turbo combining algorithm, at each round k, the update of $\overline{\boldsymbol{\xi}}_{t,j}^{(k)}(s)$ involves $T_s N_T N_{\text{iter}} \lvert\mathcal{S}\rvert$ arithmetic additions, with N_{iter} denotes the number of turbo iterations at each ARQ round. Table 4.3 summarizes the implementation requirements of the chip-level turbo combining scheme and the symbol-level turbo combining scheme. Note that the implementation cost of both algorithms does not depend on the same 'parameters'. While chip-level turbo combining scheme implementation cost involves the number of transmit antennas and the factor $\frac{N}{C}$, the implementation cost of symbol-level turbo combining scheme depends mainly on the constellation length and the number of turbo iterations.

4.4.2 Performance Evaluation

The system used for the evaluation has $N_T = 2$ transmit antennas, $N_R = \{1, 2, 4\}$ receive antennas, spreading factor $N = 16$, Quadrature Phase Shift Keying (QPSK) modulation and 16 states convolutional encoder with polynomial generators $(35, 23)_8$. The length of the coded frame is 1024 bits including tails. The MIMO channel has $L = 10$ chip spaced paths with equally distributed power. The CP length is $T_{CP} = 10$. We employ the Max-Log-MAP algorithm for SISO decoding. The E_c/N_0 ratio appearing in all figures is the SNR per chip per receive antenna. We have noticed via simulations that no remarkable performance improvement is obtained when the number of iterations is greater than three. The turbo process is therefore stopped after three iterations for each transmission and the maximum number of transmissions is set to $K = 3$. we evaluate the performance of the proposed multi-antenna multi-code CP-CDMA receivers in term of BLER and Throughput η. The MFB is used to evaluate the diversity achievement of the proposed algorithms. In

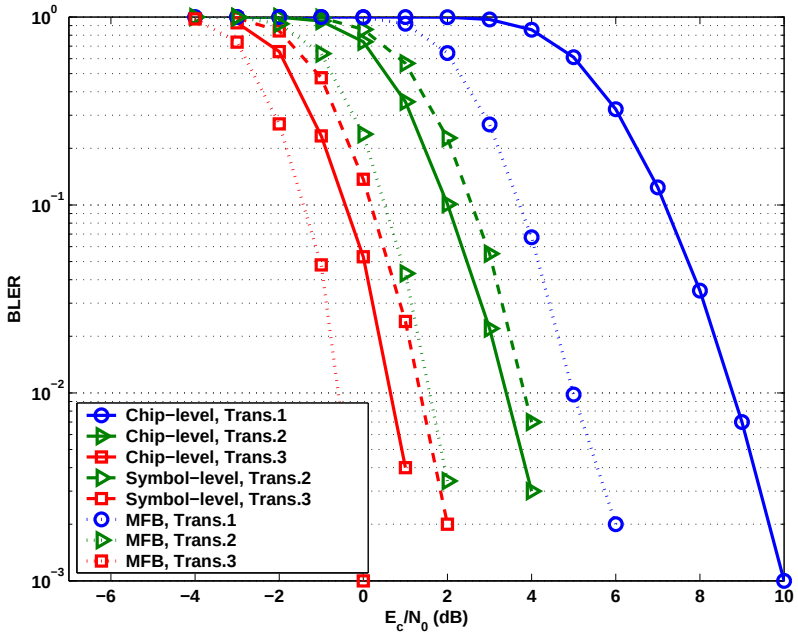

Figure 4.4: BLER performance with $N_T = 2$, $N_R = 2$, $C = 16$, $L = 10$ equal power taps profile, spectrum efficiency = 32bits/channel use.

term of complexity, the number of arithmetic additions is relatively insignificant compared with the whole computational cost of the receiver. Therefore, we consider the memory requirements as the major parameter to take into account to evaluate the studied combining schemes in term of implementation cost.

We first investigate performance for balanced configurations, i.e., $N_T = N_R$, with all codes are assigned to one user ($C = 16$). Fig. 4.4 compares the BLER performance for the chip-level and symbol-level combining with MFB. As expected, the chip-level combining outperform symbol-level combining. This result is due to the fact that in chip-level combining, each ARQ round is considered as a set of virtual N_R receive antennas. However, in term of implementation cost, symbol-level requires 66% less memory capacity than chip-level combining with a performance gap of 0.7dB at 10^{-2} BLER for both second and third transmissions. Fig. 4.4 plots also the MFB to evaluate the diversity achievement of proposed algorithms. We observe that with chip-level combining a maximum of diversity is achieved and the gap between the proposed combining scheme and MFB is reduced from 4dB in the first transmission to 1dB in the third transmission at 10^{-2} BLER. We also evaluate the system configuration with large number of antennas $N_T = N_R = 4$. In this configuration, the chip-level combining is still the best in term of performance (Fig. 4.5). However, it requires a memory capacity almost 5 times the one required by the symbol-level combining. As the performance gap between this two combining schemes is less than 1dB, the symbol-level combining can be the best candidate for system where all codes are

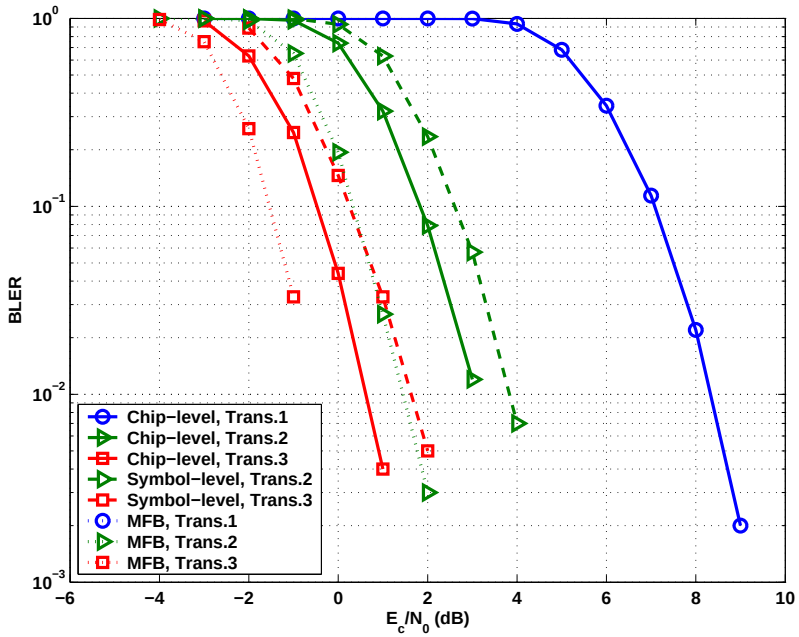

Figure 4.5: BLER performance with $N_T = 4$, $N_R = 4$, $C = 16$, $L = 10$ equal power taps profile, spectrum efficiency = 64bits/channel use.

assigned to one user with large number of antennas and low level modulation. In Fig. 4.6, we examine overloaded configuration where $N_T = 2$ and $N_R = 1$. Chip-level combining significantly outperforms symbol-level combining, the gap between this two techniques is more than 5dB for the second transmission and 3dB for the third transmission at 10^{-2} BLER.

Now, we turn to the case where all codes are not necessarily assigned to one user. We start by evaluating the throughput of the considered system with $N_T = N_R = 2$. The simulation results are depicted in Fig. 4.7 where three sets of curves are shown for $C = 4$, 8 and 16. In this configuration, both combining schemes yield quasi-identical performance, the gap between the proposed packet combining techniques is less than 0.7dB. We also evaluate multiple input single output transmission systems which are of special interest for downlink radio mobile applications. Fig. 4.8 plots throughput for $N_T = 2$ and $N_R = 1$. Chip-Level turbo combining scheme clearly outperforms symbol-Level turbo combining scheme. The performance gap is more than 5dB for systems with high ICI, i.e., $C = 16$. In systems with less ICI, i.e. $C = 4$, this gap is reduce to 1dB. In term of implementation cost, note that in balanced configuration, since both schemes have quasi-identical performance, symbol-level combining scheme is the best candidate with the least memory requirements. In the overloaded systems scenario, the chip-level combining scheme is the best in term of performance. In the case when $C = N$, this scheme needs just 50% more memory than symbol-level turbo combining scheme and can be chosen as the best candidate. However,

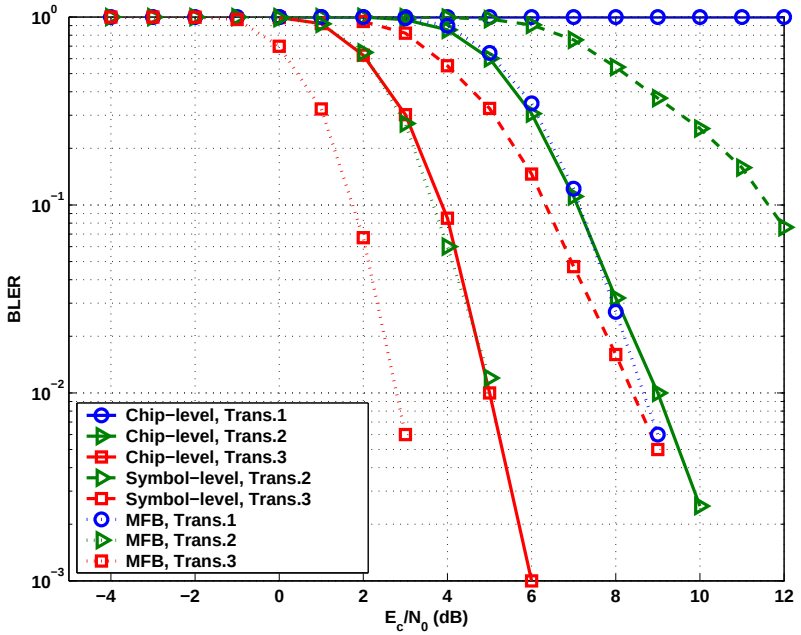

Figure 4.6: BLER performance with $N_T = 2$, $N_R = 1$, $C = 16$, $L = 10$ equal power taps profile, spectrum efficiency = 32bits/channel use.

when less multiplexed codes are used, i.e $C = 4$, the performance gap between the proposed schemes is reduced as the complexity gap becomes huge. In this case the symbol-level turbo combining scheme becomes be the best candidate.

4.5 Conclusions

In this chapter, efficient turbo receiver schemes for single user multi-code CP-CDMA transmission with ARQ operating over a broadband MIMO channel was introduced. The key idea of the proposed schemes is to exploit the diversity among all transmissions with a very low cost by introducing new variables recursively computed. Two packet combining algorithms were presented. The first algorithm consists in performing packet combining jointly with frequency domain chip level turbo equalization. The second proposed algorithm performs packet combining jointly with turbo demapping. Complexity evaluation showed that each combining scheme could be the most attractive in term of implementation cost depending on the number of transmit antennas, the factor $\frac{N}{C}$, the constellation length, and the number of turbo iterations. Moreover, simulations demonstrated that the presented combining schemes yield quasi-identical performance in a system with the same number of transmit and receive antennas. However, the chip-level packet combining scheme outperforms symbol-level packet combining scheme for overloaded configurations.

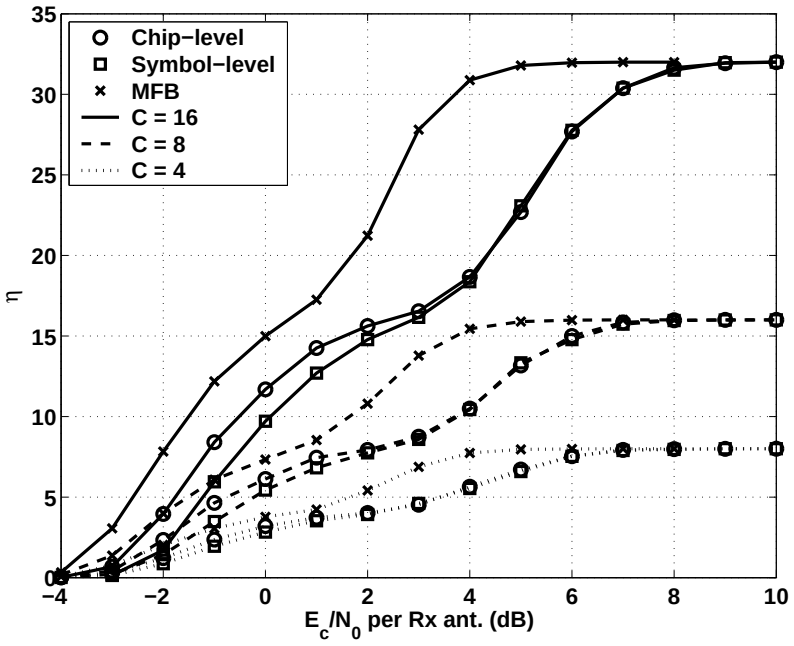

Figure 4.7: Throughput performance with $N_T = 2$, $N_R = 2$, $L = 10$ equal power taps profile.

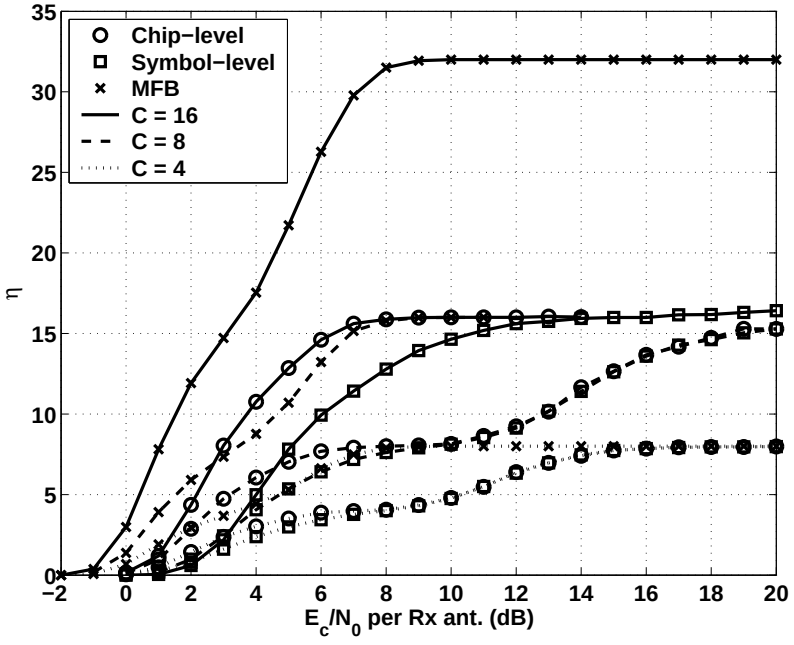

Figure 4.8: Throughput performance with $N_T = 2$, $N_R = 1$, $L = 10$ equal power taps profile.

Chapter 5

Turbo Packet Combining for Relaying Schemes over Multi-Antenna Broadband Channels

5.1 Introduction

ARQ combined with FEC is a popular mechanism to exploit temporal diversity. However, it suffers from temporal diversity limitations especially in slow fading environments due to the long-term static dynamic of the ARQ fading channel where multiple ARQ rounds see the same channel realizations. In [7], the authors have proposed cooperative relaying transmission as a solution for mitigating these diversity limitations. This cooperative diversity version exploits the broadcast nature of the wireless channel and adds spatial diversity by incorporating relays in the network. The relays play the role of packet retransmitters instead of the source, thereby creating an independent channel to increase the diversity order. Cooperative relaying presents a good alternative to classical ARQ and has recently received a lot of attention in the research community (see for instance [8], [9]). In this new transmission mechanism, one or more relays assist the communication between the source and destination to form a MIMO system and therefore build up space-time diversity branches that are exploited at the destination. In this chapter, we focus on cooperative ARQ communications where the feedback from the destination is exploited and the packet relaying is activated only if the destination fails to decode the data packet [66, 67]. The cooperative ARQ can be viewed as extension of the classical ARQ to the relay context where the relay retransmits the packet upon the reception of a NACK feedback from the

destination.

In relay communications, different approaches can be used to relay the message from the source to the destination.The well known modes are amplify-and-forward (AF) and decode-and-forward (DF). The AF scheme represents the simplest way that a relay may cooperate with the source and the destination. Under this scheme, the relay simply amplifies the received signal and forwards it towards the destination. However, in the DF scheme, the relay first decodes the signal received from the source, re-encodes and retransmits it to the destination. This approach suffers from error propagation when the relay transmits an erroneously decoded data block [65, 68]. Selective DF, where the relay only transmits when it can reliably decode the data packet, has been introduced as an efficient method to reduce error propagation [69]. However, the unsuccessful detection of the data packet by one or more relays can limit the benefit of relaying. In fact, for each incorrectly detected packet, there is a waste of one slot. To prevent the occurring "silence", a modified selective DF scheme has been proposed in [65], [70], and [71]. In this scheme, when the relay fails to correctly decode the packet, it sends back a NACK message to the source that directly transmits the packet to the destination during the allocated relay slot. In this work, we refer to this scheme as modified selective DF.

To improve spatial diversity of a relaying system, signals received over the source-destination and the relay-destination links are combined at the receiver side. In [72], the authors have introduced a maximum ratio combining (MRC)-aided strategy for AF scheme operating under protocol I[1]. Block equalization has been proposed in [74] for protocol III[2]. As a generalization of ARQ mechanisms, protocol II has been proposed in [65] and [73]. In this protocol, the operation mode during the first slot is similar to that of protocol I, while during the second slot only the relay sends the packet to the destination. To the best of the authors knowledge, previous works proposed under the framework of protocol II didn't present a real study of packet combining and simply suggest the use of one of combining techniques widely studied in the classical point-to-point hybrid ARQ [65, 75]. However, the extension of this combining strategies, especially *virtual antenna* based combining, to cooperative communications is not straightforward and this is what this chapter aims to show.

In this chapter, we consider three relaying schemes, AF, selective DF, and modified selective DF. Our main contribution is to build an appropriate system model to mask the cooperation and simplify the application of *virtual antenna* based combining. The proposed communication model is of a great use especially in practical cooperative networks where the different relays selected to assist the data packet transmission between the source and the destination do not necessarily use the same relaying schemes or perform us-

[1]In protocol I, the source broadcasts the data packet to both the relay and the destination during the first slot, and both the source and the relay re-send the packet to the destination during the relaying slot [73].

[2]In protocol II, the broadcast nature of the channel is not considered, i.e., the source sends to the relay during the first slot, and both the source and the relay send to the destination in the relaying slot [73].

ing an hybrid AF/DF scheme[3]. In contrast with point-to-point hybrid ARQ, transmissions over relaying links in AF scheme suffer from colored noise as well as correlation between source-to-relay and relay-to-destination multi-path channels. To mask this cooperation problems, we perform whitening using Cholesky decomposition and derive an equivalent source-to-relay-to-destination channel. In DF schemes, the need of an equivalent system to mask the cooperation comes from the heterogeneous nature of cooperative networks where the different nodes are equipped with different number of antennas. As far as we know, previous works that studied packet combining for multi-antenna DF cooperative relaying assume the space-time encoder used by both the source and the relays to be the same. In this work, we focus on multi-rate DF cooperative relaying where the source and the relays use the same encoder but are equipped with different number of antennas. In order to cover the cooperation, we derive a fixed rate equivalent multi-antenna system communication model. In this equivalent system, the multi-rate multi-node received signals can be viewed as direct retransmissions from a virtual node with a fixed transmission rate. As a second contribution, we investigate the outage probability of different relaying schemes. To the best of the authors knowledge, previous works that addressed outage analysis of relay communication systems have focused on the case of single relay transmissions over flat fading channels (see for instance [69] and [71]). In this chapter, we provide outage analysis of multi-relay cooperative ARQ systems operating over multi-antenna frequency selective fading channels. Using simulations, we show that the studied relaying schemes outperform each other depending on relay locations and demonstrate that the multi-relay transmissions provide better diversity gain than the conventional hybrid-ARQ. We also extend the turbo packet combiner inspired by MMSE criterion we have introduced in chapter 2, to the case of cooperative ARQ systems.

The remainder of the chapter is organized as follows: In Section 5.2, we introduce the unified communication model for the relaying schemes together with the multi-slot block communication model. In Section 5.3, we propose the structure of the turbo MAP packet combiner and investigate the outage probability of the considered relaying schemes. In section 5.4, we briefly describe the MMSE-based turbo combining scheme. Performance evaluation is provided in Section 5.5. Finally, the chapter is concluded in Section 5.6.

5.2 Relay System model

5.2.1 Multi-Relay Transmission Scheme

We consider a multi-relay-assisted wireless communication system, where the M_{S} antenna source terminal denoted as S transmits information blocks to the M_{D} antenna destination terminal denoted as D with the assistance of $K-1$ dedicated relays denoted as

[3]In hybrid AF/DF scheme, depending on the channel condition of the source-to-relay link, the better scheme between AF and DF is selected [**?**].

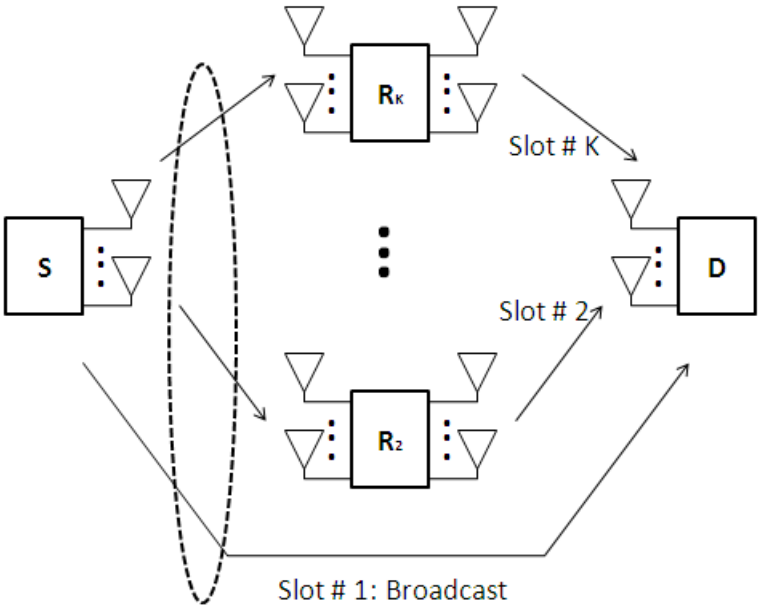

Figure 5.1: Block diagram of the considered multi-relay assisted systems.

$\mathrm{R}_2, \cdots, \mathrm{R}_k, \cdots, \mathrm{R}_K$. Each relay R_k is equipped with M_{R_k}transmit and receive antennas. We consider a relaying system using up to K time slots for sending one information block from the source to the destination to guarantee orthogonal transmissions. During the first time slot, the source broadcasts the data packet to the $K-1$ relays and the destination. During the following slots, each relay participates to the packet retransmission during the allocated slot and keeps silent during the other slots. This protocol scheme presents a generalization of ARQ mechanisms and is widely regarded as an efficient relaying scheme for increasing the overall throughput with a very well battery life saving [65, 73]. The block diagram of the considered system is depicted in Fig. 5.1. In this work, we focus on cooperative ARQ communication where the feedback from the destination is exploited and *packet retransmission is activated only if the destination fails to decode the data packet.* Therefore, during the relaying slots, once decoding is successful, the destination broadcasts an ACK message to the source and the relays to stop relaying the current block and move on to the next information block. We suppose perfect packet error detection and assume that the one bit ACK/NACK feedback message is error-free. The source-relay ($\mathrm{S} \rightarrow \mathrm{R}_k$), source-destination ($\mathrm{S} \rightarrow \mathrm{D}$), and relay-destination ($\mathrm{R}_k \rightarrow \mathrm{D}$) links are assumed to be frequency selective. The channel matrices corresponding to the $\mathrm{A} \rightarrow \mathrm{B}$ link are $\mathbf{H}_0^{(\mathrm{AB})}, \cdots, \mathbf{H}_{L_{\mathrm{AB}}-1}^{(\mathrm{AB})} \in \mathbb{C}^{M_{\mathrm{B}} \times M_{\mathrm{A}}}$ with L_{AB} denotes the number of symbol-spaced taps, $\mathrm{A} \in \{\mathrm{S}, \mathrm{R}_k\}$, and $\mathrm{B} \in \{\mathrm{R}_k, \mathrm{D}\}$. Their entries are zero-mean circularly symmetric complex Gaussian random variables. CP-aided transmission is assumed for all links. The average energies of the different links are E_{SR_k}, E_{SD} and $E_{\mathrm{R}_k\mathrm{D}}$, and take into account the

path-loss and shadowing effects of each link. We suppose that no CSI at the transmitter is available and assume perfect CSI at the relays and the destination.

First, the source encodes its data blocks using a ST–BICM encoder. The source node transmission rate is denoted $\mathcal{R}_1$. Moreover, to have independent transmitted symbols, we suppose infinitely deep interleaving. The resulting symbol vector is given by,

$$\mathbf{s} \triangleq \left[\mathbf{s}_0^{(1)^\top}, \cdots, \mathbf{s}_{T_1-1}^{(1)^\top}\right]^\top \in \mathcal{S}^{M_1 T_1}, \tag{5.1}$$

where

$$\mathbf{s}_i^{(1)} \triangleq \left[s_{1,i}^{(1)}, \cdots, s_{t,i}^{(1)}, \cdots, s_{M_{\mathrm{S}},i}^{(1)}\right]^\top \in \mathcal{S}^{M_1}, \tag{5.2}$$

is the symbol vector at channel use $i = 0, \cdots, T_1 - 1$, $M_1 = M_S$, and $\mathcal{S}$ is the symbol constellation set. During the first slot, the source inserts a CP symbol word of length $T_{CP}^{(1)} \geq \max_{k=2,\cdots,K} (L_{\mathrm{SR}_k}, L_{\mathrm{SD}})$, then broadcasts the resulting symbol frame. After CP deletion, the baseband $M_{\mathrm{D}} \times 1$ signal vector obtained at the destination side is given by,

$$\mathbf{y}_i^{(1)} = \sqrt{E_{\mathrm{SD}}} \sum_{l=0}^{L_{\mathrm{SD}}-1} \mathbf{H}_l^{(1)} \mathbf{s}_{(i-l) \bmod T_1}^{(1)} + \mathbf{n}_i^{(1)}, \tag{5.3}$$

where $\mathbf{H}_l^{(1)} = \mathbf{H}_l^{(\mathrm{SD})}$, and $\mathbf{n}_i^{(1)} \sim \mathcal{N}\left(\mathbf{0}_{M_{\mathrm{D}} \times 1}, \sigma^2 \mathbf{I}_{M_{\mathrm{D}}}\right)$ is the thermal noise. During the following $K-1$ slots, the transmission strategy depends on the considered relaying scheme. In the remainder of this subsection, our main focus is to derive a unified communication model to mask the cooperation.

5.2.1.1 Decode-and-Forward Relaying

In both DF schemes, i.e., selective DF and modified selective DF, each relay first decodes the received signal packet. If the decoding outcome is correct, the relay re-encodes the information block and upon the reception of an NACK message from the destination, the relay retransmits the resulting symbol block during the allocated slot. If the relay k decoding outcome is erroneous, the packet retransmission is not activated during slot k for selective DF. However, for modified selective DF, the relay broadcasts a NACK message to both the destination and the source to indicate that during the allocated slot the source is going to directly send the symbol frame to the destination. In this work, we assume that all relays use the same BICM encoder as the source, i.e., the same channel encoder, the same interleaver and the same constellation set. However, the transmission rate can change from slot to slot depending on the number of relay transmit antennas. As far as we know, previous works that studied DF relay communication systems have focused on fixed transmission rate. It has been assumed that the number of relay antennas is greater than the number of source antennas, i.e., $M_{\mathrm{R}_k} \geq M_{\mathrm{S}}$, and the relay uses only M_{S} transmit antennas for packet relaying. This reduces the inter-symbol interferences and

simplify the signal level packet combining at the destination side [69]. This assumption does not necessarily hold when the different nodes in the network are equipped with different number of antennas. In this work, we consider a general case where some relays could have less number of antennas than the source, i.e., $M_{\mathrm{R}_k} < M_{\mathrm{S}}\ \exists k$. In this chapter, we refer to this kind of systems as multi-rate cooperative system. Note that for the case where $M_{\mathrm{R}_k} \geq M_{\mathrm{S}}$, the relay k uses only M_{S} transmit antennas for packet relaying.

Therefore, if the data packet is correctly decoded, the relay re-encodes it using the same BICM encoder as the source. During the allocated slot, the relay retransmits the resulting symbol vector to the destination using M_k transmit antennas, i.e., $M_k = M_{\mathrm{S}}$ if $M_{\mathrm{R}_k} \geq M_{\mathrm{S}}$ otherwise $M_k = M_{\mathrm{R}_k}$. Note that the transmission rate of the relay k is then $\mathcal{R}_k = \frac{M_k}{M_{\mathrm{S}}}\mathcal{R}_1$. As a result, we get multi–rate transmissions where the same symbol block at the output of the BICM encoder is mapped over different number of transmit antennas. At slot $k = 2, \cdots, K$, the resulting symbol vector at channel use $i = 0, \cdots, T_k - 1$ is given by,

$$\mathbf{s}_i^{(k)} \triangleq \left[s_{1,i}^{(k)}, \cdots, s_{t,i}^{(k)}, \cdots, s_{M_k,i}^{(k)}\right]^{\top} \in \mathcal{S}^{M_k}, \tag{5.4}$$

where $T_k = \frac{M_{\mathrm{S}}}{M_k}T_1$ is the number of channel uses during slot k. Before transmission, the relay inserts a CP symbol word of length $T_{CP}^{(k)} \geq L_{\mathrm{R}_k\mathrm{D}}$. Therefore, at slot $k = 2, \cdots, K$, the received signal at the destination side is expressed as

$$\widehat{\mathbf{y}}_i^{(k)} = \sqrt{E_k}\sum_{l=0}^{L_k^{'}-1}\widehat{\mathbf{H}}_l^{(k)}\mathbf{s}_{(i-l)\bmod T_k}^{(k)} + \widehat{\mathbf{n}}_i^{(k)}, \tag{5.5}$$

where $\widehat{\mathbf{H}}_l^{(k)} = \mathbf{H}_l^{(\mathrm{R}_k\mathrm{D})} \in \mathbb{C}^{M_{\mathrm{D}}\times M_k}$, $L_k^{'} = L_{\mathrm{R}_k\mathrm{D}}$, and $E_k = E_{\mathrm{R}_k\mathrm{D}}$. For modified selective DF, if the relay decoding outcome is erroneous, the relay broadcasts a NACK message to both the destination and the source to indicate that during the allocated slot the source is going to directly send the symbol frame to the destination. In that case, the received signal at the destination side is expressed as in (5.5), with $T_k = T_1$, $M_k = M_1$, $\mathbf{s}_i^{(k)} = \mathbf{s}_i^{(1)}$, $\widehat{\mathbf{H}}_l^{(k)} = \mathbf{H}_l^{(\mathrm{SD})}$, $L_k^{'} = L_{\mathrm{SD}}$, and $E_k = E_{\mathrm{SD}}$.

At each slot $k = 1, \cdots, K$, the block communication model at the destination side can be written as,

$$\mathbf{y}^{(k)} = \boldsymbol{\mathcal{H}}^{(k)}\mathbf{s} + \mathbf{n}^{(k)}, \tag{5.6}$$

where

$$\begin{cases} \mathbf{y}^{(k)} \triangleq \left[\mathbf{y}_0^{(k)^{\top}}, \cdots, \mathbf{y}_{T_k-1}^{(k)^{\top}}\right]^{\top} \in \mathbb{C}^{M_{\mathrm{D}}T_k} \\ \mathbf{s} \triangleq \left[\mathbf{s}_0^{(k)^{\top}}, \cdots, \mathbf{s}_{T_k-1}^{(k)^{\top}}\right]^{\top} \in \mathcal{S}^{M_kT_{\mathrm{k}}} \\ \mathbf{n}^{(k)} = \left[\mathbf{n}_0^{(k)^{\top}}, \cdots, \mathbf{n}_{T_k-1}^{(k)^{\top}}\right]^{\top} \in \mathbb{C}^{M_{\mathrm{D}}T_k}, \end{cases} \tag{5.7}$$

$\boldsymbol{\mathcal{H}}^{(k)} \in \mathbb{C}^{T_kM_{\mathrm{D}}\times T_kM_k}$ is a block circulant matrix whose first $T_kM_{\mathrm{D}} \times M_k$ column matrix is $\left[\mathbf{H}_0^{(k)^{\top}}, \cdots, \mathbf{H}_{L_k-1}^{(k)^{\top}}, \mathbf{0}_{M_k\times(T_k-L_k)M_{\mathrm{D}}}\right]^{\top}$, and M_k and T_k are, respectively, the number of

transmit antennas and number of channel uses during slot k. Note that the slot index k is not used for the symbol vector $\mathbf{s}$ because it is the same for all slots (the source and the relays use the same BICM encoder).

Our main focus is to derive a fixed rate equivalent MIMO system block communication model where the multi-rate multi-node received signals can be viewed as direct retransmissions from a virtual node with a fixed transmission rate. Using communication model (5.6), the studied relaying system can be viewed as a classical ARQ system with $M = \mathrm{lcm}(M_1, \cdots, M_k)$ transmit antennas and $N_k = m_k M_{\mathrm{D}}$ receive antennas, where $m_k = \frac{M}{M_k}$. The equivalent MIMO system has a fixed transmission rate $\mathcal{R} = \frac{M}{M_{\mathrm{S}}}\mathcal{R}_1$. At each slot $k = 1, \cdots, K$, the symbol vector at the output of the fixed rate virtual transmitter node is given by

$$\begin{cases} \mathbf{s} \triangleq \left[\mathbf{s}_0^\top, \cdots, \mathbf{s}_{T-1}^\top\right]^\top \in S^{MT}, \\ \mathbf{s}_i \triangleq \left[s_{1,i}, \cdots, s_{M,i}\right]^\top \in S^M, \end{cases} \tag{5.8}$$

where $T = \frac{T_k}{m_k}$ is the fixed number of channel uses in the equivalent MIMO system. The virtual MIMO channel has $L_k = \left\lceil \frac{L_k^{'}}{m_k} \right\rceil$ symbol spaced taps. The channel matrix of the lth equivalent tap is expressed as,

$$\mathbf{H}_l^{(k)} = \begin{bmatrix} \widehat{\mathbf{H}}_{l\,m_k}^{(k)} & \widehat{\mathbf{H}}_{l\,m_k-1}^{(k)} & \cdots & \widehat{\mathbf{H}}_{(l-1)\,m_k+1}^{(k)} \\ \widehat{\mathbf{H}}_{l\,m_k+1}^{(k)} & \ddots & \ddots & \vdots \\ \vdots & \ddots & \ddots & \widehat{\mathbf{H}}_{l\,m_k-1}^{(k)} \\ \widehat{\mathbf{H}}_{(l+1)\,m_k-1}^{(k)} & \cdots & \widehat{\mathbf{H}}_{l\,m_k+1}^{(k)} & \widehat{\mathbf{H}}_{l\,m_k}^{(k)} \end{bmatrix} \in \mathbb{C}^{N_k \times M}, \tag{5.9}$$

with

$$\widehat{\mathbf{H}}_l^{(k)} = \mathbf{0}_{M_{\mathrm{D}} \times M_k} \quad \forall l < 0 \ \text{ and } \ l > L_k - 1. \tag{5.10}$$

The $N_k \times 1$ virtual received signal at channel use $i = 1, \cdots, T$ can therefore be expressed similarly to (5.5) as

$$\mathbf{y}_i^{(k)} = \sqrt{E_k} \sum_{l=0}^{L_k-1} \mathbf{H}_l^{(k)} \mathbf{s}_{(i-l) \bmod T} + \mathbf{n}_i^{(k)}, \tag{5.11}$$

where $\mathbf{n}_i^{(k)} \sim \mathcal{N}\left(\mathbf{0}_{N_k \times 1}, \sigma^2 \mathbf{I}_{N_k}\right)$ is the thermal noise at the virtual receiver.

5.2.1.2 Amplify-and-Forward Relaying

In AF scheme, the relay amplifies and sends the block of received signals to the destination. At each relay R_k, the $M_{\mathrm{R}_k} \times 1$ received signal, after CP removal, is expressed as,

$$\mathbf{y}_i^{(\mathrm{SR}_k)} = \sqrt{E_{\mathrm{SR}_k}} \sum_{l=0}^{L_{\mathrm{SR}_k}-1} \mathbf{H}_l^{(\mathrm{SR}_k)} \mathbf{s}_{(i-l) \bmod T_1}^{(1)} + \mathbf{n}_i^{(\mathrm{SR}_k)}, \tag{5.12}$$

where $\mathbf{n}_i^{(\mathrm{SR}_k)} \sim \mathcal{N}\left(\mathbf{0}_{M_{\mathrm{R}_k}\times 1}, \sigma^2\mathbf{I}_{M_{\mathrm{R}_k}}\right)$ is the thermal noise at the relay. The relay first normalizes received signals $\mathbf{y}_i^{(\mathrm{SR}_k)}$ as,

$$\tilde{\mathbf{y}}_i^{(\mathrm{SR}_k)} = \frac{1}{\sqrt{M_{\mathrm{S}}E_{\mathrm{SR}_k}+\sigma^2}}\mathbf{y}_i^{(\mathrm{SR}_k)}, \tag{5.13}$$

then inserts a CP signal word of length $T_{CP}^{(k)} \geq L_{\mathrm{R}_k\mathrm{D}}$ and transmits the resulting signal packet to the destination during slot k. After CP deletion, the $M_{\mathrm{D}} \times 1$ received signal, at the destination side, during slot k can be expressed as

$$\mathbf{y}_i^{(\mathrm{R}_k\mathrm{D})} = \sqrt{\frac{E_{\mathrm{R}_k\mathrm{D}}E_{\mathrm{SR}_k}}{M_{\mathrm{S}}E_{\mathrm{SR}_k}+\sigma^2}} \sum_{l=0}^{L_{\mathrm{SR}_k\mathrm{D}}-1} \mathbf{H}_l^{(\mathrm{SR}_k\mathrm{D})}\mathbf{s}_{(i-l) \bmod T_1}^{(1)} + \widetilde{\mathbf{n}}_i^{(\mathrm{SR}_k\mathrm{D})}, \tag{5.14}$$

where $\mathbf{H}_0^{(\mathrm{SR}_k\mathrm{D})}, \cdots, \mathbf{H}_{L_{\mathrm{SR}_k\mathrm{D}}-1}^{(\mathrm{SR}_k\mathrm{D})} \in \mathbb{C}^{M_{\mathrm{D}}\times M_{\mathrm{S}}}$ is the equivalent multi-path channel corresponding to link $\mathrm{S} \rightarrow \mathrm{R}_k \rightarrow \mathrm{D}$, and has $L_{\mathrm{SR}_k\mathrm{D}} = L_{\mathrm{SR}_k} + L_{\mathrm{R}_k\mathrm{D}} - 1$ symbol-spaced taps. The lth equivalent tap channel matrix is the discrete convolution of channels corresponding to $\mathrm{S} \rightarrow \mathrm{R}_k$ and $\mathrm{R}_k \rightarrow \mathrm{D}$ links and expressed as,

$$\mathbf{H}_l^{(\mathrm{SR}_k\mathrm{D})} = \begin{cases} \sum_{n=\max(0,l-L_{\mathrm{SR}_k}+1)}^{\min(l,L_{\mathrm{R}_k\mathrm{D}}-1)} \mathbf{H}_n^{(\mathrm{R}_k\mathrm{D})}\mathbf{H}_{l-n}^{(SR)}, \text{ if } L_{\mathrm{R}_k\mathrm{D}} \geq L_{\mathrm{SR}_k} \\ \sum_{n=\max(0,l-L_{\mathrm{R}_k\mathrm{D}}+1)}^{\min(l,L_{\mathrm{SR}_k}-1)} \mathbf{H}_{l-n}^{(\mathrm{R}_k\mathrm{D})}\mathbf{H}_n^{(\mathrm{SR}_k)}, \text{ otherwise.} \end{cases} \tag{5.15}$$

In (5.14), the effective zero-mean Gaussian noise is given by,

$$\widetilde{\mathbf{n}}_i^{(\mathrm{SR}_k\mathrm{D})} = \sqrt{\frac{E_{\mathrm{R}_k\mathrm{D}}}{M_{\mathrm{S}}E_{\mathrm{SR}_k}+\sigma^2}} \sum_{l=0}^{L_{\mathrm{R}_k\mathrm{D}}-1} \mathbf{H}_l^{(\mathrm{R}_k\mathrm{D})}\mathbf{n}_{(i-l) \bmod T_1}^{(\mathrm{SR}_k)} + \mathbf{n}_i^{(\mathrm{R}_k\mathrm{D})}, \tag{5.16}$$

and has conditional covariance matrix, (i.e., conditioned upon $\mathbf{H}^{(\mathrm{R}_k\mathrm{D})}$),

$$\mathbf{\Theta}_{|\mathbf{H}^{(\mathrm{R}_k\mathrm{D})}} = \sigma^2\left(\mathbf{I}_{M_{\mathrm{D}}} + \frac{E_{\mathrm{R}_k\mathrm{D}}}{M_{\mathrm{S}}E_{\mathrm{SR}_k}+\sigma^2} \sum_{l=0}^{L_{\mathrm{R}_k\mathrm{D}}-1} \mathbf{H}_l^{(\mathrm{R}_k\mathrm{D})}\mathbf{H}_l^{(\mathrm{R}_k\mathrm{D})^H}\right). \tag{5.17}$$

Note that the effective noise at the destination is colored due to the convolution by the $\mathrm{R}_k \rightarrow \mathrm{D}$ channel. We therefore proceed to a Cholesky decomposition aided whitening, i.e., $\mathbf{\Theta}_{|\mathbf{H}^{(RD)}} = \sigma^2\mathbf{L}\mathbf{L}^H$, where $\mathbf{L}$ is a $M_{\mathrm{D}} \times M_{\mathrm{D}}$ lower triangular matrix. This yields signal vector,

$$\mathbf{y}_i^{(k)} = \mathbf{L}^{-1}\mathbf{y}_i^{(\mathrm{R}_k\mathrm{D})}. \tag{5.18}$$

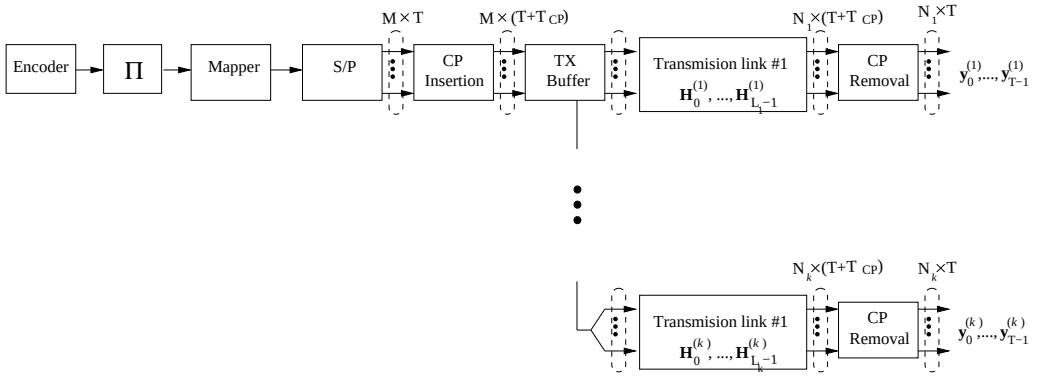

Figure 5.2: The equivalent ST–BICM diagram for multi-rate multi-relay systems.

The received signal at the destination side can therefore be expressed as in (5.11) where

$$\begin{cases} \mathbf{H}_l^{(k)} & = \mathbf{L}^{-1}\mathbf{H}_l^{(\mathrm{SR}_k\mathrm{D})}, \\ \mathbf{s}_i & = \mathbf{s}_i^{(1)}, \\ L_k & = L_{\mathrm{SR}_k\mathrm{D}}, \\ E_k & = \frac{E_{\mathrm{R}_k\mathrm{D}}E_{\mathrm{SR}_k}}{M_{\mathrm{S}}E_{\mathrm{SR}_k}+\sigma^2}, \\ M & = M_{\mathrm{S}}, \\ T & = T_1, \\ N_k & = M_{\mathrm{D}}, \end{cases} \tag{5.19}$$

and $\mathbf{n}_i^{(k)} \sim \mathcal{N}\left(\mathbf{0}_{M_{\mathrm{D}}\times 1}, \sigma^2\mathbf{I}_{M_{\mathrm{D}}}\right)$ is the whitened effective noise at the destination side.

5.2.2 Multi-Slot Block Communication Model

Using the unified communication model (5.11), the received signals during the relaying slots can be viewed as a direct retransmissions from the source as it is shown in Fig. 5.2. In fact, (5.11) is of a great importance as it allows us to apply the *virtual antenna* concept at the destination side, i.e., each relaying slot can be viewed as an additional set of virtual receive antennas. Therefore, after k slots, the system (source, $k-1$ relays, and destination) can be viewed as a point to point MIMO link with M transmit and $\underline{N}_k = \sum_{u=1}^{k} N_u$ receive antennas. First, we introduce

$$\underline{\mathbf{y}}_i^{(k)} \triangleq \left[\ \mathbf{y}_i^{(1)^\top}, \cdots, \mathbf{y}_i^{(k)^\top}\ \right]^\top \in \mathbb{C}^{\underline{N}_k}, \tag{5.20}$$

where reception over multiple slots can be viewed as multi-antenna reception. Then, we construct the $\underline{N}_k T \times 1$ block received signal vector $\underline{\mathbf{y}}^{(k)}$ as,

$$\underline{\mathbf{y}}^{(k)} \triangleq \left[\underline{\mathbf{y}}_0^{(k)^\top}, \cdots, \underline{\mathbf{y}}_{T-1}^{(k)^\top}\right]^\top \in \mathbb{C}^{\underline{N}_k T}. \tag{5.21}$$

The block communication model corresponding to this k-slot scheme is given by,

$$\underline{\mathbf{y}}^{(k)} = \underline{\boldsymbol{\mathcal{H}}}^{(k)}\mathbf{s} + \underline{\mathbf{n}}^{(k)}, \tag{5.22}$$

where $\underline{\boldsymbol{\mathcal{H}}}^{(k)} \in \mathbb{C}^{\underline{N}_k T \times MT}$ is a block circulant matrix whose first $\underline{N}_k T \times M$ block column matrix is

$$\left[\underline{\mathbf{H}}_0^{(\mathrm{k})^\top}, \cdots, \underline{\mathbf{H}}_{L-1}^{(\mathrm{k})^\top}, \mathbf{0}_{M\times(T-L)\underline{N}_k}\right]^\top, \tag{5.23}$$

with

$$\begin{cases} L = \max\limits_{k=1,\cdots,K}(L_k), \\ \underline{\mathbf{H}}_l^{(k)} \triangleq \left[\ \sqrt{E_1}\,\mathbf{H}_l^{(1)^\top}, \cdots, \sqrt{E_k}\,\mathbf{H}_l^{(k)^\top}\ \right]^\top \in \mathbb{C}^{\underline{N}_k \times M} \end{cases} \tag{5.24}$$

correspond to the order and the lth tap of the virtual MIMO channel, respectively. Vector

$$\underline{\mathbf{n}}^{(k)} = \left[\underline{\mathbf{n}}_0^{(k)^\top}, \cdots, \underline{\mathbf{n}}_{T-1}^{(k)^\top}\right]^\top \in \mathbb{C}^{\underline{N}_k T}, \tag{5.25}$$

denotes the thermal noise present in the k-slot equivalent MIMO system, where $\underline{\mathbf{n}}_i^{(k)} \triangleq \left[\ \mathbf{n}_i^{(1)^\top}, \cdots, \mathbf{n}_i^{(k)^\top}\ \right]^\top \sim \mathcal{N}\left(\mathbf{0}_{\underline{N}_k\times 1}, \sigma^2\mathbf{I}_{\underline{N}_k}\right)$. Applying the DFT to the k-slot block signal vector (5.22) yields the following frequency domain block communication model,

$$\underline{\mathbf{y}}_f^{(k)} = \underline{\boldsymbol{\Lambda}}^{(k)}\mathbf{s}_f + \underline{\mathbf{n}}_f^{(k)}, \tag{5.26}$$

where

$$\begin{cases} \underline{\boldsymbol{\Lambda}}^{(k)} \triangleq \mathrm{diag}\left\{\underline{\boldsymbol{\Lambda}}_0^{(k)}, \cdots, \underline{\boldsymbol{\Lambda}}_{T-1}^{(k)}\right\} \in \mathbb{C}^{\underline{N}_k T \times MT}, \\ \underline{\boldsymbol{\Lambda}}_i^{(k)} = \sum_{l=0}^{L-1} \underline{\mathbf{H}}_l^{(k)} e^{-j(2\pi il/T)} \in \mathbb{C}^{\underline{N}_k \times M}. \end{cases} \tag{5.27}$$

5.3 Frequency Domain Turbo Packet Combining and Outage Analysis

In this section, we provide a general description of the multi-relay turbo receiver we propose in this chapter. We also investigate the outage probability of different relaying schemes. Using simulations, we show that these schemes outperform each other depending on relay locations and demonstrate that the multi-relay transmissions provide better diversity gain than the conventional hybrid-ARQ.

5.3.1 Iterative Receiver Scheme

After k slots, the receiver constructs the frequency domain block signal vector $\underline{\mathbf{y}}_f^{(k)}$ and the corresponding CFR $\underline{\boldsymbol{\Lambda}}^{(k)}$. The decoding of the information frame is iteratively performed

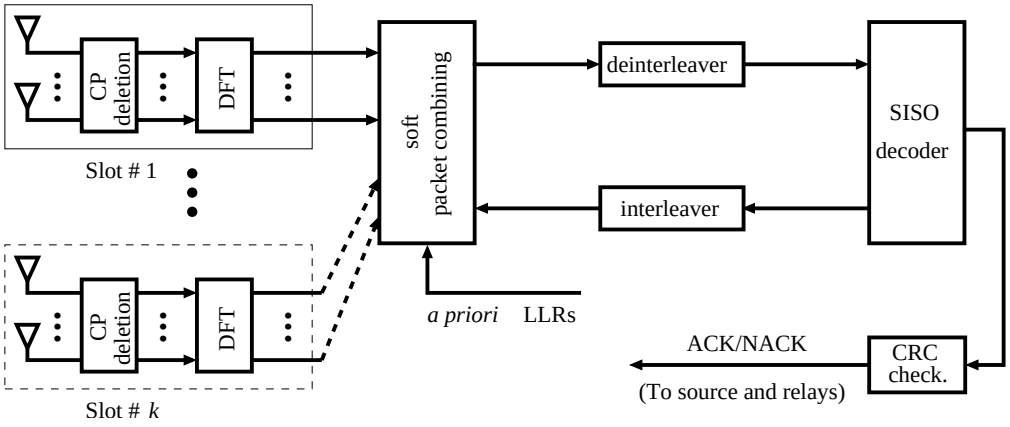

Figure 5.3: The block diagram of the turbo packet combining receiver scheme at slot k.

through the exchange of soft information between the soft combiner and the SISO decoder. First, the soft combiner computes extrinsic LLR about coded and interleaved bits using *a priori* information and signals received during slots $1, \cdots, k$. Second, the generated soft output is deinterleaved, and transferred to the SISO decoder to compute *a posteriori* LLR on useful bits and extrinsic information on coded bits. After a preset number of iterations, the decision about the data packet is performed. If the packet is incorrectly decoded, a NACK message is sent to relay $k+1$ to start packet retransmission at slot $k+1$. If the packet is correctly decoded, the destination broadcasts an ACK message to the source and the relays to stop relaying and move on to the next data packet during the next slot. The general block diagram of the iterative receiver is presented in Fig. 5.3. Let N_{iter} denote the preset number of turbo iterations performed between the soft combiner and the SISO decoder (index $n = 1, \cdots, N_{\text{iter}}$), and $\phi^{(a)}_{t,i,m,n}(k)$ denote the *a priori* LLR of coded bit $b_{t,i,m}$ available at the input of the soft combiner at iteration n of slot k. Using the MAP criterion, extrinsic LLR about coded and interleaved bit $b_{t,i,m}$ can be computed as,

$$\phi^{(e)}_{t,i,m,n}(k) = \log \frac{\sum\limits_{\mathbf{s}\in\mathcal{S}_1^{m,t,i}} \exp\left\{-\frac{1}{2\sigma^2}\left\|\underline{\mathbf{y}}_f^{(k)} - \underline{\mathbf{\Lambda}}^{(k)}\mathbf{s}_f\right\|^2 + \sum\limits_{(m',t',i')\neq(m,t,i)} \phi^{(a)}_{t',i',m',n}\lambda_{m'}\left\{s_{t',i'}\right\}\right\}}{\sum\limits_{\mathbf{s}\in\mathcal{S}_0^{m,t,i}} \exp\left\{-\frac{1}{2\sigma^2}\left\|\underline{\mathbf{y}}_f^{(k)} - \underline{\mathbf{\Lambda}}^{(k)}\mathbf{s}_f\right\|^2 + \sum\limits_{(m',t',i')\neq(m,t,i)} \phi^{(a)}_{t',i',m',n}\lambda_{m'}\left\{s_{t',i'}\right\}\right\}}, \quad (5.28)$$

where $\mathcal{S}_\beta^{m,t,i}$ is the set of symbol vectors having the mth bit in symbol $s_{t,i}$ set to $\beta \in \{0,1\}$, i.e., $\mathcal{S}_\beta^{m,t,i} = \left\{\mathbf{s} \in \mathcal{S}^{M_S T} : \lambda_m\left\{s_{t,i}\right\} = \beta\right\}$.

5.3.2 Outage Probability

The outage probability is regarded as a meaningful tool for evaluating the performance of non-ergodic channels, i.e., block fading quasi-static channels, as it provides a lower bound on the BLER [50, p. 187]. For a given SNR γ per receive antenna, the outage probability of the direct link (i.e., S $\rightarrow$ D link), at a target transmission rate $\mathcal{R}$, is defined as the probability that the mutual information I between the transmitter alphabet and the received signal is below $\mathcal{R}$,

$$P_{\text{out}}^{\text{Direct}}(\mathcal{R}, \gamma, k=1) = \Pr\left\{ I(\mathbf{s}_f, \mathbf{y}_f^{(1)} \mid \mathbf{\Lambda}^{(1)}, \gamma) < \mathcal{R} \right\}, \tag{5.29}$$

where $\mathbf{s}_f$ is the frequency domain transmitted symbol vector, $\mathbf{y}_f^{(1)}$ is the frequency domain received signal over link S $\rightarrow$ D (during slot $k=1$), and $\mathbf{\Lambda}^{(1)}$ is the corresponding CFR. In this work, we are interested in analyzing cooperative ARQ communications where packet relaying is activated only if the destination fails to decode the initially transmitted data packet. In such a scenario, packet combining starts when the direct link is in outage, i.e., $k \geq 2$.

At each slot $k \geq 2$, k copies of the transmitted packet are available at the destination side, one from the direct link and $k-1$ from relaying links, except for selective DF scheme where the number of transmitted packet copies depends on the quality of S $\rightarrow$ R link realizations. In fact, for selective DF, packet retransmission does not occur at slot u ($2 \leq u \leq k$) if the S $\rightarrow$ R$_u$ link is in outage. However, for the sake of simplicity, we assume that slot u is allocated for packet retransmission even when relaying is deactivated. Therefore, the k-slot relaying system can be viewed as a repetition coding scheme where k parallel sub-channels are used to transmit one symbol message [50, p. 194]. Using the unified communication model (5.26), the outage probability of the studied relaying schemes can be expressed as in [52], i.e.,

$$P_{\text{out}}(\mathcal{R}, \gamma, k) = \Pr\left\{ \frac{1}{k} I(\mathbf{s}_f, \underline{\mathbf{y}}_f^{(k)} \mid \underline{\mathbf{\Lambda}}^{(k)}, \gamma) < \mathcal{R},\, \mathcal{A}_1, \cdots, \mathcal{A}_{k-1} \right\}, \tag{5.30}$$

where $\mathcal{A}_u$ denotes the event that the destination sends a NACK message at slot u. In the case of i.i.d circularly symmetric complex channel inputs, the mutual information $I(\mathbf{s}_f, \underline{\mathbf{y}}_f^{(k)} \mid \underline{\mathbf{\Lambda}}^{(k)}, \gamma)$ in (5.30) can be expressed as in [76], i.e.,

$$I(\mathbf{s}_f, \underline{\mathbf{y}}_f^{(k)} \mid \underline{\mathbf{\Lambda}}^{(k)}, \gamma) = \frac{1}{T} \sum_{i=0}^{T-1} \log_2 \left(\det \left(\mathbf{I}_{\underline{N}_k} + \frac{\gamma}{M} \underline{\mathbf{\Lambda}}_i^{(k)} \underline{\mathbf{\Lambda}}_i^{(k)^{\text{H}}} \right) \right). \tag{5.31}$$

Moreover, in the special case of DF schemes, the outage probability can be expressed using the outage probabilities of S $\rightarrow$ R links. More details can be found in the Appendix B.

5.3.3 Outage Analysis

In this subsection, we analyze the outage probability of the studied relaying schemes. We use Monte Carlo simulations to evaluate system outage probability given by (5.30). First, we generate MIMO channel matrices corresponding to the S →D link and compute the mutual achievable rate using (5.31) for $k = 1$. If the achievable rate is greater than $\mathcal{R}$, the system is declared in a non outage, relaying is therefore deactivated, and the system moves on to the transmission of the next block. However if the target rate $\mathcal{R}$ is not reached when $k = 1$, the first relaying link MIMO channel matrices are generated depending on the relaying scheme in use and the mutual achievable rate is re-calculated for $k = 2$. The relaying process is stopped and the processing of the next block transmission is started, either because the achievable rate is greater than $k\mathcal{R}$ at slot $k \leq K$ or the system is in outage, i.e., the achievable rate is below $K\mathcal{R}$ at the last slot K. For simulations, we choose $T = 258$ channel use. For the sake of simplicity, we assume that all relays are at the same distance from both the source and the destination. We consider a homogeneous case where the distances between the source and relay l_{SR}, relay and destination l_{RD}, and source and destination l_{SD} are normalized in such a way that $l_{\mathrm{SR}} + l_{\mathrm{RD}} = l_{\mathrm{SD}} = 1$. All links have the same frequency-selective fading channel profile, i.e., $L = 3$ equal power paths with the same path loss exponent $\kappa = 3$. The link average energy is $E_{AB} = (l_{AB})^{-\kappa}$ with $A = \mathrm{S}$ or R, and $B = \mathrm{R}$ or D.

First, we consider a one-relay cooperative ARQ system ($K = 2$ slots) where all nodes are equipped with two antennas, i.e., $M_{\mathrm{S}} = M_{\mathrm{R}} = M_{\mathrm{D}} = 2$ and the target rate is $\mathcal{R} = 2$. In Fig. 5.4, we report the outage probability versus l_{SR} for S →D link SNR, i.e., $\mathrm{SNR}_{\mathrm{SD}} =$ 3dB. In the legend, ACK/NACK-DF (Slow Ch) and ACK/NACK-DF (fast Ch) denote the modified selective DF scheme operating over an S → D long-term static channel where the channel is constant over K consecutive slots, and a S → D short-term static channel where the channel independently changes from slot to slot, respectively. From Fig. 5.4, we notice that the optimal relay location for all studied schemes is $l_{\mathrm{SR}} = 0.5$. Moreover, the results show that AF and DF relaying outperform each other depending on the relay location. In fact, AF scheme seems to be more suitable for locations close to the destination, i.e., $l_{\mathrm{SR}} > 0.6$. However, for locations close to the source, the relay experiences better radio conditions, and the probability of successful data packet decoding becomes higher. In this case, DF schemes are more suitable. Furthermore, the studied DF schemes have similar performances when $l_{\mathrm{SR}} < 0.6$. For relay locations where $l_{\mathrm{SR}} > 0.6$, modified selective DF scheme clearly outperforms selective DF scheme. However, when the S → D link experiences slow fading the gap becomes too small. In this case, selective DF can be considered as the best DF relaying scheme as it does not involve the source during the relaying slots.

Now, we consider a multi-relay cooperative ARQ system where the source and the relays are equipped with two antennas, i.e., $M_{\mathrm{S}} = M_{\mathrm{R}} = 2$, and the target rate is $\mathcal{R} = 2$. In Fig.

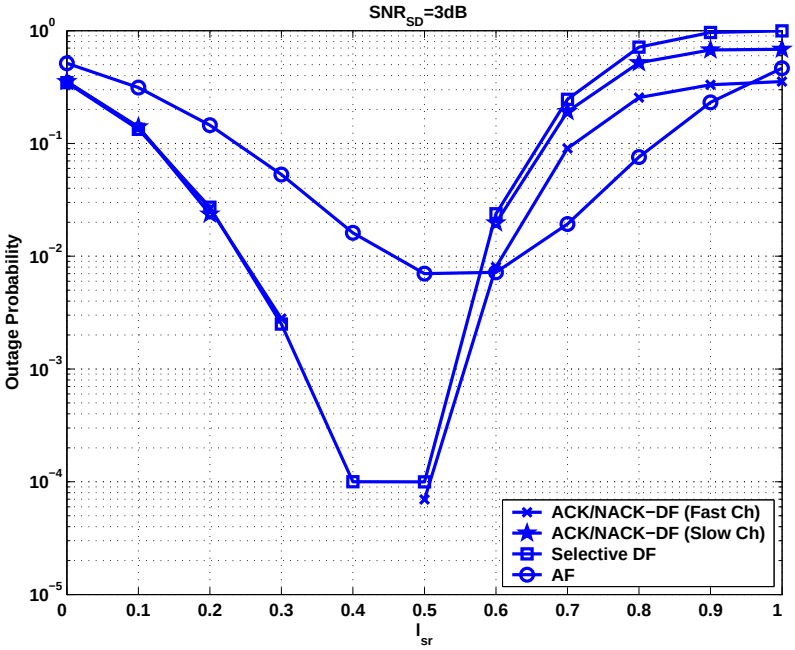

Figure 5.4: Outage probability versus l_{SR} for $M_{\mathrm{S}} = M_{\mathrm{R}} = M_{\mathrm{D}} = 2$, $K = 2$, $L = 3$, and the path loss exponent $\kappa = 3$.

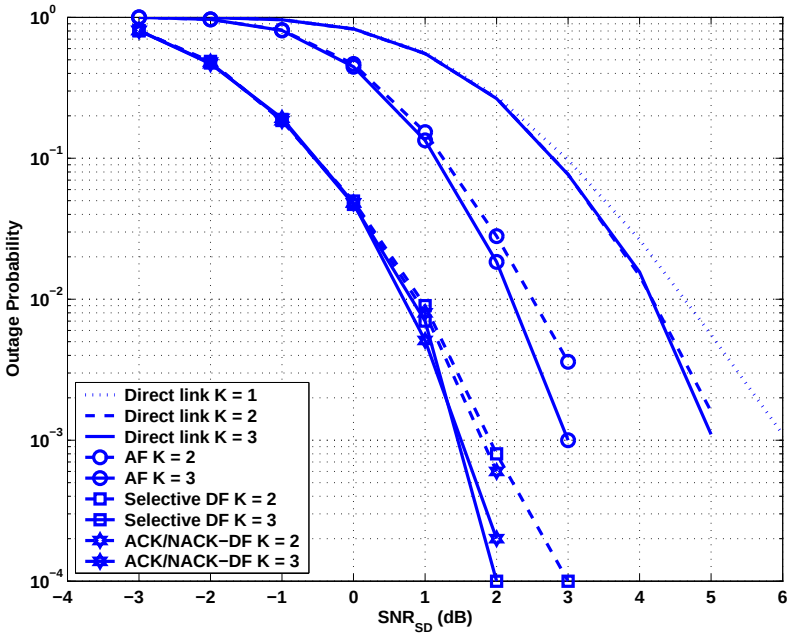

Figure 5.5: Outage probability versus $\mathrm{SNR}_{\mathrm{SD}}$ for $M_{\mathrm{S}} = M_{\mathrm{R}} = M_{\mathrm{D}} = 2$, $l_{SR} = 0.5$, $L = 3$, and the path loss exponent $\kappa = 3$.

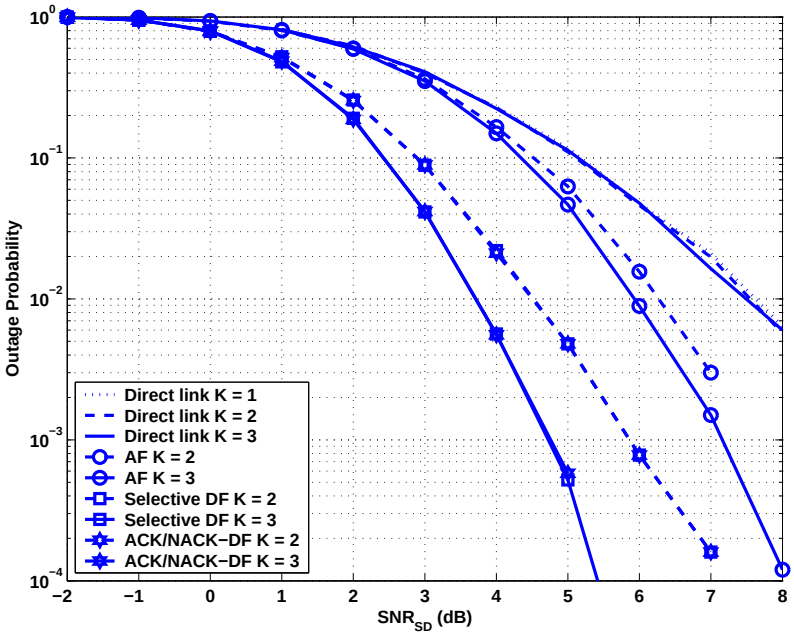

Figure 5.6: Outage probability versus $\mathrm{SNR_{SD}}$ for $M_{\mathrm{S}} = M_{\mathrm{R}} = 2$, $M_{\mathrm{D}} = 1$, $l_{SR} = 0.5$, $L = 3$, and the path loss exponent $\kappa = 3$.

5.5 and Fig. 5.6, we plot outage probability versus $\mathrm{SNR_{SD}}$ at $l_{\mathrm{SR}} = 0.5$ for one and two-relay cooperative ARQ systems ($K = 2$ and $K = 3$). In both figures, we use conventional hybrid–ARQ as a reference to evaluate the behavior of the studied relaying schemes. In this conventional packet retransmission scheme, the packet is directly retransmitted by the source without relay assistance. In the following, we assume that the $\mathrm{S} \rightarrow \mathrm{D}$ link experiences short-term quasi-static fading. This corresponds to the best scenario for conventional hybrid–ARQ where re-transmission rounds see different and independent channel realizations. In Fig. 5.5, all nodes are equipped with two antennas. In this case, for $K = 2$, the SNR gain due to packet retransmission diversity in conventional hybrid–ARQ is less than 1dB at 10^{-3} outage compared with $K = 1$. However, when relays are incorporated in the network to play the role of packet re-transmitters, this gain is increased to more than 2dB for AF relaying scheme and 5dB for DF. This high diversity gain can be reached when the relay is at the optimal location $l_{\mathrm{SR}} = 0.5$. Also, note that in conventional hybrid–ARQ transmission, the outage performance saturates after $K = 2$ while for relaying transmission, the two-relay system has a diversity gain of 0.5dB at 10^{-3} outage compared to the one-relay system. In Fig. 5.6, we notice that for overloaded multi-relay cooperative ARQ systems, i.e., $M_{\mathrm{S}} = M_{\mathrm{R}} = 2$ and $M_{\mathrm{D}} = 1$, the diversity gain is increased to 1dB for DF relaying schemes.

5.4 MMSE-based Frequency Domain Turbo Packet Combining

In this section, we briefly describe the proposed multi-relay turbo packet combining strategy using the MMSE criterion. Let us suppose that, at relaying slot k, all received signals and channel matrices corresponding to previous slots $k-1, \cdots, 1$ are available at node D receiver. First, the multi-relay frequency domain block signal vector $\underline{\mathbf{y}}_f^{(k)} \triangleq \mathbf{U}_{T,\underline{N}_k}\underline{\mathbf{y}}^{(k)}$ and CFR $\underline{\mathbf{\Lambda}}^{(k)}$ are constructed. Then, at each turbo iteration of relaying-slot k, the multi-relay soft MMSE packet combiner produces the MMSE estimate $\mathbf{z}_f^{(k)}$ on $\mathbf{s}_f$ with the aid of the unified communication model (5.26) and *a-priori* information fed back by the SISO decoder. The output $\mathbf{z}_f^{(k)}$ of the soft MMSE filter can be expressed as,

$$\mathbf{z}_f^{(k)} = \underline{\mathbf{\Phi}}^{(k)}\underline{\mathbf{y}}_f^{(k)} - \underline{\mathbf{\Psi}}^{(k)}\tilde{\mathbf{s}}_f, \tag{5.32}$$

where $\tilde{\mathbf{s}}_f$ denotes the DFT of the conditional expectation (i.e., computed based on *a-priori* LLRs) of $\mathbf{s}$, and $\underline{\mathbf{\Phi}}^{(k)} = \text{diag}\left\{\underline{\mathbf{\Phi}}_0^{(k)}, \cdots, \underline{\mathbf{\Phi}}_{T-1}^{(k)}\right\}$ and $\underline{\mathbf{\Psi}}^{(k)} = \text{diag}\left\{\underline{\mathbf{\Psi}}_0^{(k)}, \cdots, \underline{\mathbf{\Psi}}_{T-1}^{(k)}\right\}$ are the multi-relay joint forward and backward filters given by,

$$\begin{cases} \underline{\mathbf{\Phi}}_i^{(k)} \triangleq \underline{\mathbf{\Lambda}}_i^{(k)^{\mathrm{H}}}\underline{\mathbf{B}}_i^{(k)^{-1}}, \\ \underline{\mathbf{B}}_i^{(k)} = \sigma^2\mathbf{I}_{\underline{N}_k} + \underline{\mathbf{\Lambda}}_i^{(k)}\tilde{\mathbf{\Xi}}\underline{\mathbf{\Lambda}}_i^{(k)^{\mathrm{H}}}, \end{cases} \tag{5.33}$$

$$\begin{cases} \underline{\mathbf{\Psi}}_i^{(k)} \triangleq \underline{\mathbf{\Phi}}_i^{(k)}\underline{\mathbf{\Lambda}}_i^{(k)} - \underline{\mathbf{\Upsilon}}^{(k)}, \\ \underline{\mathbf{\Upsilon}}^{(k)} = \frac{1}{T}\sum_{i=0}^{T-1}\underline{\mathbf{\Phi}}_i^{(k)}\underline{\mathbf{\Lambda}}_i^{(k)}. \end{cases} \tag{5.34}$$

In (5.33), $\tilde{\mathbf{\Xi}}$ denotes the unconditional symbol covariance matrix computed as the time average of conditional covariances $\mathbf{\Xi}_i$ defined as,

$$\mathbf{\Xi}_i \triangleq \text{diag}\left\{\sigma_{1,i}^2, \cdots, \sigma_{M,i}^2\right\}, \tag{5.35}$$

where $\sigma_{t,i}^2$ is the conditional variance of symbol $s_{t,i}$. The inverse DFT of $\mathbf{z}_f^{(k)}$ is then computed, yielding thereby the time domain equalized vector,

$$\mathbf{z}^{(k)} = \mathbf{U}_{T,M}^{\mathrm{H}}\mathbf{z}_f^{(k)}. \tag{5.36}$$

The MMSE estimate $z_{t,i}^{(k)}$ corresponding to antenna t and channel use i can simply be extracted from $\mathbf{z}^{(k)}$ as $z_{t,i}^{(k)} = \mathbf{e}_{t,i}^{\mathrm{H}}\mathbf{z}^{(k)}$. Extrinsic LLR values $\phi_{t,i,m,n}^{(e)}$ corresponding to coded and interleaved bits $b_{t,i,m}$ are calculated similarly to (2.24). The calculated extrinsic LLRs are then desinterleaved and fed back to the SISO decoder.

5.5 Performance Evaluation

In this section, we evaluate the proposed packet combining strategy in term of BLER. Our main focus is to show the behavior of the studied relaying schemes depending on the relays location and to demonstrate the gain offered by the proposed turbo packet combiner.

5.5.1 Simulation Settings

In all simulations, we consider a system configuration similar to that presented in 5.3.3, using a QPSK modulation, and a 16 state convolutional encoder with polynomial generators $(35, 23)_8$. The length of the code frame is 2048 bits including tails, and the CP length is $T_{CP} = 3$. For SISO decoding, we use the Max-Log-MAP version of the MAP decoding algorithm. The iterative MMSE receiver at the destination runs three turbo iterations. We consider relay-assisted systems with one, two, and three relays. First, we verify the behavior of both AF and DF schemes depending on the relay location, already demonstrated in subsection 5.3.3 using outage probability. For this purpose, two relay locations have been considered. The location close to the source, i.e. $l_{\mathrm{SR}} = 0.3$, and the location close to the destination, i.e. $l_{\mathrm{SR}} = 0.7$. We then compare the resulting performance with outage probability to evaluate the diversity gain achieved by the introduced combining strategy. Note that for the purpose of fair comparison, the computation of the outage probability does not take into account the rate distortion as in (5.30). We also use the conventional LLR-level packet combining as a reference to evaluate our receiver performance.

5.5.2 Analysis

First, we consider a relaying system with two relays, i.e., $K = 3$, and the same number of transmit and receive antennas $M_{\mathrm{S}} = M_{\mathrm{R}} = M_{\mathrm{D}} = 2$. Fig. 5.7 plots the BLER for two relay locations, $l_{\mathrm{SR}} = 0.3$ and $l_{\mathrm{SR}} = 0.7$. We can see clearly that AF and DF schemes outperform each other depending on relay location. AF scheme seems to be the best for $l_{\mathrm{SR}} = 0.7$. In fact, it outperforms DF schemes by 4dB at 10^{-2} BLER. For $l_{\mathrm{SR}} = 0.3$, DF schemes perform better that AF. However, the performance gap is less than 2dB at 10^{-2} BLER.

Fig. 5.8 shows the performance of AF relaying system with $l_{\mathrm{SR}} = 0.7$. Two MIMO configurations are studied. The configuration where the source, the relays, and the destination have the same number of transmit and receive antennas, i.e., $M_{\mathrm{S}} = M_{\mathrm{R}} = M_{\mathrm{D}} = 2$ and an overloaded configuration, where $M_{\mathrm{S}} = M_{\mathrm{R}} = 2$ and $M_{\mathrm{D}} = 1$. Note that for both configurations, the improvement in BLER performance becomes only incremental for systems with more than one relay, i.e., $K > 2$. We can see clearly that relaying systems with $M_{\mathrm{S}} = M_{\mathrm{R}} = M_{\mathrm{D}} = 2$, achieve the diversity gain only for $K = 2$, since its BLER curve and the outage probability have similar slopes. However, for relaying systems with

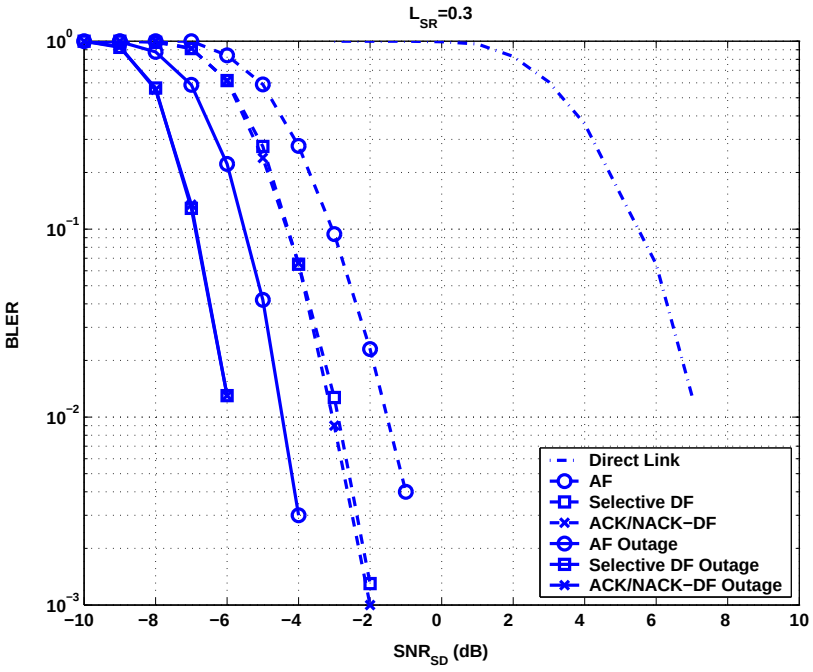

(a)

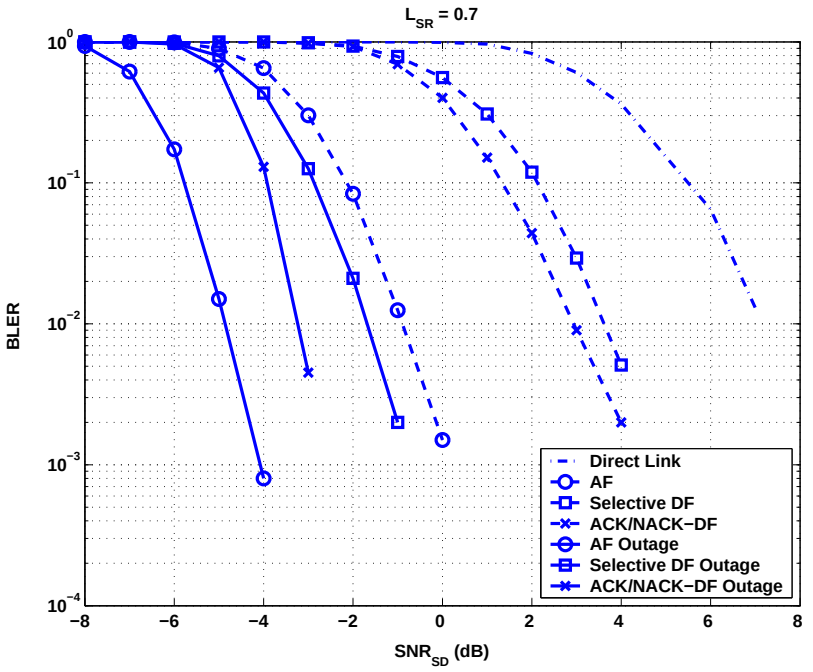

(b)

Figure 5.7: BLER performance for CC $(35, 23)_8$, QPSK, $M_{\mathrm{S}} = M_{\mathrm{R}} = M_{\mathrm{D}} = 2$, $K = 3$, $L = 3$ equal energy paths, and the path loss exponent $\kappa = 3$.

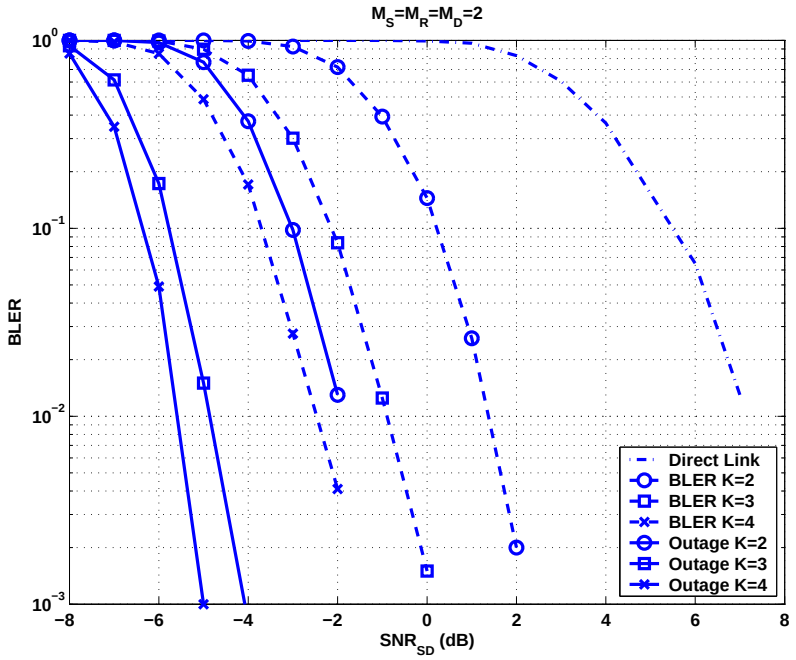

(a)

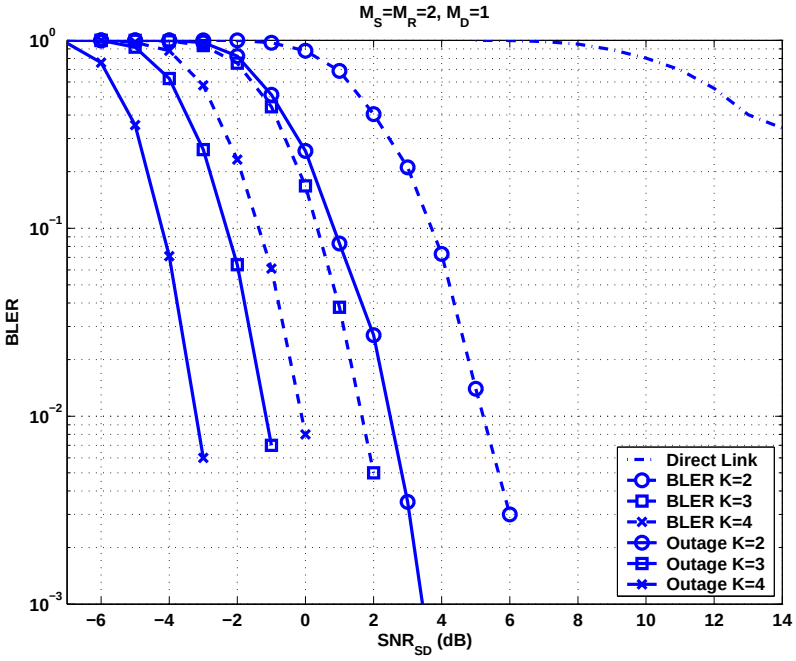

(b)

Figure 5.8: AF relaying scheme BLER performance for CC $(35, 23)_8$, QPSK, $L = 3$ equal energy paths, $l_{SR} = 0.7$, and the path loss exponent $\kappa = 3$.

$M_S = M_R = 2$ and $M_D = 1$, the proposed receiver still achieves the asymptotic slope of the outage probability for $K > 2$.

In Fig. 5.9, our main concern is to show the superior performance of the proposed combining strategy compared to LLR-level combining. First, we consider a selective DF relaying system with the same number of transmit and receive antennas $M_S = M_R = M_D = 2$. We observe that the proposed combining strategy clearly outperforms LLR-level combining. However, the performance gap, at 10^{-2} BLER, is less than 1dB for systems with one, two and three relays. For overloaded systems where $M_S = M_R = 2$ and $M_D = 1$, the proposed combining strategy significantly outperforms LLR-level combining, i.e., the performance gap is more than 2dB at 10^{-2} BLER for systems with one relay and 1.5dB for systems with three relays.

Now, we turn to DF relaying with muti-rate transmission. For that we consider a source node with $M_S = 4$ transmit antennas and relay nodes equipped with the same number of antennas, i.e., $M_R = M_{R_2} = M_{R_3} = M_{R_4} = 2$. First, we consider in Fig. 5.10 a relaying system with $M_D = 2$. The virtual equivalent MIMO system has then $M = 4$ transmit antennas and $N = 6$, $N = 10$, and $N = 14$ receive antennas for relaying system with one, two, and three relays, respectively. We observe that the proposed combining strategy outperforms LLR-level combining. The performance gap, at 10^{-2} BLER, is more than 3dB. Fig. 5.11 shows the performance of a relaying system with $M_D = 1$. In this case, the virtual equivalent MIMO system has $M = 4$ transmit antennas and $N = 3$, $N = 5$, and $N = 7$ receive antennas for relaying system with one, two, and three relays, respectively. For this configuration, the proposed scheme offers higher diversity order than LLR-level combining. In Fig. 5.11, we see clearly that the LLR-level combining curves tend to saturate for high SNR_{SD} values. Moreover, the performance gap is more than 10dB at 10^{-2} BLER for systems with two and three relays.

5.6 Conclusion

In this chapter, we proposed an efficient turbo packet combining for different relaying schemes, AF, selective DF and modified selective DF, operating over a multiple-antenna frequency-selective channels. First of all, we proposed an appropriate communication model in order to mask the cooperation and simplify the application of *virtual antenna* based combining. We examined the outage probability of different relaying schemes and showed that this schemes outperform each other depending on the relays location. Then, we briefly described the MMSE-based turbo combining scheme. Finally, we presented simulation results, and showed that the proposed packet combining strategy provides better BLER performance than the conventional LLR-level combining.

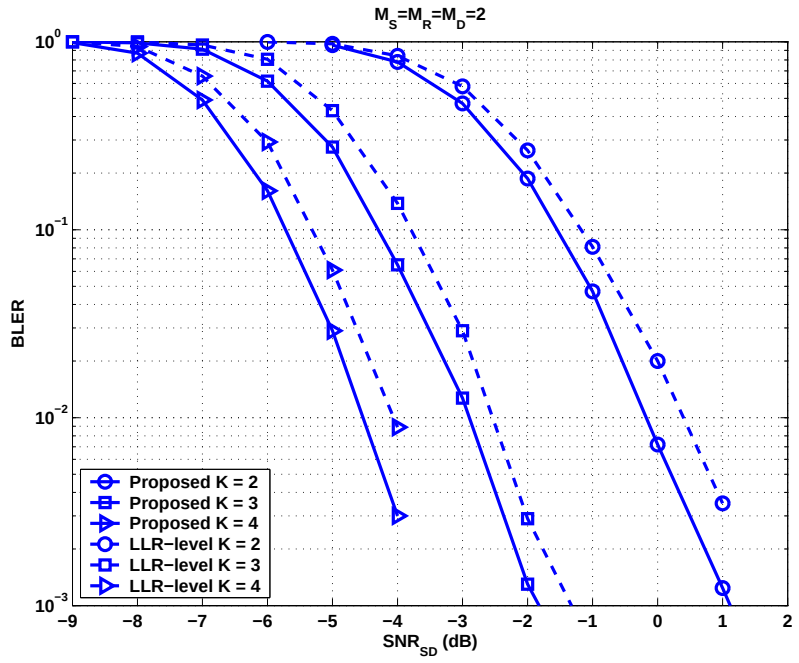

(a)

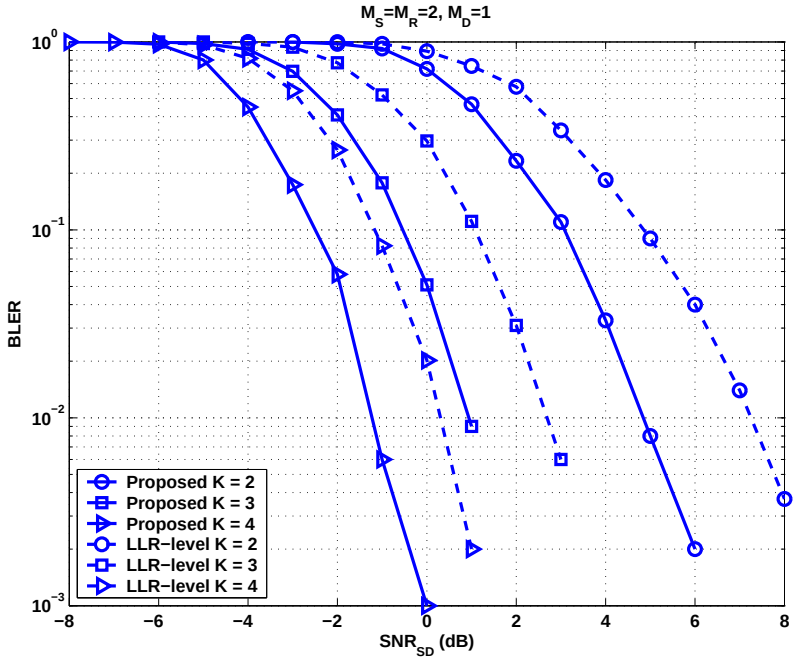

(b)

Figure 5.9: Selective DF relaying scheme BLER performance for CC $(35, 23)_8$, QPSK, $L = 3$ equal energy paths, $l_{SR} = 0.3$, and the path loss exponent $\kappa = 3$.

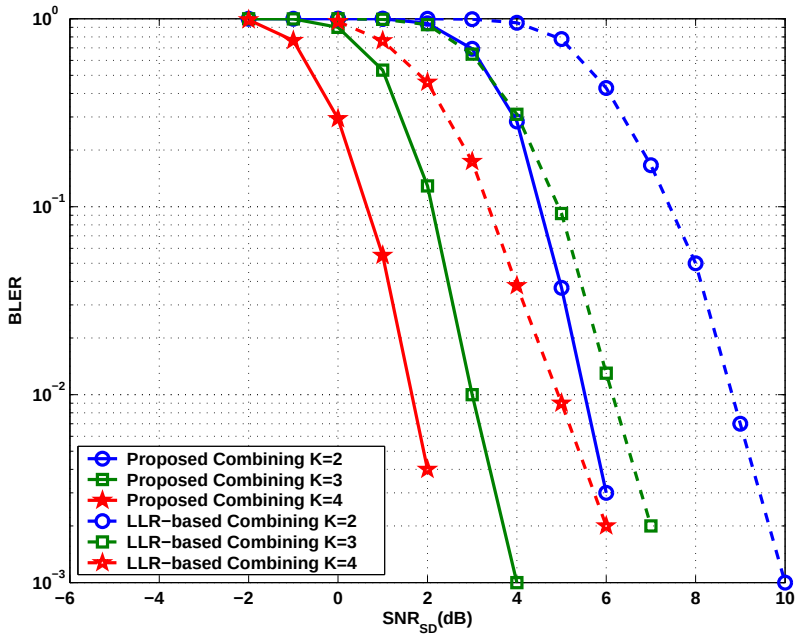

Figure 5.10: ACK/NACK DF relaying scheme BLER performance for CC $(35, 23)_8$, QPSK, $M_{\mathrm{S}} = 4$, $M_{\mathrm{R}} = M_{\mathrm{D}} = 2$, $L = 3$ equal energy paths, $l_{SR} = 0.3$ and the path loss exponent $\kappa = 3$.

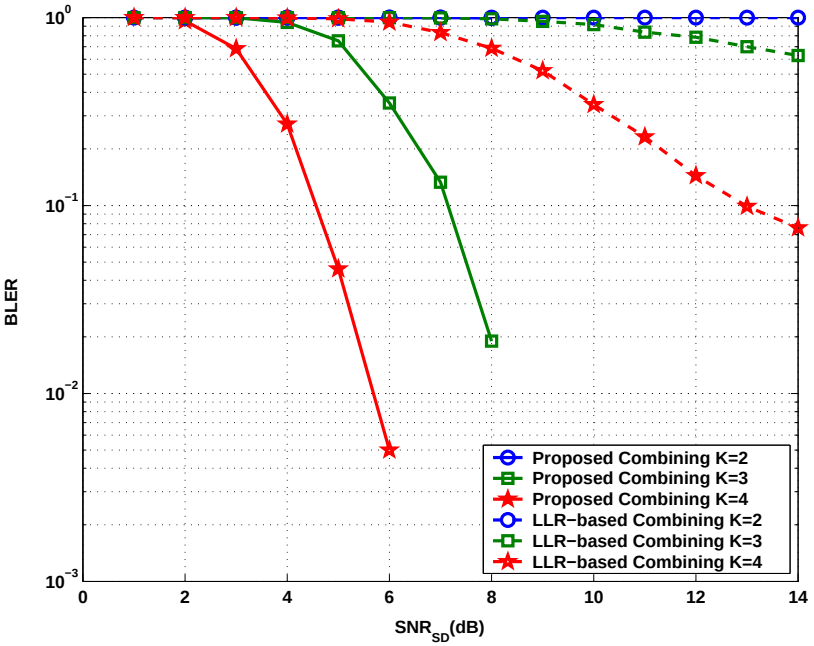

Figure 5.11: ACK/NACK DF relaying scheme BLER performance for CC $(35, 23)_8$, QPSK, $M_{\mathrm{S}} = 4$, $M_{\mathrm{R}} = 2$, $M_{\mathrm{D}} = 1$, $L = 3$ equal energy paths, $l_{SR} = 0.3$ and the path loss exponent $\kappa = 3$.

Chapter 6

Conclusions

6.1 Summary of Contributions

In this dissertation, turbo packet combining strategies for single carrier broadband MIMO-ARQ transmissions were investigated for different frameworks. First of all, a new frequency domain soft MMSE-based signal-level combining technique where received signals and CFRs corresponding to all retransmissions are used to decode the data packet, was proposed in chapter 2. The proposed scheme involves a complexity order cubic against the number of ARQ rounds. Furthermore, we showed that it requires a huge memory size that linearly increases with the increase in the number of rounds. To cope with this implementation issues, we provided a recursive implementation algorithm for the introduced scheme, and showed that both its computational complexity and memory requirements are quite insensitive to the ARQ delay. We also introduced an adaptive packet combining algorithm that enables to reduce the receiver implementation cost for overloaded configurations. Simulation results demonstrated that the proposed combining provides better BLER and throughput performances than that of the conventional LLR-level combining.

In chapter 3, the proposed combining approach was extended to a general case, where the broadband MIMO channel suffers from unknown co-channel interference caused by other transmitters who simultaneously use the same radio resource. The proposed frequency domain soft MMSE packet combiner performs soft ISI cancellation and retransmission combining in the presence of unknown CCI jointly over all received signal blocks. The covariance of the overall (over all ARQ rounds) CCI plus noise required by the frequency domain MMSE soft packet combiner is constructed by separately computing the covariance related to each round. We analyzed the effect of CCI channel rank on performance. Interestingly, under a sum-rank condition, the frequency domain MMSE soft packet combiner can completely remove CCI for asymptotically high SNR. Simulation results showed that the proposed combining scheme achieves BLER performance superior to LLR-level combining, and offers high CCI cancellation capability and diversity order

for many interference scenarios.

In chapter 4, two packet combining algorithms were proposed for multi-code CP-CDMA transmissions with ARQ operating over broadband MIMO channel. The chip-level technique performs packet combining jointly with chip-level frequency domain soft MMSE. The symbol-level scheme combines multiple transmissions at the level of the soft demapper. We analyzed the complexity and memory size required by both techniques, and showed that, from an implementation point of view, chip-level is more attractive than symbol-level combining for systems with high modulation order and load factor (number of codes with respect to the spreading factor). We also investigated BLER and throughput performances. Simulations demonstrated that both techniques approximately have similar performance for balanced MIMO configurations. In the case of unbalanced configurations (more transmit than receive antennas), chip-level combining outperforms symbol-level combining especially for full load factors.

The last part of this work focused on the extension of the proposed combining approach to multi-slot cooperative ARQ systems using AF, selective DF and modified selective DF, operating over multiple-antenna frequency-selective channels, and was reported in chapter 5. First of all, we proposed an appropriate communication model in order to mask the cooperation and simplify the application of *virtual antenna* based combining. Then, we examined the outage probability of the considered relaying schemes in section 5.3. We showed that the studied relaying schemes outperform each other depending on the relay location and demonstrated that the multi-relay transmissions provide better diversity gain than the conventional hybrid-ARQ. Using an unified communication model, derived in section 5.2, we extended the turbo packet combiner inspired by MMSE criterion to the case of cooperative ARQ systems. The unified communication model presents an important ingredient in the proposed combining scheme for cooperative ARQ systems as it allows us to view each received signal during the relaying slots as a direct retransmission from the source.

6.2 Future Research Directions

This dissertation proposed new iterative (turbo) receiver architectures with reduced complexity for broadband MIMO communications with Chase-type ARQ. Future research directions might be explored as extensions of the current work:

1. In this dissertation, the presented results are mainly limited to single-user communications. It would be of practical importance to extend this work to uplink multi-user space division multiple access (SDMA) framework where users which are located in different spatial positions, transmit simultaneously their information blocks [77, 78]. At the receiver side, in addition to ISI and CAI, multi-user transmission induces a multi-user interference (MUI) term in the received signal. The combining scheme

proposed in chapter 2 can be redesigned to cope with different interference sources in such a way to separate between users signals.

2. We can also investigate the influence of imprecise CSI on the proposed turbo receiver performance for both classical ARQ presented in chapter 2 and 4 and cooperative ARQ presented in chapter 5. In the last few years, channel re-estimation techniques have been introduced as an efficient method for improving the performance of iterative receivers [79, 80]. While in classical CSI estimation algorithms, channel estimation is performed based on the training sequence, the iterative CSI estimation concept exploits posterior LLR values at the output of the channel decoder for constructing extra training symbols.

3. A key underlying assumption in chapter 5 is that all relays are located at the same distance to the source and have the same frequency-selective fading profile with no communication between relays. Therefore, in this work, no selective transmission strategy is considered, i.e., each relay participates to data packet retransmission during the allocated slot. This assumption is not easy to keep in practical relaying systems where relays experience different channel profile. Moreover, using a selective transmission strategy where only the "best" relays participate in the retransmission will considerably reduce the overall relaying system cost.

4. In chapter 5, we showed that AF and DF relaying schemes outperform each other depending on relay locations. A hybrid scheme of AF and DF for OFDM system has been proposed in [81]. Depending on channel condition of the source-relay link on each sub-carrier, the better relaying scheme is selected. A potential future research area is to investigate this advanced selection scheme in broadband multi-user SDMA framework and redefine the problem of packet combining for such a scenario.

Appendix A

Proof of Theorem 1

Under the assumption of perfect LLR feedback from the SISO decoder, the frequency domain soft packet combiner output (3.21), at ARQ round k, can be expressed as,

$$\mathbf{z}^{(k)}_{f_{\text{perfect LLR}}} = \mathbf{A}\mathbf{s}_f + \mathbf{x}^{(k)}_f, \tag{A.1}$$

where $\mathbf{A}$ is the diagonal matrix of frequency domain symbol gains,

$$\mathbf{A} = \text{diag}\left\{(\mathbf{G}^{(k)}_0)_{1,1}, \cdots, (\mathbf{G}^{(k)}_0)_{N_T,N_T}, \cdots, (\mathbf{G}^{(k)}_{T-1})_{1,1}, \cdots, (\mathbf{G}^{(k)}_{T-1})_{N_T,N_T}\right\}, \tag{A.2}$$

with $\mathbf{G}^{(k)}_i = \underline{\mathbf{\Lambda}}^{(k)^H}_i \mathbf{\Xi}^{-1}_k \underline{\mathbf{\Lambda}}^{(k)}_i$, and $\mathbf{x}^{(k)}_f$ is the filtered CCI plus thermal noise at the output of the packet combining filter. Its covariance matrix is

$$\mathbf{G}^{(k)} = \text{diag}\left\{\mathbf{G}^{(k)}_0, \cdots, \mathbf{G}^{(k)}_{T-1}\right\}. \tag{A.3}$$

Now, let us examine the structure of matrix $\mathbf{G}^{(k)}_i$ for asymptotically high SNR, i.e., $\sigma^2 \to 0$.

Let $\mathbf{\Pi}_1\mathbf{\Pi}^H_1, \cdots, \mathbf{\Pi}_k\mathbf{\Pi}^H_k$ be the low-rank decompositions of matrices $\mathbf{\Theta}^{\text{CCI}}_1, \cdots, \mathbf{\Theta}^{\text{CCI}}_k$, where $\mathbf{\Pi}_1 \in \mathbb{C}^{N_R \times \rho_1}, \cdots, \mathbf{\Pi}_k \in \mathbb{C}^{N_R \times \rho_k}$. For the sake of notation simplicity, we write $\sum_{u=1}^{k} \rho_u = \rho$. It follows that the rank of $\mathbf{\Pi} = \text{diag}\{\mathbf{\Pi}_1, \cdots, \mathbf{\Pi}_k\}$ is ρ, and $\mathbf{\Xi}_k = \mathbf{\Pi}\mathbf{\Pi}^H + \sigma^2\mathbf{I}_{kN_R}$ is a square invertible matrix. Therefore, it has an eigenvalue decomposition (E.V.D) that can be expressed as,

$$\mathbf{\Xi}_k = \underbrace{\left[\begin{array}{cc} \mathbf{P}_\rho & \mathbf{P}_{kN_R-\rho} \end{array}\right]}_{\mathbf{P}} \left[\begin{array}{cc} \mathbf{\Upsilon} + \sigma^2\mathbf{I}_\rho & \\ & \sigma^2\mathbf{I}_{kN_R-\rho} \end{array}\right] \left[\begin{array}{c} \mathbf{P}^H_\rho \\ \mathbf{P}^H_{kN_R-\rho} \end{array}\right], \tag{A.4}$$

where $\mathbf{P}\mathbf{P}^H = \mathbf{P}^H\mathbf{P} = \mathbf{I}_{kN_R}$ since $\mathbf{\Xi}_k$ is symmetric. This condition yields the following set of equalities,

$$\mathbf{P}_\rho^H \mathbf{P}_\rho = \mathbf{I}_\rho, \tag{A.5a}$$

$$\mathbf{P}_{kN_R-\rho}^H \mathbf{P}_{kN_R-\rho} = \mathbf{I}_{kN_R-\rho}, \tag{A.5b}$$

$$\mathbf{P}_\rho^H \mathbf{P}_{kN_R-\rho} = \mathbf{0}, \tag{A.5c}$$

$$\mathbf{P}_\rho \mathbf{P}_\rho^H + \mathbf{P}_{kN_R-\rho} \mathbf{P}_{kN_R-\rho}^H = \mathbf{I}_{kN_R}. \tag{A.5d}$$

Therefore, a Taylor expansion of $\mathbf{\Xi}_k^{-1}$ when $\sigma^2 \to 0$, is given as,

$$\mathbf{\Xi}_k^{-1} = \mathbf{P}_\rho \mathbf{\Upsilon}^{-1} \mathbf{P}_\rho^H + \sigma^{-2} \mathbf{I}_{kN_R} + \mathcal{O}\left(\sigma^2\right). \tag{A.6}$$

Note that $\mathbf{\Upsilon}$ does not have any null diagonal element, i.e., $\mathbf{\Upsilon}$ is invertible. Indeed, multiplying the left and right sides of (A.4) by $\mathbf{P}^H$ and $\mathbf{P}$, respectively, and with respect to (A.5a), we get, $\mathbf{P}_\rho^H \mathbf{\Pi}\mathbf{\Pi}^H \mathbf{P}_\rho = \mathbf{\Upsilon}$. By noting that $\mathbf{P}_\rho^H \mathbf{\Pi}$ is $\rho \times \rho$ and has rank equal to ρ, it follows that $\mathbf{\Upsilon}^{-1} = \left(\mathbf{\Pi}^H \mathbf{P}_\rho\right)^{-1} \left(\mathbf{P}_\rho^H \mathbf{\Pi}\right)^{-1}$. Therefore, when $\sigma^2 \to 0$, we have,

$$\mathbf{G}_i^{(k)} = \underline{\mathbf{\Lambda}}_i^{(k)^H} \mathbf{P}_\rho \mathbf{\Upsilon}^{-1} \mathbf{P}_\rho^H \underline{\mathbf{\Lambda}}_i^{(k)} + \sigma^{-2} \underline{\mathbf{\Lambda}}_i^{(k)^H} \underline{\mathbf{\Lambda}}_i^{(k)} + \mathcal{O}\left(\sigma^2\right). \tag{A.7}$$

Since the time domain channel coefficients are i.i.d., it follows that the $kN_R \times N_T$ matrix $\underline{\mathbf{\Lambda}}_i^{(k)}$ has full-column rank unless all fading coefficients are equal to zero. If $\rho + N_T < kN_R$, i.e., $\rho < kN_R - N_T$, then all the first ρ columns of $\mathbf{\Xi}_k$ (column vectors of $\mathbf{P}_\rho$) are in the kernel of $\underline{\mathbf{\Lambda}}_i^{(k)^H}$, i.e., $\underline{\mathbf{\Lambda}}_i^{(k)^H} \mathbf{P}_\rho = \mathbf{0}_{N_T \times \rho}$. It follows that, when $\sigma^2 \to 0$,

$$\mathbf{G}_i^{(k)} = \sigma^{-2} \underline{\mathbf{\Lambda}}_i^{(k)^H} \underline{\mathbf{\Lambda}}_i^{(k)} + \mathcal{O}\left(\sigma^2\right). \tag{A.8}$$

Therefore, when SNR$\to \infty$, we get

$$\begin{aligned} \mathrm{SINR} &= \frac{1}{\sigma^2} T \sum_{i=0}^{T-1} \mathrm{tr}\left\{ \underline{\mathbf{\Lambda}}_i^{(k)^H} \underline{\mathbf{\Lambda}}_i^{(k)} \right\} + \mathcal{O}\left(\sigma^2\right) \\ &= \underbrace{\frac{1}{\sigma^2} \sum_{l=0}^{L-1} \sum_{u=1}^{k} \mathrm{tr}\left\{ \underline{\mathbf{H}}_l^{(u)^H} \underline{\mathbf{H}}_l^{(u)} \right\}}_{\mathrm{SNR_{MF}}} + \mathcal{O}\left(\sigma^2\right), \end{aligned} \tag{A.9}$$

where $\mathrm{SNR_{MF}}$ corresponds to the instantaneous matched filter (MF) SNR in the case of k rounds CCI-free MIMO-ISI ARQ channel. ■

Appendix B

DF Schemes Outage Expressions

For DF modes, the received signals available at the destination side after k slots, depend on the quality of S $\rightarrow$ R links. Let $\mathcal{E}_k$ denote the event that the relaying system {Source, $k-1$ relays, destination} is in outage at slot k, and $\mathcal{C}_{k,\tau}$ denote the event that τ source-relay links among the $k-1$ available source-relay links (i.e., S $\rightarrow$ R$_2, \cdots,$ S $\rightarrow$ R$_k$) are in outage. The outage probability of the DF relaying system at slot k can be expressed as,

$$P_{\text{out}}^{\text{DF}}(\mathcal{R},\gamma,k) = \sum_{\tau=0}^{k-1} \Pr\left\{\mathcal{E}_k, \mathcal{C}_{k,\tau}, \mathcal{A}_1, \cdots, \mathcal{A}_{k-1}\right\}. \tag{B.1}$$

In the case of selective DF mode, packet retransmission does not occur at slot u ($2 \leq u \leq k$) if the S $\rightarrow$ R$_u$ link is in outage. Let $\mathbf{R}_{k,\tau} \subset \{\text{R}_2, \cdots, \text{R}_k\}$ denote the set of τ relays involved in event $\mathcal{C}_{k,\tau}$, and $\overline{\mathbf{R}}_{k,\tau} \triangleq \{\text{R}_2, \cdots, \text{R}_k\} \setminus \mathbf{R}_{k,\tau}$. For selective DF relaying, the outage probability (B.1) can then be expressed as,

$$P_{\text{out}}^{\text{SDF}}(\mathcal{R},\gamma,k) = \sum_{\tau=0}^{k-1} \sum_{\mathbf{R}_{k,\tau}} P_{\text{out}}^{\text{S},\overline{\mathbf{R}}_{k,\tau}\rightarrow\text{D}} \prod_{\text{R}\in\mathbf{R}_{k,\tau}} P_{\text{out}}^{\text{S}\rightarrow\text{R}} \prod_{\text{R}'\in\overline{\mathbf{R}}_{k,\tau}} \left(1 - P_{\text{out}}^{\text{S}\rightarrow\text{R}'}\right), \tag{B.2}$$

where $P_{\text{out}}^{\text{S}\rightarrow\text{R}}$ denotes the outage probability of the S $\rightarrow$R link and is computed as,

$$P_{\text{out}}^{\text{S}\rightarrow\text{R}} = \Pr\left\{\frac{1}{k} I(\mathbf{s}_f, \mathbf{y}_f^{(\text{SR})} \mid \mathbf{\Lambda}^{(\text{SR})}, \gamma) < \mathcal{R},\, \mathcal{A}_1, \cdots, \mathcal{A}_{k-1}\right\}. \tag{B.3}$$

In (B.3), $\mathbf{y}_f^{(\text{SR})}$ denotes the frequency domain received signal over the S $\rightarrow$ R link, and $\mathbf{\Lambda}^{(\text{SR})}$ is the corresponding CFR. While $P_{\text{out}}^{\text{S},\overline{\mathbf{R}}_{k,\tau}\rightarrow\text{D}}$ is the outage probability of the system after combining at slot k using relays in set $\overline{\mathbf{R}}_{k,\tau}$. It is computed similarly to (5.30) using R $\rightarrow$D link channel matrices corresponding to relays in set $\overline{\mathbf{R}}_{k,\tau}$. Note that when $\mathbf{R}_{k,0} = \emptyset$

and $\overline{\mathbf{R}}_{k,k-1} = \emptyset$, the corresponding multiplicative terms in (B.2) are assumed equal to 1.

In the case of modified selective DF mode, the packet is directly retransmitted by the source during slot u if the link S $\rightarrow$ R$_u$ is in outage. Let $\mathbf{S}_{k,\tau}$ denote the set of τ time slots during which the source is involved in the packet retransmission. The outage probability (B.1) can be expressed as,

$$P_{\text{out}}^{\text{ACK/NACK-DF}}(\mathcal{R},\gamma,k) = \sum_{\tau=0}^{k-1} \sum_{\mathbf{R}_{k,\tau}} P_{\text{out}}^{\mathbf{S}_{k,\tau},\overline{\mathbf{R}}_{k,\tau}\rightarrow \text{D}} \prod_{\text{R}\in\mathbf{R}_{k,\tau}} P_{\text{out}}^{\text{S}\rightarrow\text{R}} \prod_{\text{R}'\in\overline{\mathbf{R}}_{k,\tau}} \left(1 - P_{\text{out}}^{\text{S}\rightarrow\text{R}'}\right), \tag{B.4}$$

where $P_{\text{out}}^{\mathbf{S}_{k,\tau},\overline{\mathbf{R}}_{k,\tau}\rightarrow \text{D}}$ denotes the outage probability of the system after combining at slot k using τ packet copies from S $\rightarrow$D links and $k-\tau$ copies from R$^{'}$ $\rightarrow$ D links where R$^{'}$ $\in \overline{\mathbf{R}}_{k,\tau}$.

Bibliography

[1] J. Peisa, S. Wager, M. Sagfors, J. Torsner, B. Goransson, T. Fulghum, C. Cozzo, and S. Grant, "High speed packet access evolution - concept and technologies," *IEEE Veh. Technol. Conf. (VTC)-Spring*, Dublin, Ireland, Apr. 2007.

[2] P. W. Wolniansky, G. J. Foschini, and R. A. Valenzuela, "V-BLAST : an architecture for realizing very high data rates over the rich scattering wireless channel," *in Proc. Int. Symp. Signals, Systems, Electron.,* Pisa, Italy, Sep. 1998.

[3] G. J. Foschini, G. D. Golden, P. W. Wolniansky, and R. A. Valenzuela, "Simplified processing for wireless communication at high spectral efficiency," *IEEE J. Sel. Areas Commun.*, vol. 17, pp. 1841-1852, 1999.

[4] D. Chase, "Code combining–a maximum-likelihood decoding approach for combining an arbitrary number of noisy packets," *IEEE Trans. Commun.,* vol. COM-33, no. 5, pp. 385-393, May 1985.

[5] F. Adachi and S. Itoh, "Efficient ARQ with time diversity reception–Time diversity ARQ," *Electronics letter*, vol. 22, pp. 1254–1258, Nov. 1986.

[6] J. Hagenauer, "Rate-compatible punctured convolutional codes (RCPC codes) and their application," *IEEE Trans. Commun.*, vol. 36, no. 4, pp. 389–400, Apr. 1988.

[7] E. Zimmermann, P. Herhold, and G. Fettweis, "The impact of cooperation on diversity-exploiting protocols," *IEEE VTC-spring*, Milan, Italy, May 2004.

[8] J. N. Laneman, G. W. Wornell, and D. N. C. Tse, "An efficient protocol for realizing cooperative diversity in wireless networks," *IEEE International Symposium on Information Theory (ISIT)*, Washington, DC, June 2001.

[9] A. Sendonaris, E. Erkip, and B. Aazhang, "User cooperation diversity – Part I & Part II," *IEEE Trans. Commun.*, vol. 51, pp. 1927-1948, Nov. 2003.

[10] S. L. Ariyavisitakul, "Turbo space-time processing to improve wireless channel capacity," *IEEE Commun. Conf.,* vol. 3, pp. 1238-1242, Jun. 2000.

[11] A. M. Tonello, "MIMO MAP equalization and turbo decoding in interleaved space time coded systems", *IEEE Trans. Commun.*, vol. 51, no. 2, pp. 155-160, Feb. 2003.

[12] H. Sari, G. Karam, and I. Jeanclaude, "Frequency domain equalization of mobile radio and terrestrial broadcast channels," *in Proc. IEEE GLOBECOM,* San Francisco, CA, Nov.–Dec. 1994.

[13] M. Tüchler and J. Hagenauer, "Turbo equalization using frequency domain equalizers," *in Proc. Allerton Conf.,* Monticello, IL, Oct. 2000. CD-ROM.

[14] D. Falconer, S. L. Ariyavisitakul, A. Benyamin-Seeyar, and B. Eidson, "Frequency domain equalization for single-carrier broadband wireless access systems," *IEEE Commun. Mag.,* vol. 40, no. 4, pp. 58–66, Apr. 2002.

[15] F. Pancaldi and G. M. Vitetta, "Block channel equalization in the frequency domain," *IEEE Trans. Commun.,* vol. 53, no. 3, pp. 463–471, Mar. 2005.

[16] R. Visoz, A. O. Berthet, and S. Chtourou, "Frequency-domain block turbo-equalization for single-carrier transmission over MIMO broadband wireless channel," *IEEE Trans. Commun.,* vol. 54, no. 12, pp. 2144-2149, Dec. 2006.

[17] L. J. Cimini, "Analysis and simulation of a digital mobile channel using orthogonal frequency division multiplexing," *IEEE Trans. Commun.,* vol. COM-33, pp. 400–411, July 1985.

[18] R. van Nee and R. Prasad, *OFDM for Wireless Multimedia Communications*, Norwood, MA: Artech House, 2000.

[19] Z.Wang and G. B. Giannakis, "Wireless multicarrier communications – Where Fourier meets Shannon," *IEEE Signal Processing Mag.*, vol. 17, pp. 29–48, May 2000.

[20] P. S. Sindhu, "Retransmission error control with memory," *IEEE Trans. Commun.,* vol. 25, pp. 473–479, May 1977.

[21] G. Benelli, "An ARQ scheme with memory and soft error detection," *IEEE Trans. Commun.,* vol. 33, pp. 285–288, Mar. 1985.

[22] S. B. Wicker, "Adaptive error control through the use of diversity combining majority logic decoding in hybrid ARQ protocol," *IEEE Trans. Commun.,* vol. 39, pp. 380–385, Mar. 1991.

[23] E. Yli-Juuti, S. S. Chakraborty, and M. Liinaharja, "An adaptive ARQ scheme with packet combining," *IEEE Commun. Lett.*, vol. 2, pp. 200–202, July 1998.

[24] M. Liinaharja, S. S. Chakraborty, and E. Yli-Juuti, "An adaptive ARQ scheme with packet combining for time varying channels," *IEEE Commun. Lett.,* vol. 3, pp. 52–54, Feb. 1999.

[25] S. Kallel, "Analysis of a type-II hybrid ARQ scheme with code combining," *IEEE Trans. Commun.,* vol. 38, pp. 1133–1137, Aug. 1990.

[26] E. N. Onggosanusi, A. G. Dabak, Y. Hui, and G. Jeong, "Hybrid ARQ transmission and combining for MIMO systems," *in Proc. IEEE Int. Conf. Commun.,* vol. 5, May 2003, pp. 3205-3209.

[27] A. Nakajima, D. Garg, and F. Adachi, "Throughput of turbo coded hybrid ARQ using single-carrier MIMO multiplexing," *61st IEEE veh. technol. conf. VTC'05 Spring*, Stockholm, Sweden, 2005.

[28] A. Nakajima, and F. Adachi, "Iterative joint PIC and 2D MMSE-FDE for turbo-coded HARQ with SC-MIMO multiplexing," *63rd IEEE veh. technol. conf. VTC'06 Spring*, pp. 2503-2507, Melbourne, Australia, May. 2006.

[29] H. Samra, and Z. Ding, "Integrated iterative equalization for ARQ systems," *in Proc. IEEE Int. Conf. on Acoustics, Speech, and Signal Processing (ICASSP)*, Orlando, FL, May 2002.

[30] H. Samra, and Z. Ding, "Integrated iterative equalization for ARQ systems," *in Proc. IEEE Int. Symp. on Info. Theory (ISIT)*, Lausanne, Switzerland, Jun., 2002.

[31] H. Samra, and Z. Ding, "Precoded integrated equalization for packet retransmissions," *in Proc. 36th IEEE Asilomar Conf. on Signals, Systems, and Computers*, Monterey, CA, Nov., 2002.

[32] H. Samra, and Z. Ding, "A hybrid ARQ protocol using integrated channel equalization," *IEEE Trans. Commun.*, vol. 53, no. 12, pp. 1996-2001, Dec. 2005.

[33] D. N. Doan, and K. R. Narayanan, "Iterative packet combining schemes for intersymbol interference channels," *IEEE Trans. Commun.*, vol. 50, no. 4, pp. 560-570, Apr. 2002.

[34] H. Samra, and Z. Ding, "Sphere decoding for retransmission diversity in MIMO flat-fading channels," *in Proc. IEEE ICASSP*, Montreal, Canada, May 2004.

[35] H. Samra, and Z. Ding, "New MIMO ARQ protocols and joint detection via sphere decoding," *IEEE Trans. Sig. Proc.* vol. 54, no. 2, pp. 473-482, Feb. 2006.

[36] S. Lin and D. Costello, *Error Control Coding: Fundamentals and Applications*. Englewood Cliffs, NJ: Prentice-Hall, 1983.

[37] D. Costello, J. Hagenauer, H. Imai, and S. Wicker, "Applications of error-control coding," *IEEE Trans. Inform. Theory,* vol. 44, pp. 2531–2560, Oct. 1998.

[38] B. A. Harvey and S. B. Wicker, "Packet combining system based on the Viterbi decoder," *IEEE Trans. Commun.,* vol. 42, pp. 1544–1557, Feb./Mar./Apr. 1994.

[39] R. Visoz, and A. O. Berthet, "Iterative decoding and channel estimation for space-time BICM over MIMO block fading multipath AWGN channel", *IEEE Trans. Commun.,* vol. 51, no. 8, pp. 1358-1367, Aug. 2003.

[40] X. Wautelet, A. Dejonghe, and L. Vandendorpe, "MMSE-based fractional turbo receiver for space-time BICM over frequency selective MIMO fading channels," *IEEE Trans. Sig. Proc.,* vol. SIG-52, pp. 1804-1809, Jun. 2004

[41] R. Visoz, A. O. Berthet, and S.Chtourou, "A new class of iterative equalizers for space-time BICM over MIMO block fading multipath AWGN channel," *IEEE Trans. Commun.*, vol. 53, no. 12, pp. 2076-2091, Dec. 2005.

[42] M. Yee, M. Sandell, and Y. Sun, "Comparison study of single-carrier and multi-carrier modulation using iterative based receiver for MIMO systems," *IEEE VTC-spring*, Milan, Italy, May 2004.

[43] T. Ait-Idir, S. Saoudi, and N. Naja, "Space-time turbo equalization with successive interference cancellation for frequency selective MIMO channels," *IEEE Trans. Veh. Technol.*, vol. 57, no. 5, pp. 2766-2778, Sep. 2008.

[44] K. Narayanan, and G. Stuber, "A novel ARQ technique using the turbo coding principle," *IEEE Commun. Lett.,* vol. 1, no. 3, pp. 49-51, Mar. 1997.

[45] S. Haykin, *Adaptive Filter Theory*, 3rd Ed. Upper Saddle River, NJ: Prentice-Hall, 1996.

[46] L. R. Bahl, J. Cocke, F. Jelinek, and J. Raviv, "Optimal decoding of linear codes for minimizing symbol error rate," *IEEE Trans. Inform. Theory,* vol. IT-20, pp. 284-287, Mar. 1974.

[47] G. Caire, and D. Tuninetti, "ARQ protocols for the Gaussian collision channel," *IEEE Trans. Inf. Theory,* vol. 47, no. 4, pp. 1971–1988, Jul. 2001.

[48] L. Zheng, and D. N. C. Tse, "Diversity and multiplexing:A fundamental tradeoff in multiple antenna channels," *IEEE Trans. Inf. Theory,* vol. 49, no. 5, pp. 1073–1096, May 2003.

[49] H. El Gamal, G. Caire, and M. O. Damen, "The MIMO ARQ channel: diversity–multiplexing–delay tradeoff," *IEEE Trans. Inf., Theory,* vol. 52, no. 8, Aug. 2006, pp. 3601-3621.

[50] D. Tse, and P. Viswanath, *Fundamentals of Wireless Communication*, Cambridge University Press, May 2005.

[51] A. Chuang, A. Guillen i Fabregas, L.K. Rasmussen, I.B. Collings, "Optimal throughput-diversity-delay tradeoff in MIMO ARQ block-fading channels," *IEEE Trans. Inf., Theory,* vol. 54, no. 9, Sep. 2008, pp. 3968-3986.

[52] T. Ait-Idir, and S. Saoudi, "Turbo packet combining strategies for the MIMO-ISI ARQ channel," *IEEE Trans. Commun.*, vol. 57, no. 12, pp. 3782-3793, Dec. 2009.

[53] T. Ait-Idir, and S. Saoudi, "Turbo packet combining for MIMO-ISI channels with co-channel interference," *in Proc, 19th Annual IEEE Symp. Personal Indoor Mobile Radio Commun. (PIMRC'08)*, Cannes, France, Sep. 2008.

[54] D. Gesbert, H. Bölcskei, D. A. Gore, and A. J. Paulraj, "Outdoor MIMO wireless channels: models and performance prediction," *IEEE Trans. Commun.,* vol. 50, no. 12, pp. 1926–1934, Dec. 2002.

[55] M. Sellathurai, and S. Haykin, "Turbo-BLAST: Performance evaluation in correlated Rayleigh-fading environment," *IEEE J. Sel. Areas Commun.,* vol. 21, no. 3, pp. 340–349, Apr. 2003.

[56] C.-L. I and R. D. Gitlin, "Multi-code CDMA wireless personal communications networks," *in Proc. IEEE Int. Conf. Commun.*, Seattle, WA, June 1995, pp. 1060-1064.

[57] U. Madhow and M. L. Honig, "MMSE Interference suppression for Direct-Sequence Spread-spectrum CDMA," *IEEE Trans. Communications*, vol. 12, no. 4, pp. 3178-3188, 1994.

[58] K. Hooli, M. J. Heikkila, P. Komulainen, M. Latva-aho, and J. Lilleberg, "Chip-level channel equalization in WCDMA downlink," *EURASIP Journal on Applied Signal Processing*, Aug.2002, pp. 757-770.

[59] J. Choi, "MMSE equalization of downlink CDMA channel utilizing unused orthogonal spreading sequences," *IEEE Trans. Signal Proc.*, vol.51, pp.1390-1402, May 2003.

[60] K. Baum, T. Thomas, F. Vook, and V. Nangia, "Cyclic-prefix CDMA: An improved transmission method for broadband DS-CDMA cellular systems," *IEEE WCNC 2002*, Vol.1, pp. 183-188, March 2002.

[61] F. Adachi, T. Sao, and T. Itagaki, "Performance of multicode DS-CDMA using frequency domain equalization in frequency selective fading channel," *Electronics letter*, vol. 39, no. 2, pp. 239- 241, Jan. 2003.

[62] J. K. Lee, T. J. Lee, H. J. Chae, and D. K. Kim, "Frequency domain turbo equalization for multicode DS-CDMA in frequency selective fading channel," *in Proc, 19th Annual IEEE Symp. Personal Indoor Mobile Radio Commun. (PIMRC'07)*, Athens, Greece, Sep. 2007.

[63] H. Huang, H. Viswanathan, and G. J. Foschini, "Multiple antennas in cellular CDMA systems: Transmission, detection, and spectral efficiency," *IEEE Trans. Wireless Commun.*, vol. 1, no. 4, pp. 383-392, Jul. 2002.

[64] D. Garg and F. Adachi, "Packet access using DS-CDMA with frequency-domain equalization ," *IEEE J. Sel. Areas Commun.*, vol. 24, no. 1, pp.161-170, Jan. 2006.

[65] J. N. Laneman, D. Tse, and G. W. Wornell, "Cooperative diversity in wireless networks: Efficient protocols and outage behavior," *IEEE Trans. Inform. Theory*, vol. 50, no. 12, pp. 3062-3080, Dec. 2004.

[66] Y. Zhang, H. H. Chen, and M. Guizani, *Cooperative Wireless Communications*, Auerbach Publications, 2009.

[67] B. Zhao and M. C. Valenti, "Practical relay networks: A generalization of hybrid-ARQ," *IEEE J. Select. Areas. Comm.*, vol. 23, no. 1, Jan. 2005.

[68] J. Boyer, D. D. Falconer, and H. Yanikomeroglu, "Multihop diversity in wireless relaying channels," *IEEE Trans. on Comm.*, vol. 52, pp. 1820-1830, Oct. 2004.

[69] F. Atay Onat, H. Yanikomeroglu, and S. Periyalwar, "Relay-assisted spatial multiplexing in wireless fixed relay networks,", *IEEE GLOBECOM*, San Francisco, USA, Nov.- Dec. 2006.

[70] P. Herhold, E. Zimmermann, and G. Fettweis, "A simple cooperative extension to wireless relaying", *Int. Zurich Seminar on Commun.*, Zurich, Switzerland, Feb. 2004.

[71] H. V. Khuong and T. Le-Ngoc, "A bandwidth-efficient cooperative relaying scheme with limited feedback information" *24th Biennial Symposium on Communication 2008*, pp. 175-178, June 2008.

[72] Q. Jia, T. Lv, and G. Ping, "An efficient scheme for joint equalization and interference cancellation in distributed cooperative diversity networks", *Communication Networks and Services Research (CNSR)*, Halifax, Canada, May 2008.

[73] R. U. Nabar, F. W. Kneubiihler, and H. Boelcskei, "Performance limits of amplify-and-forward based fading relay channels", *IEEE International Conference on Acoustics, Speech, and Signal Processing (ICASSP*), Montreal, Canada, May 2004.

[74] H. Mheidat, M. Uysal, and N. Al-Dhahir, "Equalization techniques for distributed space-time block codes with amplify-and-forward relaying," *IEEE Trans. Signal Process.*, vol. 55, pp. 1839-1852, 2007.

[75] H. Xiong and J. X. P. Wang, "Frequency-domain equalization and diversity combining for demodulate-and-forward cooperative systems", *IEEE ICASSP*, Las Vegas, Nevada, USA, March-April 2008.

[76] H. El Gamal, A. R. Hammons, Y. Liu, M. P. Fitz, and O. Y. Takeshita, "On the design of space–time and space–frequency codes for MIMO frequency-selective fading channels," *IEEE Trans. Inform. Theory*, vol. 49, no 9, pp. 2277–2292, Sep. 2003.

[77] G. Tsoulos, M. Beach, and J. McGeehan, "Wireless personal communications for the 21st century: European technological advances in adaptive antennas," *IEEE Commun. Magazine*, pp. 102-109, Sept. 1997.

[78] J. Winters, "Smart antennas for wireless systems," *IEEE Personal Commun. Magazine*, Feb. 1998.

[79] M. Loncar, J. Wehinger, R. Muller, and C. Mecklenbrauker, T. Abe. "Iterative channel estimation and data detection in frequency-selective fading MIMO channels", *Europ. Trans. Telecoms.*, vol. 15, no. 5, pp. 459-470, Sep./Oct. 2004.

[80] R. Otnes and M. Tuchler, "Iterative channel estimation for turbo equalization of timevarying frequency-selective channels," *IEEE Trans. Wireless. Commun.*, vol. 3, no. 6, pp. 1918-1923, Nov. 2004.

[81] B. Can, H. Yomo, and E. D. Carvalho, "Hybrid forwarding scheme for cooperative relaying in OFDM based networks," *in Proc. IEEE International Commun. Conf.*, Istanbul, Turkey, Jun. 2006, pp. 4520–4525.

Publications List

- Tarik Ait-Idir, Houda Chafnaji, Samir Saoudi, and Athanasios V. Vasilakos, "Advanced Hybrid-ARQ Receivers for Broadband MIMO Communications," Chapter in "Radio Communications", Alessandro Bazzi (Ed.), ISBN: 978-953-307-091-9, INTECH.

- Houda Chafnaji, Tarik Ait-Idir, Halim Yanikomeroglu, and Samir Saoudi, "Relaying Schemes and Joint Turbo Processing for Spatial Multiplexing over Broadband MIMO Channels," Submitted to *IEEE Transactions on Wireless Communications*, Mar. 2010.

- Houda Chafnaji, Tarik Ait-Idir, Samir Saoudi, and Athanasios V. Vasilakos, "Frequency Domain Hybrid-ARQ Chase Combining for Broadband MIMO CDMA Systems," Submitted to *EURASIP Journal on Wireless Communications and Networking*.

- Tarik Ait-Idir, Houda Chafnaji, and Samir Saoudi, "Turbo Packet Combining for Broadband Space-Time BICM Hybrid-ARQ Systems with Co-Channel Interference," *IEEE Transactions on Wireless Communications*, vol. 9, no. 5, pp. 1686-1697, May 2010.

- Houda Chafnaji, Tarik Ait-Idir, Halim Yanikomeroglu, and Samir Saoudi, "Signal-level turbo packet combining for multi-rate relay-assisted systems over multi-antenna broadband channels," Accepted to *IEEE GLOBECOM 2010*, 6-10 December 2010, Miami, Florida, USA.

- Houda Chafnaji, Tarik Ait-Idir, and Samir Saoudi, "A comparative study of frequency domain HARQ Chase combining schemes for broadband single carrier MIMO CDMA systems," Accepted, *Workshop on Broadband Single Carrier and Frequency Domain Communications, IEEE GLOBECOM 2010*, Miami, FL, Dec. 2010

- Houda Chafnaji, Tarik Ait-Idir, Halim Yanikomeroglu, and Samir Saoudi, "Analysis of Packet Combining for Single Carrier Multi-Relay Broadband Systems," *IEEE International Workshop on Signal Processing Advances in Wireless Communications, SPAWC 2010*, Marrakech, Morocco, Jun. 2010.

- Houda Chafnaji, Tarik Ait-Idir, Halim Yanikomeroglu, and Samir Saoudi, "Turbo Packet Combining Techniques for Multi-Relay-Assisted Systems over Multi-Antenna Broadband Channels," *ACM International Wireless Communications and Mobile Computing Conference, IWCMC 2010*, Caen, France, Jun. 2010.

- Houda Chafnaji, Tarik Ait-Idir, Halim Yanikomeroglu, and Samir Saoudi, "On the Design of Turbo Packet Combining Schemes for Relay-Assisted Systems over Multi-Antenna Broadband Channels," *IEEE 71st Semi-Annual VTC10Spring*, Taipei, Taiwan, May 2010.

- Tarik Ait-Idir, Houda Chafnaji, and Samir Saoudi, "Frequency Domain Hybrid–ARQ Chase Combining for Broadband MIMO Communication with Co-Channel Interference," *IEEE GLOBECOM 2009*, Honolulu, Hawaii, Nov-Dec. 2009.

- Tarik Ait-Idir, Houda Chafnaji, Halim Yanikomeroglu, and Samir Saoudi, "Turbo Packet Combining for Boadband MIMO Relay Communication," *9th IEEE Mediterranean Microwave Symposium, MMS 2009*, Tangiers, Morocco, Nov. 2009. (*Invited Paper*).

- Houda Chafnaji, Tarik Ait-Idir, Halim Yanikomeroglu, and Samir Saoudi, "Joint Turbo Equalization for Relaying Schemes over Frequency-Selective Fading Channels,"' *ACM IWCMC 2009*, Leipzig, Germany, Jun. 2009.

- Houda Chafnaji, Tarik Ait-Idir, and Samir Saoudi, "Packet Combining and Chip Level Frequency Domain Turbo Equalization for Multi-Code Transmission over Multi-Antenna Broadband Channel," *19th Annual IEEE Symposium PIMRC 2008*, Cannes, France, Sep. 2008.

- Houda Chafnaji, Tarik Ait-Idir, and Samir Saoudi, "Implementation and Complexity evaluation of Packet Combining for Multi-Code Transmission over Multi-Antenna Broadband Channel," *IEEE IWCMC 2008*, Crete Island, Greece, Aug. 2008.

- Tarik Ait-Idir, Houda Chafnaji, and Samir Saoudi, "Frequency Domain Packet Combining with Integrated MMSE Block Turbo Equalization for Broadband MIMO Communicatio," *4th International Symposium on Image/Video Communications over Fixed and Mobile Networks, ISIVC 2008*, Bilbao, Spain, Jul. 2008 (*Invited Paper*).

- Tarik Ait-Idir, Houda Chafnaji, and Samir Saoudi, "Joint Hybrid ARQ and Iterative Space-Time Equalization for Coded Transmission over MIMO-ISI Channel," *IEEE WCNC 2008*, Las Vegas, NV, Mar-Apr. 2008.